Processing of behaviorally relevant stimuli at different levels in the bee brain

Die Verarbeitung verhaltensrelevanter Stimuli auf unterschiedlichen Ebenen im Bienengehirn

Doctoral thesis for a doctoral degree
at the Graduate School of Life Sciences,
Julius-Maximilians-Universität Würzburg,
Section Integrative Biology

submitted by

Fabian Dominik Schmalz

from

Regensburg

Würzburg 2022

Submitted on: …………………………………………………………………….

Members of the Thesis Committee

Chairperson: Prof. Dr. Christian Wegener

Primary Supervisor: Dr. Martin Strube-Bloss

Supervisor (Second): Prof. Dr. Basil el Jundi

Supervisor (Third):   Prof. Dr. Martin Nawrot

Date of Public Defence: …………………………………………………………………….

Date of Receipt of Certificates: …………………………………………………………………….

Contents

Summary

The behavior of honeybees and bumblebees relies on a constant sensory integration of abiotic or biotic stimuli. As eusocial insects, a sophisticated intraspecific communication as well as the processing of multisensory cues during foraging is of utter importance. To tackle the arising challenges, both honeybees and bumblebees have evolved a sophisticated olfactory and visual processing system.

In both organisms, olfactory reception starts at the antennae, where olfactory sensilla cover the antennal surface in a sex-specific manner. These sensilla house olfactory receptor neurons (ORN) that express olfactory receptors. ORNs send their axons via four tracts to the antennal lobe (AL), the prime olfactory processing center in the bee brain. Here, ORNs specifically innervate spheroidal structures, so-called glomeruli, in which they form synapses with local interneurons and projection neurons (PN). PNs subsequently project the olfactory information via two distinct tracts, the medial and the lateral antennal-lobe tract, to the mushroom body (MB), the main center of sensory integration and memory formation. In the honeybee calyx, the sensory input region of the MB, PNs synapse on Kenyon cells (KC), the principal neuron type of the MB. Olfactory PNs mainly innervate the lip and basal ring layer of the calyx. In addition, the basal ring receives input from visual PNs, making it the first site of integration of visual and olfactory information. Visual PNs, carrying sensory information from the optic lobes, send their terminals not only to the to the basal ring compartment but also to the collar of the calyx. Receiving olfactory or visual input, KCs send their axons along the MB peduncle and terminate in the main output regions of the MB, the medial and the vertical lobe (VL) in a layer-specific manner. In the MB lobes, KCs synapse onto mushroom body output neurons (MBON). In so far barely understood processes, multimodal information is integrated by the MBONs and then relayed further into the protocerebral lobes, the contralateral brain hemisphere, or the central brain among others.

This dissertation comprises a dichotomous structure that (i) aims to gain more insight into the olfactory processing in bumblebees and (ii) sets out to broaden our understanding of visual processing in honeybee MBONs.

The first manuscript examines the olfactory processing of *Bombus terrestris* and specifically investigates sex-specific differences. We used behavioral (absolute conditioning) and electrophysiological approaches to elaborate the processing of ecologically relevant odors

(components of plant odors and pheromones) at three distinct levels, in the periphery, in the AL and during olfactory conditioning. We found both sexes to form robust memories after absolute conditioning and to generalize towards the carbon chain length of the presented odors. On the contrary, electroantennographic (EAG) activity showed distinct stimulus and sex-specific activity, e.g. reduced activity towards citronellol in drones. Interestingly, extracellular multi-unit recordings in the AL confirmed stimulus and sex-specific differences in olfactory processing, but did not reflect the differences previously found in the EAG. Here, farnesol and 2,3-dihydrofarnesol, components of sex-specific pheromones, show a distinct representation, especially in workers, corroborating the results of a previous study. This explicitly different representation suggests that the peripheral stimulus representation is an imperfect indication for neuronal representation in high-order neuropils and ecological importance of a specific odor.

The second manuscript investigates MBONs in honeybees to gain more insights into visual processing in the VL. Honeybee MBONs can be categorized into visually responsive, olfactory responsive and multimodal. To clarify which visual features are represented at this high-order integration center, we used extracellular multi-unit recordings in combination with visual and olfactory stimulation. We show for the first time that information about brightness and wavelength is preserved in the VL. Furthermore, we defined three specific classes of visual MBONs that distinctly encode the intensity, identity or simply the onset of a stimulus. The identity-subgroup exhibits a specific tuning towards UV light. These results support the view of the MB as the center of multimodal integration that categorizes sensory input and subsequently channels this information into specific MBON populations.

Finally, I discuss differences between the peripheral representations of stimuli and their distinct processing in high-order neuropils. The unique activity of farnesol in manuscript 1 or the representation of UV light in manuscript 2 suggest that the peripheral representation of a stimulus is insufficient as a sole indicator for its neural activity in subsequent neuropils or its putative behavioral importance. In addition, I discuss the influence of hard-wired concepts or plasticity induced changes in the sensory pathways on the processing of such key stimuli in the peripheral reception as well as in high-order centers like the AL or the MB. The MB as the center of multisensory integration has been broadly examined for its olfactory processing capabilities and receives increasing interest about its visual coding properties. To further

unravel its role of sensory integration and to include neglected modalities, future studies need to combine additional approaches and gain more insights on the multimodal aspects in both the input and output region.

Zusammenfassung

Honigbienen und Hummeln sind aufgrund ihrer Lebensweise auf die ständige Verarbeitung sensorischer Eindrücke abiotischen und biotischen Ursprungs angewiesen. Als eusoziale Insekten ist hierbei für beide Arten die Wahrnehmung innerartlicher Kommunikation wie auch die Verarbeitung multisensorischer Einflüsse während der Nahrungssuche von essenzieller Bedeutung. Um die daraus resultierenden vielfältigen Herausforderungen erfolgreich bewältigen zu können, verfügen Honigbienen und Hummeln über eine fortschrittliche Verarbeitung olfaktorischer und visueller Reize.

In beiden Arten beginnt die Geruchsrezeption an den Antennen, welche geschlechtsspezifisch von zahlreichen olfaktorischen Sensillen besetzt sind. Diese beinhalten olfaktorische Rezeptorneurone (ORN), in welchen die Expression der Geruchsrezeptoren stattfindet. Axone der ORNs laufen dabei gebündelt über vier verschiedene Trakte in den Antennallobus (AL), das erste olfaktorische Verarbeitungszentrum im Bienengehirn. Im AL verschalten ORNs mit lokalen Interneuronen und Projektionsneuronen (PN) in kugelförmigen Strukturen, den sogenannten Glomeruli. PNs leiten die olfaktorische Information daraufhin über zwei charakteristische Trakte, den medialen und lateralen Antennallobustrakt, in den Pilzkörper (MB), das Verarbeitungszentrum für die Integration sensorischer Eindrücke und Gedächtnisbildung. Im Calyx der Honigbiene, der sensorischen Eingangsregion des MB, bilden die Endköpfchen der PNs synaptische Verbindungen mit Kenyonzellen (KC), den primären Nervenzellen im MB. Die Innervation des Calyx durch die PNs ist dabei spezifisch in drei verschiedenen Zonen organisiert, nämlich in Lippe, Hals und basalen Ring. Während die Lippe vornehmlich olfaktorische Information von PNs aus dem AL erhält, wird der basale Ring zusätzlich auch von visuellen PNs, welche Informationen aus dem optischen Lobus einbringen, angesteuert. Der basale Ring der Honigbiene wird dabei Ort der ersten räumlichen Integration visuellen und olfaktorischen Eingangs. Wiederum ähnlich zum unimodalen Eingang der Lippe, bezieht auch der Hals des Calyx grundsätzlich nur sensorischen Eingang einer Modalität, nämlich visuelle Information von PNs aus dem optischen Lobus. KCs verschalten im weiteren Verlauf die olfaktorischen und visuellen Informationen an Pilzkörperausgangsneurone (MBON). In einem bisher kaum erforschten Vorgang wird diese multimodale Information dabei verarbeitet und dann mithilfe der MBONs in verschiedene Bereiche des Gehirns geleitet, z.B. in die protocerebralen Loben, die kontralaterale Gehirnhemisphäre oder das

Zentralgehirn.

Diese Dissertation ist zweigeteilt und behandelt zuerst (i) die geschlechtsspezifische Verarbeitung olfaktorischer Reize in Hummeln und bespricht im zweiten Teil (ii) neue Einblicke in die neuronale Weiterverarbeitung visueller Reize durch MBONs in der Honigbiene. Manuskript 1 untersucht die Abläufe der Geruchsverarbeitung von *Bombus terrestris* und beschreibt geschlechtsspezifische Unterschiede. Hierbei wurden sowohl verhaltensbasierte als auch elektrophysiologische Methoden genutzt um die Wahrnehmung ökologisch relevanter Duftstoffe (Komponenten unterschiedlicher Pflanzendüfte oder Pheromone) auf drei verschiedene Weisen zu untersuchen, nämlich in der Peripherie, im AL und mittels olfaktorischer Konditionierung. Wir fanden in beiden Geschlechtern eine robuste Gedächtnisbildung nach absoluter Konditionierung und eine ausgeprägte Generalisierung anhand der Kohlenstoffkettenlänge der präsentierten Duftstoffe. Anders stellten sich die Ergebnisse der elektroantennographischen (EAG) Untersuchungen dar. Hier zeigten sowohl Drohnen als auch Arbeiterinnen neuronale Aktivität mit spezifischen Unterschieden zwischen den Stimuli, aber auch zwischen den Geschlechtern auf, z.B. löste die Applikation von Citronellol eine deutliche verringerte Reaktion in der EAG Aktivität der Drohnen aus. Interessanterweise zeigten auch extrazelluläre Ableitungen im AL stimulus- und geschlechtsspezifische Unterschiede, jedoch in unterschiedlicher Konstellation als in den EAG-Experimenten. Besonders Farnesol und 2,3-Dihydrofarnesol wiesen vor allem bei Arbeiterinnen eine deutliche Repräsentation in der neuronalen Aktivität auf; ein Alleinstellungsmerkmal welches für Farnesol bereits in einer früheren Studie beschrieben wurde. Diese explizit unterschiedliche neuronale Darstellung von Farnesol und 2,3-Dihydrofarnesol in der Peripherie und im AL führt zu der Annahme, dass die rezeptive Darstellung eines Stimulus in der Peripherie keine zuverlässigen Rückschlüsse über die neuronale Repräsentation in höheren Zentren oder die ökologische Relevanz zulässt. Im zweiten Manuskript stehen MBONs der Honigbiene im Fokus, um mehr Einblicke in die visuelle Verarbeitung im VL zu erlangen. Bisher können MBONs in folgende Klassen unterteilt werden: Visuelle, olfaktorische und multimodale MBONs, welche sensitiv für beide Modalitäten sind.

Kern dieser Arbeit ist, mittels extrazellulärer Ableitungen festzustellen, welche zusätzlichen Aspekte eines visuellen Stimulus in diesem zentralen Verarbeitungszentrum repräsentiert

sind. Dabei konnte zum ersten Mal gezeigt werden, dass Informationen über die Wellenlänge und die Intensität des Lichtstimulus im VL erhalten sind. Im weiteren Verlauf konnte eine Spezifizierung der bisherigen Kategorisierung visueller und multimodaler MBONs in drei weitere Untergruppen vollzogen werden: MBONs die spezifisch die Intensität, die Identität und dein Eingang eines Stimulus kodieren. Des Weiteren zeigte vor allem die Gruppe der Identitäts-MBONs eine bemerkenswerte Kategorisierung von UV-Licht. Diese neuen Erkenntnisse bestätigen die Ansicht, dass der MB, als Zentrum für sensorische Integration, eine Kategorisierung der verarbeiteten Eindrücke vornimmt und diese daraufhin auf die MBONs verschaltet wird.

Abschließend diskutiere ich Unterschiede in der peripheren Repräsentation von Stimuli und ihrer späteren neuronalen Verarbeitung. Hier zeige ich, die Aktivität von Farnesol in MS1 und UV-Licht MS2 als Beispiel nehmend, dass die periphere Repräsentation eines Stimulus keine sicheren Schlussfolgerungen über die nachfolgend induzierte neurale Aktivität oder die verhaltensrelevante Bedeutung zulässt. Im weiteren Verlauf werden dabei die Einflüsse konservierter Strukturen und plastischer Änderungen auf die Abläufe der sensorischen Peripherie oder der höheren Verarbeitungszentren, wie dem AL oder dem MB gezeigt. Obwohl der MB, das Zentrum für multimodale Integration und Gedächtnis, hinsichtlich seiner Rolle in der Geruchswahrnehmung ausgiebig erforscht ist, gibt es bezüglich der visuellen Verarbeitung oder dem Einfluss anderer Modalitäten noch ungeklärte Abläufe und Fragen. Wenngleich auch hier die Kenntnis speziell über die visuelle Verarbeitung im MB stetig zunimmt, sollten zukünftige Arbeiten mithilfe weiterer Methoden den MB Eingang und Ausgang explizit auf den Einfluss weiterer Modalitäten untersuchen, um so ein umfassenderes Bild über die Abläufe multimodaler Integration zu erhalten.

"Man is nothing else but what he purposes, he exists only in so far as he realizes himself, he is therefore nothing else but the sum of his actions, nothing else but what his life is."

Jean-Paul Sartre

1 General Introduction

1.1 Sensory perception

Action and decision making is usually proceeded by an evaluation of options and simultaneous interpretation of environmental cues. The interpretation of the environment is a process that is mainly based on the neural integration of the received sensory stimuli. This sensory input often consists of multiple modalities, depending on the receptive repertoire of the respective organism and its surroundings. For example, human sensation comprises the "classic five senses", namely sight, hearing, touch, smell, and taste. Moreover, humans are subconsciously able to receive various additional modalities, e.g. temperature, or body position & balance. The definition of a stimulus or its description is therefore always based on the subjective experience or ability to detect it and thus the comprehension of a stimulus outside of the own receptive range can be challenging. A prominent example for this phenomenon is the perception of visible light. Equipped with a trichromatic vision, humans are able to receive light within a wavelength range from about 400 nm to 700 nm (Wald, 1945). Whenever one tries to comprehend the concept off a differing color perception, e.g. a shifted trichromatic vision like in honeybees (300-600 nm, Dyer et al. 2011) or the dichromatic vision like in most mammals (Li and DeVries, 2006), one is struggling to find matching color attributes or values to describe the difference. The same holds true for the understanding of sensory modalities that cannot be received by humans but are essential for other organisms' perception, e.g. magnetoreception during navigation of various invertebrates and vertebrates (Fleischmann et al., 2018; Mouritsen, 2018) or the orientation of electric fish via electroreception (Moller, 1976; von der Emde et al., 1998). Since this study will mainly address the processing of olfactory and visual stimuli in bees, I will introduce the sensory perception of these modalities in various models and discuss the current state of research and experimental approaches in honeybees and bumblebees.

1.2 Human vision and olfaction

The sensory perception of an organism is highly adapted to its ecology, thus the receptive capabilities of humans and our closest relatives, the primates, are very similar and comprise the same senses. Primates are described to rely heavily on visual cues and evolved a powerful visual sense, especially the mostly diurnal haplorhines (humanoids, old world monkeys, new world monkeys, and tarsiers), the only reported mammal species with a trichromatic vision so

far (Matsui et al., 2010). The visual reception starts at the retina in the eyes, a thin layered tissue that houses photoreceptors. Humans are known to express two types of photoreceptors, i.e. the rods, mainly tuned to low light levels, and the cones, tuned to bright light conditions and especially important for spatial acuity and color vision (Sterling and Demb, 2004). Upon activation, the photoreceptors forward the visual information via bipolar cells to ganglion cells that bundle the information and project to various brain areas, mainly the visual cortex (Soucy et al., 1998; Grill-Spector and Malach, 2004; Do and Yau, 2010). Throughout evolution, human visual perception has become more and more sophisticated, with humans being able to discriminate up to 2.3 million surface colors (Pointer and Attridge, 1998), an accurate discrimination no other species has so far been found to exhibit (Jacobs, 2009). The evolution of this sophisticated trichromatic vision in haplorhines was initially thought to correlate with the degeneration of the olfactory receptor (OR) gene repertoire (Gilad et al., 2004, 2007; Nei et al., 2008), but was later reported to occur gradually across the lineages (Matsui et al., 2010). Moreover, an adapted emphasis of vision over olfaction is also reflected in the formation of the vomeronasal organ (VNO). The VNO is a chemoreceptor organ, occurring in most amphibians, reptiles, and nonprimate mammals and is considered as a key component in pheromone processing (Keverne, 1999; Grammer et al., 2005). Many species of the trichromatic haplorhines, including humans, are reported to either exhibit only an impaired VNO or to lack a functional VNO (Bhatnagar and Meisami, 1998; Keverne, 1999; Smith et al., 2011). Until today, the functionality or condition of the human VNO and thus the ability of humans to perceive pheromonal signals is still under discussion (Keverne, 1999; Grammer et al., 2005). Despite the fact that research often underestimated human olfaction, humans are still relying on this modality to integrate biologically relevant information, especially during sociosexual interactions (reviewed in Grammer et al. 2005). Furthermore, humans were shown to be able to distinguish more than one trillion odors (Bushdid et al., 2014), a discrimination ratio that by far exceeds the visual discrimination ratios mentioned before. To efficiently perceive and distinguish this amount of different olfactory stimuli, humans depend on a broad tuning of their olfactory receptive range. The human genome is found to express up to 388 olfactory receptors (OR), about a third of the number of ORs in mice (1200, Young et al. 2003), rats (1430, Gibbs et al. 2004) or dogs (1070, Quignon et al. 2003). Molecular analyses of the mammalian genome identified the ORs as G-protein coupled

receptors (Buck and Axel, 1991). Located in olfactory receptor neurons (ORN) in the nasal epithelium, the ORs are the binding site for airborne odor molecules. Interestingly, the ORNs are not projecting directly in the environmental air but are instead innervating a fluid-filled space that in turn is directly connected to the surrounding air (reviewed in Ache and Young 2005). This concept of an aqueous intermediate space holds for the later discussed olfactory reception of bees (Foret and Maleszka, 2006) and as well for various other species (Ache and Young, 2005). The binding process of the odor molecules to the ORs can thereby be subject to an interaction with protein complexes in the liquid milieu, especially with so-called odorant binding proteins (OBP). OBPs occur in various classes and are found in the human mucus as well as in various other terrestrial animals, e.g. insects, sheep, pigs, and frogs, suggesting a convergent evolution (Pevsner et al., 1988; Pelosi and Maida, 1990; Briand et al., 2002; Fan et al., 2011). Up to today, the distinct function of OBPs is still under discussion, but OBPs are theorized to modulate the binding of odor molecules in various ways, e.g. binding inhibition, neutralization of components, facilitation of fluid transfer or specific delivery of pheromone compounds (Ache and Young, 2005; Schiefner et al., 2015). Subsequent to the reception of the odor, ORNs convey the olfactory information to mitral and tufted cells located in the olfactory bulb, the first olfactory processing center in mammals. Here, periglomerular cells synapse with ORNs, mitral or tufted cells, and form spheroidal structures, the glomeruli. In the glomeruli, olfactory information is integrated via lateral inhibition of periglomerular cells and granular cells and is subsequently projected to the olfactory cortex (Shepherd, 1972). Independent of their peripheral distribution, ORNs expressing the same OR are found to specifically converge onto one or few glomeruli (mouse: Mombaerts et al. 1996; fly: Vosshall et al. 2000; Wang et al. 2003), resulting in a spatial pattern of odor induced glomerular activity. Since odorants are not restricted to a single OR but are binding to various ORs, each odorant evokes an individual combination of glomerular activity (reviewed in Ache and Young 2005). This spatial combinatorial code in the olfactory bulb is the neural basis for humans to detect trillions of odors despite having only around 400 ORs expressed (Malnic et al., 1999).

1.3 Processing of visual and olfactory stimuli in insects

Worldwide, over one million insect species occur and recent studies estimate additional four million species to be undescribed so far (Stork, 2018). As part of this vast abundance of species and corresponding ecological demands, insect vision has evolved multiple times resulting in

various adaptions. In general, two photosensitive organs, the ocelli and the compound eyes, receive visual input in insects. While the ocelli are shown to project directly to the central brain area, the visual input processed by the compound eyes is conveyed to the optic lobes (Strausfeld, 1976). Depending on their morphology, insect compound eyes can be categorized into three types: apposition, optic super-position, and neural superposition eyes (reviewed in Agi et al. 2014). Compound eyes of all categories are comprised of single units, the ommatidia. The number of ommatidia can range from a few dozens, e.g. in zygentoma (Elofsson, 1970) up to almost 30,000 in odonata (Sherk, 1978). Each ommatidium houses a species-specific number of retinulacells that house layers of microvilli (rhabdomere) expressing the photoreceptors (Land and Fernald, 1992; Hardie and Raghu, 2001; Schwarz et al., 2011). Rhabdomeres of a single ommatidium form the so-called rhabdom, which is fused in both apposition eyes and optic-superposition, with all containing rhabdomeres in direct contact to each other. While small rhabdoms of apposition eyes restrict the visual input only to the own ommatidium, the enlarged rhabdoms of optic super-position eyes receive additional visual input from neighboring ommatidia. This leads to a high spatial resolution during bright light conditions in apposition eyes and to high light sensitivity and low spatial resolution in optic-superposition eyes. As a consequence, these specifications are reflected in an abundance of diurnal insects with apposition eyes and nocturnal insects with optic-superposition eyes (for reviews see: Land and Fernald 1992; Agi et al. 2014). The third category, the neural superposition eye, evolved most likely from the apposition type and has an open rhabdom, with no contact between the single rhabdomeres. The neural superposition eye provides a high spatial resolution without a decrease of light sensitivity. It is most common in brachycera flies, but seems to also have evolved convergently in mosquitoes and march flies (Agi et al., 2014). Photoreceptors of all three categories project further into the optic lobe (OL) and innervate the lamina (LA) where the photoreceptors synapse on interneurons, forming so-called cartridges. Cartridges in the neural superposition eye of the fly comprise receptor axons from all neighboring ommatidia, whereas cartridges in the apposition and optic-superposition eyes contain receptor axons from only a single ommatidium (Strausfeld, 1989). The cartridge-organized architecture in the lamina is found to be maintained in the OL medulla and lobula. Visual information is then further processed in the medulla and the lobula and conveyed to the motor control system or the central brain via projection neurons (reviewed in Kinoshita

and Homberg, 2017).

The reception of olfactory stimuli in insects starts mainly at the antennal level. Here, ORNs innervate several classes of olfactory sensillae that are distributed across the antennal surface. The type and morphology of olfactory sensillae varies widely across insect species and even across sexes of the same species (reviewed in Steinbrecht, 2007). For example, olfactory sensillae of honeybees can be categorized into three types, *Sensilla placodea*, *Sensilla trichoidea*, and *Sensilla basiconica* (Lacher, 1964; Esslen and Kaissling, 1976). In contrast to honeybees, fruit flies have *Sensilla coeloconica* instead of *S. placodea* (Stocker, 2001). In general, insect sensilla exhibit pores in their single or double walled cuticle, which allow odor molecules to enter an aqueous intermediate space. The hydrophilic odorant interacts with OBPs and eventually binds to the OR, a highly conserved concept and convergently evolved with odorant binding processes in vertebrates and humans, as described above (Pelosi and Maida, 1990; Foret and Maleszka, 2006). Whereas various processes and concepts in the olfactory reception and later processing show high similarities between vertebrates and invertebrates, the ORs of insects are fundamentally different from G-protein coupled ORs in mammals and additionally rely on an expression of a co-receptor, the so-called ORCO (reviewed by Zufall and Domingos, 2018). Until today, the exact functioning of ORCO is still under discussion, but it is generally accepted that ORCO has an essential role in the membrane localization of ORs. Furthermore, additional functions of ORCO are still under discussion. For example, ORCO could serve as a modulator of the odor response kinetics or as a key element underlying ionotropic signal transduction in insect odorant reception (reviewed in Stengl and Funk, 2013). After reception of the odorant molecule, ORNs project the information to the antennal lobe (AL), the insect pendant of the mammalian olfactory bulb. Similar to the olfactory bulb, the AL comprises glomeruli, the functional units of the AL. Here, the specific number and consistent position of glomeruli enables a mapping of the glomerular organization for various insect species, e.g. fruit fly, honeybee or cockroaches (reviewed in Anton and Homberg, 1999). Thus, the concept of a spatial combinatorial coding via glomerular activity as described above for humans, applies as well for the insect AL (Hildebrand and Shepherd, 1997; Vosshall, 2000). Identified populations of glomeruli in the fruit fly and the honeybee show specific activity depending on odor identity (Couto et al., 2005; Sandoz, 2006) or odor moiety (Sachse et al., 1999; Paoli and Galizia, 2021). Odor induced activity in the

glomerulus is then integrated by local interneurons and subsequently projected by PNs to the mushroom body and lateral horn via three distinct olfactory pathways, the medial (mALT), the medio-lateral (mlALT), and the lateral antennal-lobe tract (lALT) (honeybee: Mobbs, 1982; sphinx moth: Homberg et al., 1988; fruit fly: Stocker et al., 1990; cockroach: Malun et al., 1993; updated nomenclature: Ito et al., 2014). The mlALT only projects to the LH, whereas the m- and lALT project to both the lateral horn and the mushroom body (MB). The MB, the center of sensory integration and memory formation (Homberg, 1984; de Belle and Heisenberg, 1994; Menzel, 2014) receives its sensory input thereby from multiple modalities, but mainly from the AL and OL. The honeybee calyx is the main input region of the MB and shows a distinct layer specific organization (Strausfeld, 2002). Visual input is projected to the collar region of the calyx, whereas olfactory information is sent to the lip region. In addition, the basal ring area of the calyx receives multimodal, visual and olfactory, input (Strausfeld, 2002; reviewed in Groh and Rössler, 2020). Whereas research in the honeybee MB clearly shows a multimodal integration of olfactory and visual input, studies of the fly MB initially neglected direct visual input to the MB calyx (Strausfeld et al., 2003) or found only a single neuronal process from to the OL to the MB calyces in cockroaches (Strausfeld and Li, 1999). However, later studies confirmed the role of MB calyces as multimodal input region in both flies and cockroaches (Nishino et al., 2012; Vogt et al., 2016). In general, the input of a relatively low number of PNs is diverged widely onto multiple Kenyon cells (KC), the MB principal neurons. The fruit fly for example exhibits around 50 olfactory PNs that diverge onto 2,000 KCs whereas in the honeybee around 900 olfactory PNs diverge onto 180,000 KCs (Groh and Rössler, 2020; Modi et al., 2020). The MB peduncle compartment is formed by the KC axons that send their terminals to the MB lobes, the main output region of the MB, that comprises the medial (ML) and the vertical lobe (VL). Here, KC axons converge heavily onto 34 (fruit fly), respectively ~400 (honeybee) mushroom body output neurons (MBON, Rybak and Menzel, 1993; Aso et al., 2014). The innervation pattern of the KC axons in the MB lobes thereby reflects the layer-specific architecture of the MB calyx, i.e. KC axons originating in a specific calyx region restrict their terminals to a certain layer in the ML or VL (cockroach: Li and Strausfeld, 1999; honeybee: Strausfeld, 2002; fruit fly: Aso et al., 2014). MBONs eventually relay information further along the motor output and behavioral pathway into brain regions like the central complex (fruit fly: Hulse et al., 2021), the contralateral brain hemisphere (Rybak and Menzel, 1993; Strausfeld,

2002) or the superior, intermediate and lateral protocerebral lobes (honeybee: Homberg, 1984; Mauelshagen, 1993; cockroach: Li and Strausfeld, 1997).

1.4 Olfaction and vision in the ecology of *Apis mellifera* and *Bombus terrestris*

Honeybees and bumblebees share a very similar lifestyle that relies heavy on the perception of olfactory and visual cues (Seeley, 1985; Goulson, 2010). Being part of a eusocially-organized colony requires workers in both species to fulfill the various needs of their nest mates and brood. Whereas the division of labor in honeybees is age-related, bumblebees exhibit a polyethism in dependence of the body size, a so-called alloethism (Seeley, 1985; O'Donnell et al., 2000; Goulson, 2010). Nevertheless, both species have common principles in their essential intraspecific communication. Due to low light conditions, the communication in the hive is primarily conveyed via olfactory and mechanic cues (von Frisch, 1965; Dornhaus and Chittka, 2001). Olfactory communication is thereby based on the emission and perception of pheromones and has been studied extensively in insects. In general, pheromones can be divided into two distinct classes: Primer and releaser pheromones. While primer pheromones are shown to change the physiology of the recipient, releaser pheromones are defined to elicit specific behavioral changes (reviewed in Keeling et al., 2004). The most prominent primer pheromone in bees is the queen retinue pheromone (QRP) of honeybees. Two major effects of the QRP are the suppression of fecundity in other sexuals and the inhibition of worker reproduction. In addition, the QRP is acting simultaneously as a releaser pheromone with various behaviorally effects, e.g. attraction of males, swarming behavior or the name giving retinue aggregation (Keeling et al., 2004). In contrast to the well examined QRP in honeybees (Brockmann and Brückner, 2001; Keeling et al., 2004; Sandoz, 2006; Wanner et al., 2007; Mariette et al., 2021), little is known about sex-specific pheromones or their processing in bumblebees. Although early research examined the behavioral context and components of male marking pheromone in several bumblebee species (Bergström et al., 1968; Kullenberg et al., 1970), it took additional 30 years until the behaviorally active compounds of the queen sex pheromone in *B. terrestris* was identified (Krieger et al., 2006). Around that time, research started to re- focus on bumblebee pheromones and pursued earlier interest in bumblebee releaser pheromones, e.g. the specific role of farnesol, a major component in the bumblebee worker recruitment process (Free, 1987; Granero et al., 2005) and also part of the honeybee Nasonov pheromone (Abdullah et al., 1990; Trhlin and Rajchard, 2011). Research that

examines further aspects of olfactory processing in bumblebees is sparse and mainly focused on the role of pheromonal components (Bergström et al., 1968; Kullenberg et al., 1970; Bergman and Bergström, 1997; Krieger et al., 2006). Until today, little is known about sex-specific differences in neural processing along the olfactory pathway or in high-order neuropils like the AL.

The perception of pheromones is of utter importance for the reproductive and trivial communication inside the hive and also for foraging activities, where honeybees and bumblebees were found to specifically tag exploitable flowers with pheromonal scent marks to increase their foraging activity (Stout and Goulson, 2001; Srinivasan and Reinhard, 2009). This naturally occurring association of an olfactory stimulus with a subsequent reward, in this case nectar, represents the cognitive foundation for over a century of extensive research on the memory and learning abilities of honeybees and later as well of bumblebees. Since von Frisch's early studies on the learning and memory capabilities of free flying honeybees, research developed numerous designs of olfactory and visual conditioning experiments to eventually establish the honeybee as model for olfactory behavior, the underlying sensory structures, pathways and physiology, as well as learning induced plasticity (e.g. von Frisch, 1914; Kirschner et al., 2006; Szyszka, 2008; Haehnel and Menzel, 2010; Strube-Bloss et al., 2011; Giurfa and Sandoz, 2012; Groh et al., 2012; Brill et al., 2013; Menzel, 2014; Lichtenstein et al., 2015; Kropf and Rössler, 2018). The analysis of learning and memory capabilities using the bee's proboscis extension response (PER) is one fundamental experimental design that evolved from this period (Bitterman et al., 1983). Here, honeybees and bumblebees are harnessed and undergo a classic Pavlovian protocol during which the animal is forming a temporal association of a novel (conditioned) stimulus (CS) with an unconditioned stimulus (US), mostly sugar. After a series of acquisition trials, the animals will then present a PER upon presentation of the CS. Since honeybees and bumblebees do not only rely on olfactory cues during the foraging process, but also integrate visual cues, PER experiments can thus be adapted to control as well for the perception of visual cues or for a compound comprising both modalities (Lichtenstein et al., 2015; Avarguès-Weber and Mota, 2016; Mansur et al., 2018; Becker et al., 2019). The integration of visual and olfactory cues during the foraging activity is thereby not only restricted to the very detection of valuable food resources by their distinct scent or color pattern (e.g. Peitsch et al., 1992; Lunau, 1993; Heiling et al., 2003;

Srinivasan and Reinhard, 2009), visual and olfactory cues are also used to navigate between the nest and the food source location. Honeybees have therefore been shown to orientate by visual cues like the sun, landmarks, panoramic characteristics, or the pattern of polarized skylight, among others (e.g. Srinivasan and Zhang, 2004; Menzel and Greggers, 2015), but also to use pheromones, like the Nasonov pheromone to guide their nest mates from the hive to the resource and back (reviewed in Srinivasan and Reinhard, 2009). It is assumed that the MB, as the center of sensory integration, is the neural basis for such multimodal integration of visual and olfactory cues. As described in the previous paragraph, the honeybee MB integrates both visual and olfactory input in specific calycal compartments, from where the KCs send their axons downwards in the ML and VL, the main output region of the MB. The layer-structured architecture of the ML and VL reflects the modality specific input of the MB calyx and is distinctly innervated by MBONs. So far, honeybee MBONs have been primarily examined for their role in olfactory processing and learning induced plasticity (e.g. Menzel and Giurfa, 2001; Haehnel and Menzel, 2010; Strube-Bloss et al., 2011). Although some studies showed multimodal activity in MBONs (e.g. Gronenberg, 1987; Mauelshagen, 1993; Rybak and Menzel, 1998; Haehnel and Menzel, 2010), only one study specifically tackled the subject of multimodal processing recently and found several classes of MBONs to code modality specific (Strube-Bloss and Rössler, 2018). However, it remains unresolved how MBONs process visual cues and to what extent specific information about stimulus identity or intensity is encoded in the MB output region.

1.5 Thesis outline

In the course of my dissertation, I am aiming to gain more insights on the processing of behaviorally relevant stimuli at different levels in the bee brain. I will focus on two specific subjects, addressed in the previous chapter:

- Sex-specific processing of olfactory cues in bumblebees

- Visual processing of honeybee mushroom body output neurons

First, I will combine behavioral and electrophysiological approaches to examine the olfactory processing of behaviorally relevant odors in drones and workers of *B. terrestris*. Analyses of proboscis extension response performance, electroantennographic activity and extracellular recordings at the antennal lobe output will be used to elaborate aspects of sex-specific processing in the bumblebee, shown in Chapter 2:

> Manuscript 1: Sex specific processing of olfactory key stimuli in the buff-tailed bumblebee

The second approach comprises of extracellular recordings in the honeybee vertical lobe during stimulation with light of varying wavelength and intensity. I will analyze the processing characteristics of visual and multimodal mushroom body output neurons and identify distinct neural subpopulations according to their response capabilities, shown in Chapter 3:

> Manuscript 2: Categorizing visual information in subpopulations of honeybee mushroom body output neurons

Sex specific processing of olfactory key stimuli in the buff-tailed bumblebee

Fabian Schmalz[1], Thomas Eltz[2], Wolfgang Rössler[1], Johannes Spaethe[1], Thomas Schmitt[3], Martin Strube-Bloss[4*]

[1] Behavioral Physiology and Sociobiology (Zoology II), Biozentrum, University of Würzburg, Würzburg, Germany

[2] Department of Animal Ecology, Evolution and Biodiversity, Faculty of Biology and Biotechnology, Ruhr-Universität Bochum, Bochum, Germany

[3] Department of Animal Ecology and Tropical Biology (Zoology III) , Biozentrum, University of Würzburg, Würzburg, Germany

[4] Department of Biological Cybernetics and Theoretical Biology, University of Bielefeld, Bielefeld, Germany

* Correspondence:
Martin Strube-Bloss
martin.strube-bloss@uni-bielefeld.de

Keywords: Antennal Lobe, Electroantennography, Olfaction, Multi-Unit Recording

This Manuscript is close to publication.

Abstract

The olfactory capabilities of insects have been studied extensively over the past decades. Because of its prominent learning & memory abilities and its olfactory communication via semiochemicals the honeybee is established as a common model in this context. Overshadowed by their popular sister tribe, bumblebees have been mostly neglected in research regarding these topics. This study aims to gain more insights on the olfactory processing of *Bombus terrestris* and specifically examines sex-specific differences in drones and workers. For the first time, we will combine behavioral and electrophysiological approaches to elaborate the processing of behaviorally relevant odors at three distinct levels. Our results show that sex-specific differences in the electroantennographic (EAG) activity are not reflected in the performance during classical conditioning. Here, both sexes exhibit a robust memory formation and generalize towards the carbon chain length of the presented odors whereas EAG activity specifically differs between odors. In addition, extracellular multi-unit recordings in the antennal lobe (AL) output of workers and drones show a distinct representation of farnesol and 2,3-dihydrofarnesol, components of sex-specific pheromones, thus corroborating findings of an earlier study, that found a distinct farnesol activity in the AL of *B. terrestris* workers.

1 Introduction

Honeybees have been studied explicitly over the past decades for their sophisticated olfactory behavior, the underlying sensory structures, pathways and physiology, as well as learning induced plasticity (Kirschner et al., 2006; Szyszka, 2008; Yamagata et al., 2009; Haehnel and Menzel, 2010; Srinivasan, 2010; Strube-Bloss et al., 2011, 2016; Giurfa and Sandoz, 2012; Groh et al., 2012; Brill et al., 2014; Kropf and Rössler, 2018). Despite this general knowledge on olfaction in bees, only little is known about sex-specific olfactory processing in bumblebees. Due to their ecological relevance as key pollinators for a wide range of plant families and climate conditions (reviewed in Parrey et al., 2021), research focusing on bumblebees is of a rising conservational and economic interest. In this study we aim to gain more insight into this topic and examine the effect of behaviorally relevant odors at three distinct stages of olfactory processing. Using behavioral and electrophysiological approaches, we will (i) compare the learning and memory performances, (ii) analyze the peripheral processing at the receptor level, and (iii) examine the neural activity in the AL in bumblebee drones and workers.

Both tribes, the Apini and Bombini, share a very similar ecology and rely heavily on an olfactory perception of environmental cues, e.g. during foraging activities or intraspecific communication (Nunes et al., 2008). These processes can thereby range from a simple association of a nectar reward with a single floral odor up to the challenging identification of intruder bees, by detecting slight differences in their complex cuticular hydrocarbon profiles (Nouvian et al., 2016). To successfully deal with these highly complex challenges in olfactory discrimination, the olfactory system of bees has evolved an elaborate tool kit of chemosensory receptors, olfactory neuropils, and high-order neural centers for the integration of olfactory information and subsequent memory formation or decision-making. Processing of olfactory cues starts in the periphery, at the antennal level. Here, three kinds of olfactory sensilla cover the antennal surface of both honeybees and bumblebees, *Sensilla placodea*, *Sensilla trichoidea*, and *Sensilla basiconica* (Lacher, 1964; Esslen and Kaissling, 1976; Getz and Akers, 1993; Ågren and Hallberg, 1996). These sensillae are innervated by olfactory receptor neurons (ORN) that express the olfactory receptors. In the honeybee, 170 olfactory receptor genes were found, compared to 159 in bumblebees (Robertson and Wanner 2006; Sadd et al. 2015). Bumblebee ORN axons bundle into six antennal-lobe input tracts, four of which (T1-4) specifically innervate glomeruli clusters in the antennal lobe, the first stage of neural

integration of olfactory information (Mertes et al., 2021). This innervation of the AL is very similar to the honeybee's AL architecture, but a detailed description of ORN innervation patterns has so far been only examined for honeybees (Abel et al., 2001; Kirschner et al., 2006). In the spheroidal glomeruli, olfactory information from the ORN conveys for further processing onto local interneurons and projection neurons (PN). PNs project via two tracts, the medial (mALT) and the lateral antennal-lobe tract (lALT) to the lateral horn (LH) and the mushroom body (MB, Müller et al. 2002; Kirschner et al. 2006; Brill et al. 2013), the center of sensory integration and memory formation in the honeybee brain (Homberg, 1984; de Belle and Heisenberg, 1994; Menzel, 2014). Stainings in this study (Fig. 1C) and a recent study in the *B. terrestris* AL (Strube-Bloss et al., 2015) show a very similar pathing of the m- and lALT in the bumblebee. Around 500 PNs of the honeybee lALT and 400 PNs of the mALT innervate specific layers in the calyx region of the MB, namely the lip and the basal ring area, and diverge their information onto kenyon cells (KC), the principal neuron type of the MB (~180,000 per hemisphere, Fahrbach 2006; Groh and Rössler 2020). From here, KCs send their axons downstream along the MB peduncle area, terminating in the main output regions of the MB, the vertical and medial lobe (Strausfeld, 2002; Zwaka et al., 2018). KC terminals synapse with mushroom body output neurons that relay the olfactory information among others into the protocerebral lobes (Homberg, 1984; Mauelshagen, 1993), the contralateral brain hemisphere (Rybak and Menzel, 1993; Strausfeld, 2002), or in case of GABA-ergic feedback neurons, back to the calyx region of the MB (Gronenberg, 1987; Grünewald, 1999; Zwaka et al., 2018).

Given this highly elaborate olfactory system, both honeybees and bumblebees are able to solve complex behavioral tasks and exhibit robust learning and memory capabilities (Giurfa, 2007; Avarguès-Weber et al., 2011; Menzel, 2012). Although many studies on this subject examined free flying or walking animals (von Frisch, 1914; Loukola et al., 2017; Howard et al., 2018; Finke et al., 2021) the most common protocol involves an examination of the proboscis extension response (PER) in harnessed bees. These experiments are based on classical Pavlovian protocol, a temporal association of a novel (conditioned) stimulus (CS) with an unconditioned stimulus (US), in this case a sugar reward. Throughout the experiment, animals will learn to associate the former unappealing CS with the sugar rewards and eventually exhibit a PER upon the presentation of the CS (Bitterman et al., 1983; Giurfa, 2007; Matsumoto et al., 2012). Whereas PER experiments on workers are well established in learning and

memory studies of honeybees and bumblebees (Hammer, 1993; Laloi et al., 1999; Riveros and Gronenberg, 2009; Strube-Bloss et al., 2011, 2016; Giurfa and Sandoz, 2012; Menzel, 2012; Sommerlandt et al., 2014; Avarguès-Weber and Mota, 2016), research focusing on males is sparse. However, it has been shown that drones of both honeybees and bumblebees not only exhibit robust PER performances, but are also capable to keep up with their female conspecifics in terms of learning and memory formation (Nagaraja and Bruckner, 2013; Lichtenstein et al., 2015).

So far, sex-specific differences in olfactory processing of bees are mostly reported at the peripheral level (antennae) and at the first stage of olfactory processing, the AL. At the antennae, drones of honeybees and several bumblebee species are reported to lack a specific class of olfactory sensillae, the *Sensilla basiconica*, but overall, have distinctly more sensillae distributed over the antennal surface (Esslen and Kaissling, 1976; Nishino et al., 2009; Shang et al., 2010; Kropf et al., 2014). Differences in sensillae abundance are thereby reported to increasingly influence activity in the electronantennogram (EAG), i.e. higher numbers of sensillae result in increased EAG amplitudes in drones and young queens (Fonta and Masson, 1984, 1987; Spaethe et al., 2007). Moreover, the AL of honeybee and bumblebee drones shows an overall reduced number of glomeruli and exhibit several distinctly enlarged glomeruli, the so-called macroglomeruli (Arnold et al., 1985; Fonta and Masson, 1987; Sandoz, 2006; Groh and Rössler, 2008; Mertes et al., 2021). Studies in honeybees reported that these macroglomeruli are responding specifically to a major component of the drone mandibular pheromone (Sandoz, 2006; Wanner et al., 2007).

To further unravel sex-specific differences in olfactory processing of bumblebees, we compared odor processing in drones and workers of *Bombus terrestris*. We used odors that have a strong ecological background either as components of floral odors or as major components of key pheromones. On the one hand, we stimulated with citral, citronellol, geraniol and farnesal, widely distributed terpenes that are not only abundant in various floral products but are also found in several species specific pheromone blends (Robacker and Hendry, 1977; Hefetz et al., 1979; Connolly and Hill, 1991; Trhlin and Rajchard, 2011). On the other hand, we presented the animals with farnesol, a pheromone component linked to swarming and aggregation (Free, 1987; Granero et al., 2005; Trhlin and Rajchard, 2011), and 2,3-dihydrofarnesol (DHF), a major component of the drone's sex pheromone and cephalic

secretions (Bergström et al., 1968; Kullenberg et al., 1970; Luxová et al., 2004). In this account, we examined sex-specific odor representation at three stages of the processing along the olfactory pathway. First, we performed PER conditioning experiments to test for memory retention and possible generalization effects. Next, we analyzed physiological data to investigate sex-specific differences in the peripheral EAG activity and finally, we analyzed the activity in the first-order processing center, the AL, towards same odor set to facilitate a comparison of odor separation at both processing levels.

2 Material & Methods

2.1 Animals

All experiments were conducted using buff-tailed bumblebees (*Bombus terrestris*). Bumblebee colonies were commercially obtained from Koppert B.V. (Berkel en Rodenrijs, the Netherlands) and kept under constant conditions (25°C, light dark cycle: 12h/12h, humidity: 70%). Dried pollen and sugar solution (Apiinvert, Südzucker AG, Mannheim, Germany) were provided ad libitum.

2.2 Behavioral experiments

Animals

Animals were captured the day before the experiments, chilled and carefully harnessed in plastic tubes by means of paper clips and adhesive tape (as described by Sommerlandt et al. 2014; Lichtenstein et al. 2015). Harnessed bumblebees were fed 30 % sucrose solution and kept overnight in an incubator (temperature: ~ 25°C; relative humidity: ~ 75%). All bees were tested for a PER prior to experimental on-set, by carefully touching the antennae with sucrose solution (50 %). Only bees that showed an intact PER were taken for the subsequent conditioning processes. Male bumblebees could be easily distinguished from females based on their bearded mandibles.

Olfactory stimulation

A semi-automated stimulus controller (Stimulus Controller CS-55, Syntech, Hilversum, the Netherlands) lead a permanent air stream (1 l/min) through a Teflon tube that pointed at the animal's antennae. Two additional channels were alternately supplied by the stimulus generator with a second, constant air stream (0.5 l/min) and entered the Teflon tube

(diameter: 8 mm), merging both air streams. Both channels were equipped with 1 cm² filter paper, containing either 10 µl pure paraffin oil or 10 µl odor-paraffin-mixture. During stimulation, the stimulus controller automatically switched the air stream from the paraffin-loaded channel to the odor-loaded channel. In doing so, we guarantee a constant air stream at the antennae and prevent volume or airspeed alterations that could elicit physical artifacts. To prevent olfactory accumulation and guarantee fresh air conditions prior to each trial, a suction device was mounted behind the stimulation site, opposite to the Teflon tube. We tested six different odors and decided to use an odor concentration of 1/100 (odor/paraffin oil) following preliminary experiments (not shown) and previous studies (Brill et al., 2013; Sommerlandt et al., 2014; Lichtenstein et al., 2015)

Absolute conditioning & retention test

The conditioning protocol for both sexes followed the established methods for paired and unpaired conditioning in previous studies (Sommerlandt et al., 2014; Lichtenstein et al., 2018). Animals were placed on a mobile slider and positioned in front of a fume hood. Each subject was granted 20 s of adaption time, after which the odor stimulus (conditioned stimulus, CS) was applied for 6 s. With a delay of 3 s to the odor on-set, the animal's antennae were touched with a sucrose wetted toothpick (unconditioned stimulus, US), and the animal was subsequently allowed to lick the solution (50% sugar solution) for further 3 s (paired conditioning). A second resting stint of 15 s closed each conditioning trial. As a control group to the paired conditioning, CS and US were presented separately to the so-called unpaired group, 10 times per stimulus in a random order. Due to the temporal separation of the CS and the US, unpaired bees underwent the double amount of acquisition trials to reach 10 trials for both, the CS and US. PER during odor application and before sucrose offering was counted as a positive response.

Memory and generalization tests started 1 hour after the absolute conditioning trials. Reactivation of the bees prior to the memory retention test with a sugar reward followed the procedures as described by Lichtenstein et al. (2015). Bees that did not respond to the presented sugar reward with an active PER were excluded from the subsequent retention test. In addition to the CS at least three novel, unpresented odors were tested once, using the same stimulation and resting intervals. With this, we not only exclude an unspecific conditioning

effect of the reactivating US prior to the tested CS but also test at the same time for a possible generalization of the presented test odors and the CS towards specific molecule characteristics like the carbon chain length or functional groups.

Analysis

Analysis and statistics were performed in MATLAB, using the 'Statistics and Machine Learning' toolbox and the pval_adjust function (Fachada and C. Rosa, 2018). Statistics for acquisition trials and memory retention tests was based on the sum of all animal's single responses to the CS or the novel odors (retention test). A chi^2 test was used to test the significance between paired & unpaired groups during acquisition trial 10. Comparison of PER performance between all odors during retention tests also used chi^2 tests for all pairings. P-values in retention test matrices were corrected using the Benjamini-Hochberg method in the pval_adjust function (Table S6/S7). Chi^2 testing of the C10 vs. C15 comparison and the aldehyde vs. alcohol comparison was corrected using a Yates correction, whenever expected cell frequencies were below 10 (Table S7/8).

2.3 Electroantennography

Animals

Animals were captured in the morning, chilled prior to the experiment, and subsequently decapitated. Heads were carefully fixed with dental wax and a specific low melting point paraffin wax (eicosane, Sigma-Aldrich, Taufkirchen, Germany) was used to adjust the antennae position in a way that enables an unobstructed exposition of the flagellum to air streams (Fig. 1A).

Olfactory stimulation

Olfactory stimulation followed the setup of a semi-automated odor stimulation via a stimulus generator as described in 2.2., including usage of the same odors and concentration levels. Stimuli were presented three times per odor, in a pseudo-randomized order (random, but not more than two presentations of the same stimulus in a row). Stimulation lasted 500 ms and was followed by an inter-stimulus-interval of 60 s (Fig. 1A).

Electrophysiology

Recording electrodes were pulled from thin-walled glass capillaries (1B100F-3, WPI, Sarasota, USA) with a DMZ-Universal puller (Zeitz-Instruments, Martinsried, Germany) and filled with KCl solution (0.1 M). To implant the electrode, we cut off the apical segment of the antenna flagellum and inserted the electrode in the opened second segment (Fig. 1A). A silver wire (AG-8T, Science-Products, Hofheim, Germany) was inserted as reference electrode posteriorly in the head capsule. The signal was tenfold amplified (Neuroprobe Amplifier 1600, A-M Systems, Sequim, USA), filtered to reduce 50Hz noise (Kemo VBF 8, Kemo Inc., Greenville, USA) and eventually digitized via an acquisition board (Labtrax 4/16, WPI, Sarasota, USA). Data was sampled at a rate of 1 kHz using the software LabScribe 3 (iWORX, Dover, NH, USA) and recorded from only one antenna per animal.

Analysis

Analysis and statistics were performed in MATLAB, using the 'Statistics and Machine Learning' toolbox (MathWorks, Natick, MA, USA) and the raacampbell/shadedErrorBar function (see Key resources table). To facilitate a robust response detection we split neural activity in 100 ms bins and tested each bin during stimulation against baseline bins (Fig. 2A/B). Activity was classified as responding when at least one bin during stimulation varied significantly to pre-stimulus bins (Fig. 2C, ANOVA for repeated measurements, followed by a Tukey-Kramer post hoc test, $p < 0.05$). EAG analysis is obtained from animals that responded at least to one of the six presented odors. Subsequent to response detection, raw data was multiplied by -1 and baseline corrected by subtracting the mean activity 500 ms before stimulus on-set from the full recording. Maximum activity was calculated during the first 1000 ms after stimulus on-set and averaged across all three trials per stimulus. Next, data was organized in stimulus-dependent population vectors to allow evaluations of the Euclidean distances (ED) and principal component analysis (PCA). EDs (L^2-Norm) were calculated using a pairwise subtraction of a population vector couple ($v^a - v^b$) as $d(t) = (\sum (v_i^a (t) - v_i^b(t))^2)^{1/2}$.

2.4 Antennal lobe recordings

Animals

Animals were captured in the morning and harnessed as described in 2.3. In addition, head capsules were fixed by strong dental wax (Deiberit 502, SILADENT Dr. Böhme & Schöps GmbH, Goslar, Germany), while the antennae were fixed by specific low melting point wax, as described in 2.3. This preparation prevented head movement, while full mobility in the proboscis was preserved and thus the ability to show an unimpaired PER. Access to the AL area was obtained by a small cut in the head cuticle and removal of glands, trachea and neural sheath above the AL, as described by Strube-Bloss et al (2015).

Olfactory stimulation

Stimulation was fully automated using Trial Control Software (Neuralynx Inc., Bozeman, MT, USA) with customized scripts, linked to a Neuralynx acquisition system unit (DL 4SX 16ch System, Neuralynx Inc., Bozeman, MT, USA) that operated seven opto-couplers which connected to solenoid valves in a 7-channel, custom-made olfactometer (adapted from Galizia et al. 1997; Strube-Bloss et al. 2011). The olfactometer was used to present seven odors, as it has been described in Schmalz et al. (2022). In short, a constant, humidified air stream (25 ml/s) was led through a Teflon tube (diameter 10 mm) and 7 pairs of channels, gated by solenoid valves (LEE HDI 3 Port, LEE Hydraulische Miniaturkomponenten GmbH, Sulzbach, Germany). Each channel pair consisted of an empty and a loaded channel (1 cm² filter paper, 10 µl odor solution) that both eventually connected to the Teflon tube, pointing at the animal's antennae. Stimulation was achieved by an on-set of a solenoid valve, which then subsequently switched the airstream from the empty channel to the odor loaded one for 3 seconds. We presented all odors in a pseudo-randomized order, 10 times per stimulus, and with an inter-stimulus-interval of 60 s (Fig. 1B). Odor dilution levels followed mixtures as described in 2.2.
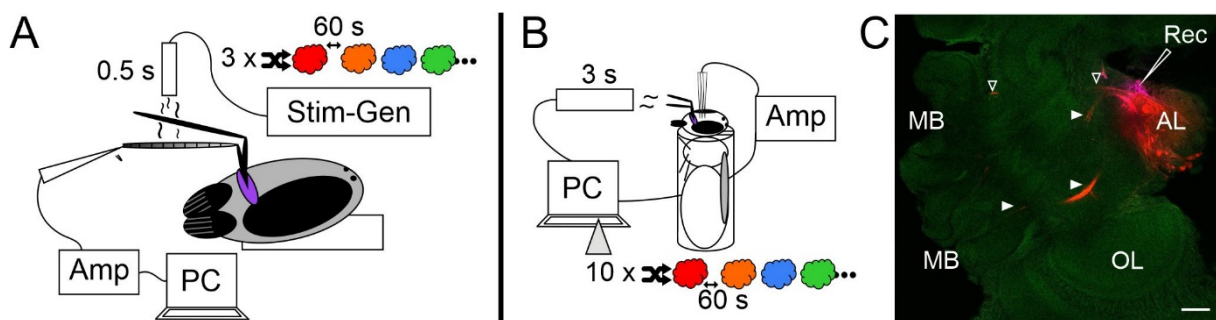
Figure 1. Electrophysiological recordings at two olfactory processing levels. A: Electro-antennographic recordings. Bee heads were fixated on a plastic holder, the antennae were immobilized by dental wax (purple spot at the antennal base), and positioned in front of an air stream. The recording electrode was inserted in the second apical segment of one antenna and the signal subsequently amplified. A silver wire was inserted as a reference in the back of the head capsule (not shown). Detailed stimulation protocol in 2.3. **B:** Extracellular multi-unit recordings. Bees were harnessed in plastic tubes, heads were immobilized by strong dental wax, and the antennae positioned as described in A. The recording triode was inserted at the output region of the lALT and mALT, as shown in C. A silver wire was used as a reference and was positioned in the dorsal region of the head capsule (not shown). Detailed stimulation protocol in 2.3. **C:** Triangle tip marks position of the recording triode (Rec) at the output area of the AL (pink staining). Arrowheads indicate position of the lALT and the mALT (filled: lALT, unfilled: mALT). Abbreviations: Amp: Amplifier, Stim-Gen: Stimulus generator, MB: Mushroom Body, OL: Optic lobe, AL: Antennal lobe, lALT: lateral antennal-lobe tract, mALT: medial antennal-lobe tract, Rec: Recording electrode.

Electrophysiology

Building and implantation of triodes was based on methods of earlier studies (Strube-Bloss et al., 2011; Brill et al., 2014). Three polyurethane insulated copper wires (P155, Elektrisola, Reichshof-Eckenhagen, Germany) were bundled using dental wax (64103015S1 Pinnacle, DeguDent GmbH, Hanau, Germany). Each single wire was connected to an electrode interface board (EIB-18; Neuralynx Inc., Bozeman, MT, USA) that was mounted on a customized electrode holder. Each single electrode channel was checked for an impedance value between 1.5-2.5 MΩ, using a nanoZ kit (Multi Channel Systems MCS GmbH, Reutlingen, Germany). Signals were pre-amplified by a head stage (HS-16, Neuralynx Inc., Bozeman, MT, USA) and subsequently digitized. We performed an online, pair-wise subtraction of all three channels to decrease global noise and electric artifacts (differential recording), using implemented tools of the Cheetah acquisition software (Cheetah 6.4, Neuralynx Inc., Bozeman, MT, USA). Activity was high-pass filter (above 300-400 Hz) and recorded at a sampling rate of 30 kHz. A silver wire (AG-8T, Science-Products, Hofheim, Germany) was inserted as reference electrode in the hemolymph of the posterior head capsule. The triode was inserted at the dorsal rim of the AL, close to the output region of the mALT and lALT, at a depth between 150 and 400 µm (Fig. 1C). The brain was subsequently sealed with two component, surgical silicon (KWIK-SIL Sarasota, FL, USA) to prevent the brain tissue from desiccation and to stabilize the triode position.

*Visualization of electrode position*

Prior to the recording, the triode was immersed in ALEXA 647 Hydrazide (A20502, Thermo Fisher Scientific GmbH, Dreieich, Germany). After the experiment, we removed the triode and injected micro-Ruby in the AL, using a glass electrode. Specimen were kept in a moist, dark chamber for 2-3 hours at room temperature, with the head openings covered. Following this, we dissected the brains out of the head capsule, removed remaining trachea tissue and transferred the brains in a fixation buffer. Fixation took place overnight in a 4% formaldehyde/phosphate-buffered saline (PBS), under dark conditions at 4°C. On the next day, brains were washed in PBS (5 x 10 min), permeabilized in 0.2% Triton X-100 (Tx) in PBS (2 x 10 minutes), and subsequently blocked in 2% normal goat serum (NGS; 005-000-121, Jackson ImmunoResearch Laboratories, West Grove, PA) in 0.2% PBS-Tx, for 1 hour at room temperature, as described in Groh et al. (2012). Synapsin labeling followed the instructions of Groh and was conducted with the primary antibody SYNORF1, diluted 1:10 in 0.2% PBS-Tx with 2% NGS and an incubation time of 4 days at 4°C. After another stage of rinsing in PBS (5x 10 minutes), brains were incubated in Alexa Fluor 488–conjugated goat anti-mouse secondary antibody (1:250) in 1% NGS-PBS for three more nights at 4°C. Brains were then washed 3 x 10 min in PBS and dehydrated in an increasing ethanol series (30%, 50%, 70%, 90%, 95%, 2x100%; 10 min each). Methyl salicylate was used to conduct the subsequent clearing and mounting of the brains in customized aluminum slides. Brain preparations were scanned with a confocal microscope (SP2, Leica, Wetzlar, Germany) under a 10x water immersion objective.

Spike Sorting

Neural activity was sorted using the semi-automatic spike sorting tools of Spike2 (Cambridge Electronic Design, Cambridge, UK) as described in previous studies (Strube-Bloss et al., 2011, 2012). Spike sorting was conducted either on single channels or simultaneously on multiple channels. All recorded events above threshold (± 3 x standard deviation above baseline) were grouped and matched to fitting templates, based on waveform and amplitude characteristics. Furthermore, we used principal component analyses (PCA) to check for a clear separation and accuracy of the assignment and, additionally, excluded all groups containing inter spike intervals below 1 ms. Timestamps of template assigned spikes were then exported to MATLAB.

Analysis, statistics, and response detection (Fig. 2, bottom panels) were performed as described in 2.2. All analyzed data was baseline corrected by subtracting the mean activity 500 ms before stimulus on-set from the full recording. In contrast to analysis performed in 2.2, the calculation of the maximum activity was restricted to the first 500 ms after stimulus on-set, but averaged across all 10 trials per stimulus. PCA and analyses of Euclidean distances followed the procedures described in 2.2.
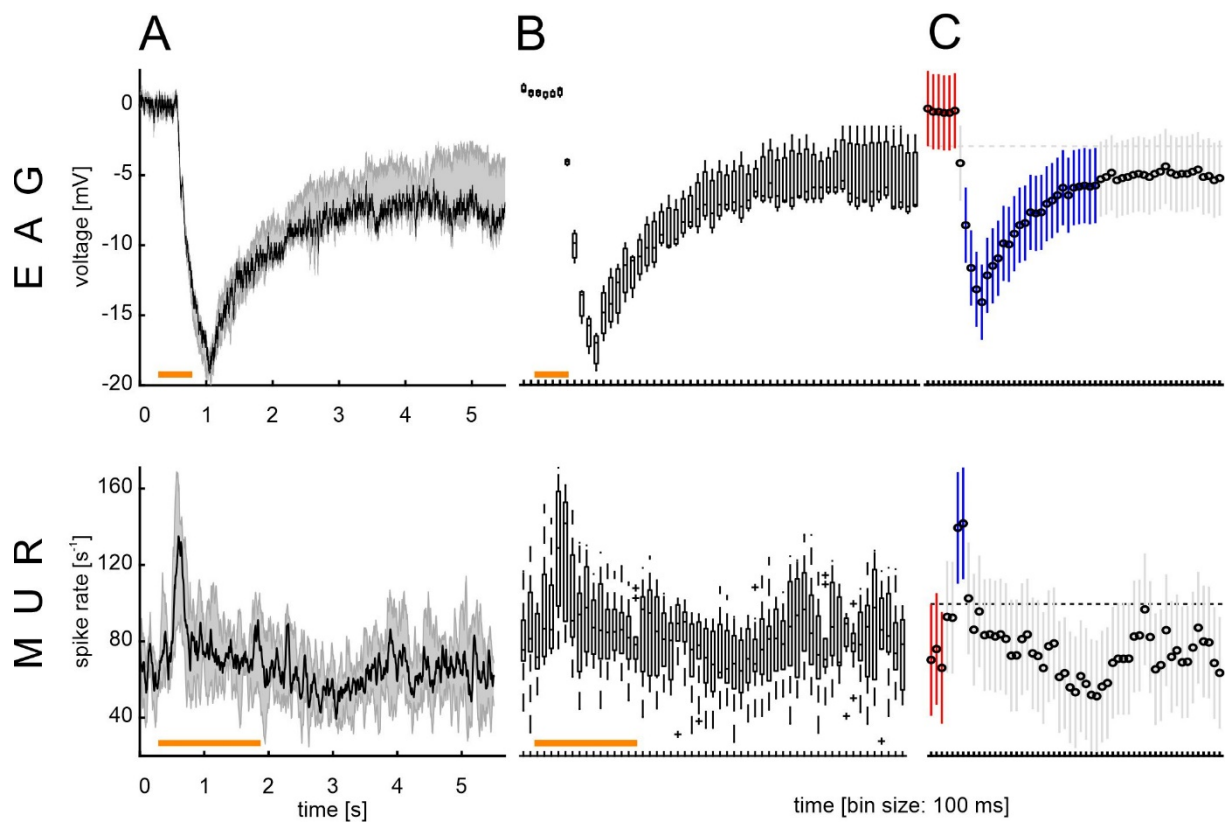
Figure 2. Exemplary neural activity and response detection. A: Top panel shows mean (black line) electroantennogram (EAG) of one exemplary bee towards citral. Stimulus starts at 250 ms and lasts for 500 ms (orange bar). Bottom panel displays spike activity during multi-unit recordings (MUR) at the AL output. Stimulus starts at 250 ms and lasts for 3 s. Shaded grey area represents standard deviation. **B:** Boxplots represent mean activity from A, split in 100 ms bin. **C:** Evaluation of response detection. Bins during stimulation window are analyzed for significant variances to base activity (red). Blue marked bins display detected responses (repeated measurements ANOVA, $p < 0.05$, post hoc test: Tukey Kramer, $p < 0.05$).

Key resources table

Substance

Farnesol	CAS RN 4602-84-0
Farnesal	CAS RN 19317-11-4
2,3 Dihydrofarnesol	CAS RN 37519-97-4
Citronellol	CAS RN 106-22-9
Citral	CAS RN 5392-40-5
Geraniol	CAS RN 106-24-1
Paraffin oil	CAS RN 8012-95-1
Potassium chloride	CAS RN 7447-40-7
ALEXA 647 Hydrazide	A20502, Thermo Fisher Scientific GmbH, Dreieich, Germany
SYNORF1	E. Buchner, University of Würzburg
Alexa Fluor 488–conjugated goat anti-mouse secondary antibody	A-11001, Molecular Probes, Eugene, OR, USA
Micro-Ruby	D7162, ThermoFisher Scientific, Dreieich, Germany
NGS Mouse	005-000-121, Jackson ImmunoResearch Laboratories, West Grove, PA, USA
Methyl salicylate	4529.1, Carl Roth, Karlsruhe, Germany

Matlab function

raacampbell/shadedErrorBar	Rob Campbell, 2022. https://github.com/raacampbell/shadedErrorBar, GitHub. Retrieved March 3, 2022.
Pval_adjust	Fachada and C. Rosa, 2018

3 Results

Behavioral data shows odor generalization based on molecule size

Absolute conditioning of bees in both sexes resulted in successful associations of all tested odors with an unconditioned stimulus. Both groups showed significant differences in PER rate between paired and unpaired conditioning after ten acquisition trials to all tested odors (Fig. 3A/B, left panels). No specific differences between the conditioned odors where found.
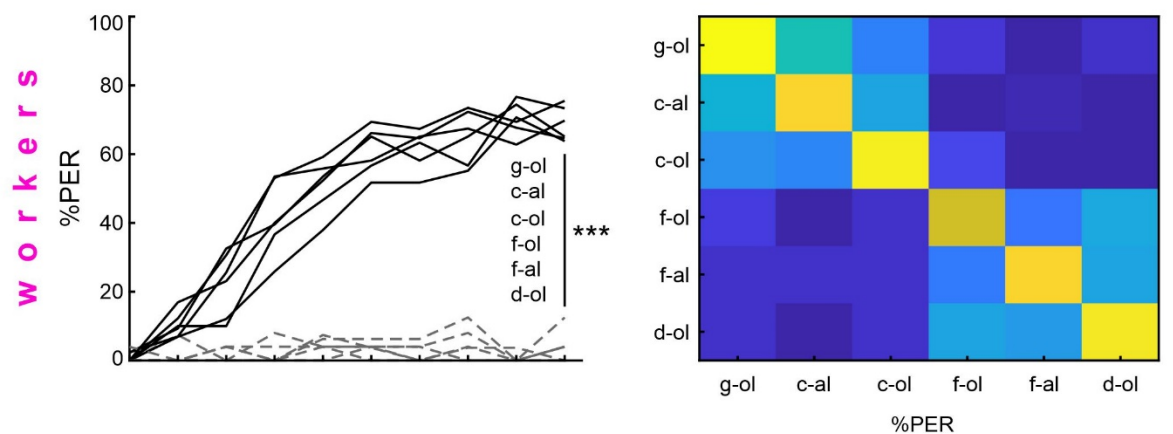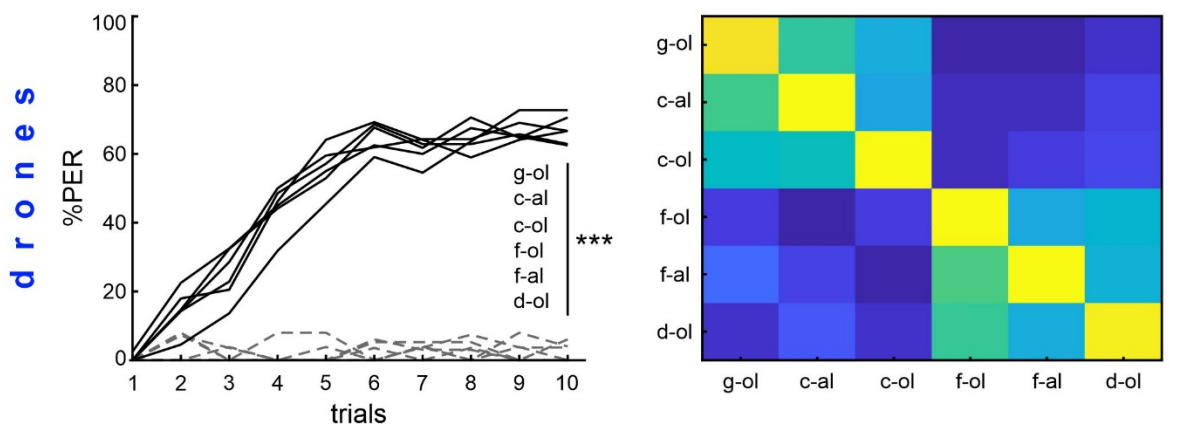

Figure 3. Absolute conditioning and memory retrieval. A: Left panel shows PER rate of bumblebee workers during absolute condition to six presented odors along ten acquisition trials. Bees underwent paired (solid line) and unpaired (grey, dashed line) conditioning to the CS (Chi² test: ***, p < 0.001). Right panel shows memory retrieval test after one hour. Bees were tested for the CS and unconditioned odors. Matrix shows memory test of all stimuli against each other. Color-coding reflects low PER rates in blue and high PER rates in yellow. **B:** Acquisition trials of absolute conditioning and retention test matrix of bumblebee drones, as explained for workers in A. Abbreviations: f-ol: farnesol, d-ol: 2,3-dihydrofarnesol, f-al: farnesal, c-ol: citronellol, g-ol: geraniol, c-al: citral. For detailed statistics see table S1-4.

Retention tests after one hour confirmed a robust memory formation and bees showed high percentages of PER to conditioned odors in contrast to novel test odors. A comparison matrix of the retention rate (Fig. 3A/B, right panels) displayed an additional generalization towards odor molecule size. Depending on the molecule size of the CS, novel odors, sharing the same carbon chain length, triggered positive PER significantly more frequent than novel odors of the second presented terpene class (Fig. 4).
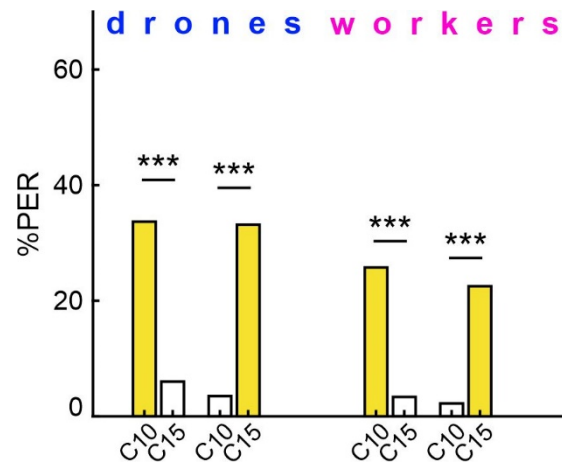

Figure 4. Molecule size dependent generalization during retention test. Both drones and workers exhibit a significant generalization of the PER to novel odor molecules sharing the same carbon chain length as the CS. Bars show averaged PER to all presented novel stimuli, grouped in C10 (monoterpenes) and C15 (sesquiterpenes) odors. Yellow filled bars indicate carbon chain length of the rewarded CS. Chi² test: ***, $p < 0.001$. For detailed statistics see table S5 & S6.

Odor detection at the antennal level is dominated by molecule size

In total, we analyzed EAG data from 24 bees, 11 drones and 13 workers. Animals from both sexes responded reliably to all presented stimuli and showed distinct EAG amplitudes in response to specific odors (Fig. S1). Analysis of the EAG levels between both sexes found no significant differences, except for a significantly lower citronellol activity in the drone population (Fig. 5A). However, the mentioned odor specificity appearing in both sexes is due to a generalization pattern based on odor molecule size (Fig. 5B). Both sexes exhibited significantly higher EAG signals to presented monoterpenes (citronellol, geraniol, and citral) compared to the sesquiterpenes (farnesol, DHF, and farnesal). Although a pooled analysis of the drone-specific data only showed a tendency for a difference between the sesqui- and
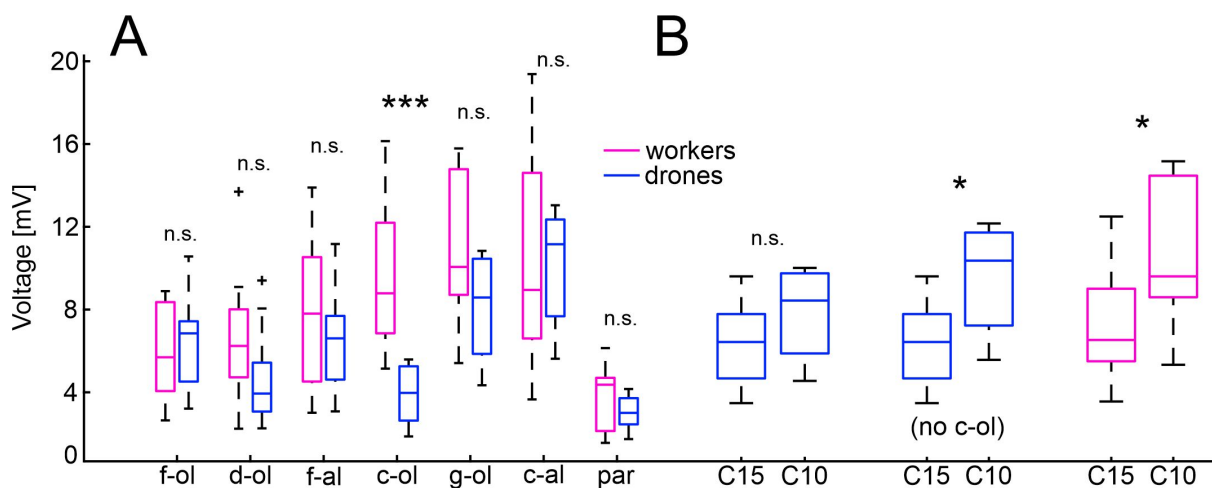
Figure 5. EAG activity A: Maximum EAG amplitudes during first 1000 ms after stimulus on-set is shown for both sexes. No difference between worker (n = 13, magenta) and drone (n = 11, blue) activity was found, except for stimulation with citronellol (Wilcoxon rank sum test, ***, p < 0.001). **B:** EAG data was pooled in regards of molecule size. A significant generalization due to molecule size was found in both sexes. Large sesquiterpenes (C15, sesquiterpenes, containing 15 carbon atoms) evoked significantly lower EAG activity than smaller monoterpenes (C10, monoterpenes, containing 10 carbon atoms). Pooling of drone data showed only significant differences after exclusion of citronellol activity. Wilcoxon rank sum test: Drones: C15/C10: p = 0.1007, C15/C10 no c-ol: p = 0.0086, Workers: C15/C10: p = 0.0159 p. Abbreviations: f-ol: farnesol, d-ol: 2,3-dihydrofarnesol, f-al: farnesal, c-ol: citronellol, g-ol: geraniol, c-al: citral, n.s.: not significant.

monoterpene evoked activity, an exclusion of the specific citronellol activity resulted in a significant difference in EAG amplitude, as already occurring in the workers' EAG responses.

Neural processing in the AL output reflects behavioral relevance rather than molecule size

In total, we recorded 27 AL neurons in 10 drones (11 AL neurons) and in 16 workers (16 AL neurons). All examined units responded with a significant increase in spike rate during stimulus on-set to at least one of the presented stimuli. Despite the fact that analyses of the averaged maximum spike rates during stimulus onset found neither intra- nor intersex-specific coding patterns (Fig. 6A/B), principal component analyses (PCA) of the averaged population activity showed stimulus specific activity in both sexes towards certain stimuli. Here, although all presented odors are uniformly processed in PC1 in both groups, PC2 displays specific activity of farnesol and DHF. Both sesquiterpenes exhibit distinctly different neural activity, especially after stimulus onset when the firing pattern transitions from a phasic onset into a tonic state (Fig. 6C/D). Evaluation of the Euclidean distances (ED) between all presented odors and the paraffin control showed stimulus specific discrimination rates in the EAG data for both sexes (Fig. 7A). Here, ED analyses of the EAG activity reflect the specifically low EAG

amplitudes of citronellol in drones and of farnesol in workers, shown in Fig. 5. Interestingly, ED analysis of the extracellular recordings in the AL revealed a specific processing of farnesol in workers, but not in drones (Fig. 7B).
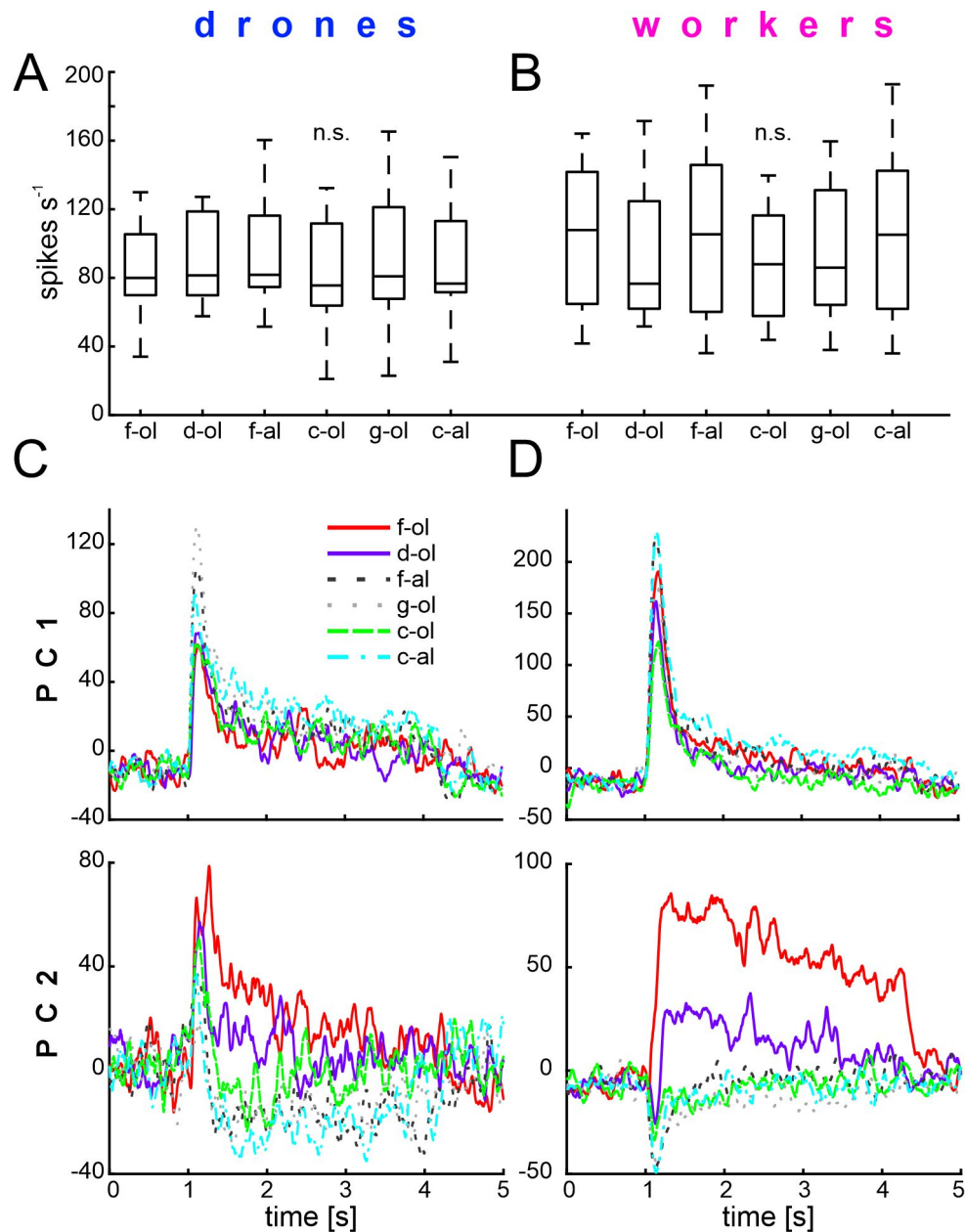
Figure 6. Neural activity in AL neurons. A: Maximum spike rate of drones AL neurons (n = 11) during 500 ms after stimulus onset. No odor specific tuning was found for any of the six tested odors (repeated measurements ANOVA, post-hoc test: Tukey-Kramer, p > 0.05). **B:** Activity of AL neurons of worker bees (n = 16) as described for A. Maximum AL spike rate of worker bees shows no stimulus specific coding. **C:** Principal component analyses (PCA) of the population activity of drone AL neurons. Top panel shows first component of the PCA (representing 40 % of the variance in the data), bottom panel depicts second component of the PCA (20 % of variance in the data). Stimulus starts at 1 s and lasts 3 s. **D:** PCA of neural activity of AL neurons of workers, as explained in C. PC1 explains 48 % and PC2 18 % of variance in the data. Abbreviations: f-ol: farnesol, d-ol: 2,3-dihydrofarnesol, f-al: farnesal, c-ol: citronellol, g-ol: geraniol, c-al: citral, n.s.: not significant.
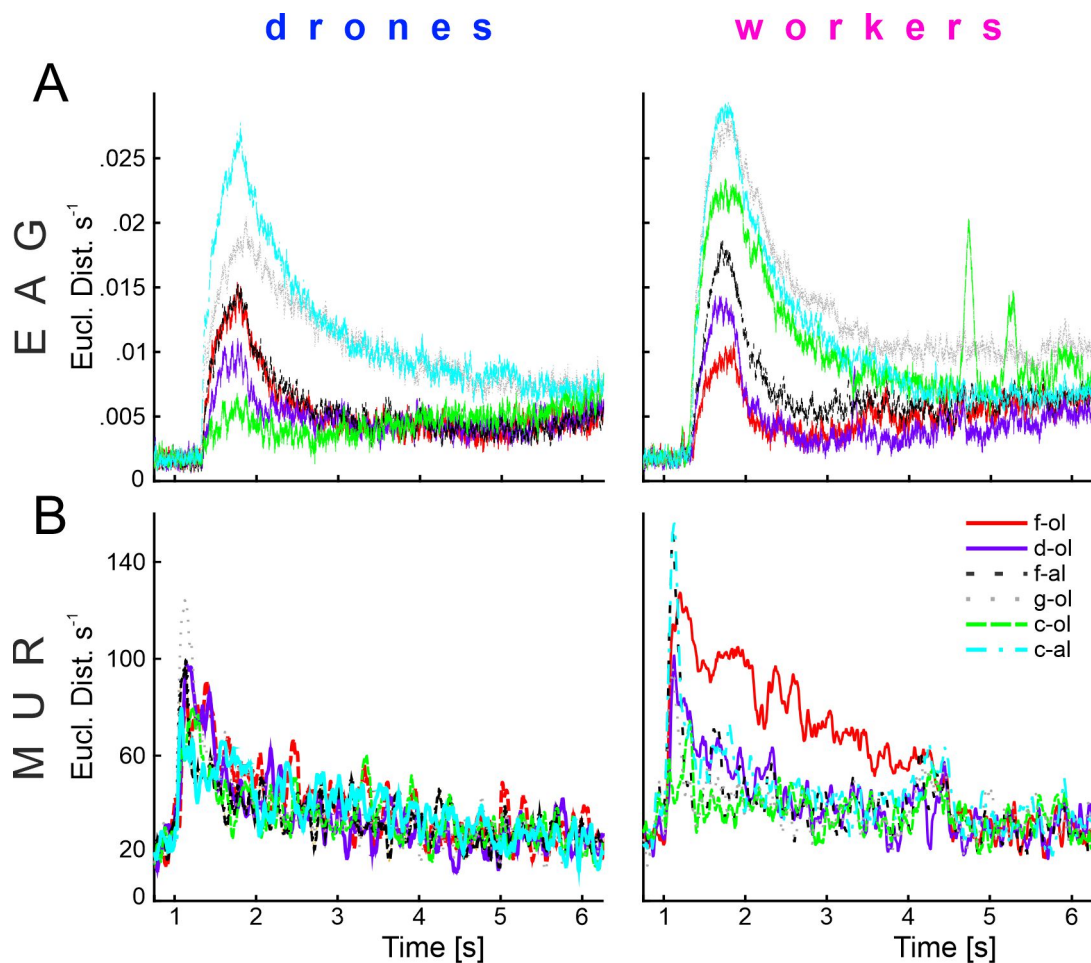
Figure 7. Temporal odor discrimination through the olfactory pathway. A: Pair wise Euclidean distances of EAG activity between all presented odors and the control. Left panel shows discrimination levels in drones (n = 11), right panel shows discrimination levels in workers (n = 13). Stimulus starts at 1 s and lasts for 500 ms. Discrimination of citronellol (green) is distinctly more pronounced in workers than in drones, while farnesol (red) shows a similar rate of discrimination in both sexes. **B:** Pair wise Euclidean distances for AL output activity as explained in A. Left panel shows discrimination levels in drone AL neurons (n = 11), right panel shows discrimination levels in worker AL neurons (n = 16). Note: Although Farnesol shows the lowest discrimination to the control in the EAG data, it shows prominent separation in AL-population activity. Stimulus starts at 1 s and lasts for 3 s. Abbreviations: f-ol: farnesol, d-ol: 2,3-dihydrofarnesol, f-al: farnesal, c-ol: citronellol, g-ol: geraniol, c-al: citral, EAG: Electro-antennography, MUR: multi-unit recording.

4 Discussion

Our trichotomous approach to examine sex-specific differences in the olfactory processing of bumblebees comprised a combination of behavioral experiments and electrophysiological recordings at two subsequent stages, in the sensory periphery (antennae) and in the AL. (i) While our behavioral approach showed a strong generalization of the presented stimuli based on their chemical structure in both sexes, (ii) recordings in the periphery found a sex-specific processing of citronellol, but neither of farnesol nor of DHF. (iii) Most interestingly, analyzes

of neural activity in the AL revealed distinct sex-specific differences in processing of these components and showed high rates of discrimination specifically for farnesol (Fig. 6 and 7), thus suggesting that the separation of behaviorally relevant stimuli is initiated in the AL neural network.

Olfactory generalization due to chemical structure

Olfactory generalization in insects (Laska et al., 1999; Daly et al., 2001; Guerrieri et al., 2005) and vertebrates (Imamura et al., 1992; Katoh et al., 1993; Linster and Hasselmo, 1999; Laska and Hübener, 2001) has been extensively investigated and revealed strong evidence for a correlation between odor generalization and chemical structure of the respective odors. Odors that share similar carbon chain lengths (CCL) underlie generalization effects significantly more often than odors with distinct differences in the CCL. The present PER experiments also confirm this concept for bumblebees and additionally show no sex-specific differences between drones and workers to any of the presented stimuli (Fig. 3, right panels; Fig. 4). Interestingly, the generalization effect of the CCL is reported to be of a linear nature, i.e. the lower the number of differing carbon atoms is, the higher is the rate of generalization (Laska et al., 1999; Daly et al., 2001; Guerrieri et al., 2005). Furthermore, honeybees show robust rates of generalization in regard to molecule moiety. Odors that share the same functional groups, like alcohols (present study: geraniol, citronellol, farnesol, DHF) or aldehydes (present study: citral, farnesal) elicit significant generalization effects (Vareschi, 1971; Smith and Menzel, 1989; Guerrieri et al., 2005). However, this moiety dependent generalization is shown to increase with high CCL but holds true only within a certain range of CCL differences of the processed odors. Whenever the CCL size difference of the compared molecules exceeds a certain level, the moiety induced generalization effects decline and the CCL impact dominates the generalization pattern (Guerrieri et al., 2005). These effects already reach significant levels by size differences of two carbon atoms in honeybees (Guerrieri et al., 2005) and are in line with the results found in this account. The presented mono-and sesquiterpenes exhibit CCL differences of five carbon atoms and neither drones nor workers showed a generalization towards a functional group (Fig. S3), but consistently generalized according to the CCL. To clarify a potential olfactory generalization based on odor moiety in both sexes of *B. terrestris*, future experiments should include a comparison of odors with closer CCLs and various classes of functional groups.

Artificial generalization and sex specific activity in the periphery

In addition to the olfactory generalization found in the PER experimental series (Fig. 4), we found in both sexes a similar neural generalization of mono- and sesquiterpenes in the periphery (Fig. 5B). In contrast to the perceptual generalization described for the PER conditioning, we assume this peripheral CCL effect to be correlated to physical artifacts, for example originating in differing vapor pressures of the presented odors (e.g. citronellol: 2.00e-2 [mm Hg], farnesol: 3.94e-5 [mm Hg], see Table S9). Since we performed extracellular recordings of multiple ORNs and our olfactory stimulation was not corrected for equalized molecule number per volume (compare Fonta and Masson, 1984), odor specific vapor pressures will directly influence molecule numbers at the antennal ORNs and thus the total EAG activity. The significant variances between the EAG amplitudes of monoterpenes (citronellol, citral, geraniol) and sesquiterpenes (farnesal, farnesol, DHF) are therefore most likely caused by a reduced number of evaporated C15 molecules. However, sex-specific differences occurring within the same class of terpenes stay uncompromised from such vapor pressure induced effects.

The most striking sex-specific difference we found is the distinct reception of citronellol (Fig. 5A). Citronellol is naturally abundant in various plant odors and is also reported to be part of the pheromone blends of several bumblebee species (Kullenberg et al., 1970; Luxová et al., 2004). A distinct presence of the citronellol in the EAG activity of the worker class is therefore in line with its foraging-related background. Moreover, the marking pheromone specifically of *B. terrestris* is shown to lack citronellol but rather comprises 2,3-dihydrofarnesol and 2,3-dihydrofarnesal, among others (Luxová et al., 2004). We assume the specifically reduced sensitivity towards citronellol in drones is a consequence of its sex-specific ecological relevance and correlates with the abundance of *Sensilla trichodea* and *S. basiconica* in bumblebee drones. Whereas the numbers of *S. trichodea* reach up to ~16,000 per flagellum in honeybee workers, it is only up to ~400 on the male antenna. Sex-specific differences regarding the occurrence of *S. trichodea* have been also reported for several bumblebee species (Shang et al., 2010). In addition, the expression of *S. basiconica* is restricted to the worker antennae in both honeybees and nine examined bumblebee species (Esslen and Kaissling, 1976; Fonta and Masson, 1987; Shang et al., 2010). This concept of sex- specific sensilla expression and EAG sensitivity applies also for a third class of olfactory sensillae,

Sensilla placodea. S. placodea are shown to occur in sex-specific numbers in various bumblebee species (Fonta and Masson, 1982; Shang et al., 2010). Moreover, *S. placodea* occur up to seven times more abundant on the male antennal surface of honeybees (Esslen and Kaissling, 1976) and are shown to exhibit distinct activity towards 9-ODA ((2E)-9-oxodecenoic acid), the major component of the queen mandibular pheromone (Brockmann et al., 1998). Observations of bumblebee nuptial flights suggest a heavy reliance on the mutual olfactory detection and exchange of the mating partner's pheromones (Bergman and Bergström, 1997). Considering these observations, we assume young queens as a main target of DHF and future analyses of the EAG activity of *B. terrestris* queens to show specific activity towards DHF as conversely reported for the 9-ODA activity in honeybee drones. Thus, a final conclusion on the peripheral sex-specific activity of the buff-tailed bumblebee should not only include examinations of the EAG activity of young queens towards DHF but also analyze caste-specific effects of the *B. terrestris* equivalent to 9-ODA.

Distinct processing of behaviorally relevant key stimuli in the AL

As previous work established the use of extracellular recordings in the AL output to show a specific processing of farnesol in *B. terrestris* workers (Strube-Bloss et al., 2015), we decided to use a similar approach to extend the examination of behaviorally key stimuli and additionally focus on sex specific processing in the AL.

Based on the highly conserved neuroanatomy of *B. terrestris* and honeybees (Rybak et al., 2010; Mertes et al., 2021; Rother et al., 2021), we performed extracellular recordings in the dorso-medial rim region of the AL, the output region of the l- and mALT tracts in both sexes (Fig. 1C, Fig. 6 A/B). Due to the spatial organization of the bee AL with its specific regional and glomerular tuning towards stimulus CCL, moiety and olfactory receptors (Sachse et al., 1999; Dahanukar et al., 2005; Sandoz, 2006; Mertes et al., 2021), we specifically aimed for the dorso-medial rim position to both minimize as much individual influence of specific glomeruli, local interneurons and ORNs as possible and to maximize the uptake of PN activity.

Here, our results corroborate the findings of a distinct processing of farnesol in *B. terrestris* workers (Strube-Bloss et al., 2015) and additionally show a similar discrimination for the processing of DHF (Fig. 6D, bottom panel). While DHF and farnesol induced activity does not reach as distinct levels in the AL activity of drones (Fig. 6C, bottom panel, Fig. 7B), all other presented stimuli show a uniformly processing in both sexes (Fig. 6 C/D, Fig. 7B). Interestingly,

farnesol exhibits a distinct, long lasting tonic activity that can hint to an increased network activity, standing in line with its described ecological role as a recruitment and alert pheromone. This specific tonic activity of farnesol has also been reported by Strube-Bloss et al. (2015). Moreover, the previously discussed sex-specific representation of citronellol in the male EAG (Fig. 5A) is not reflected in the AL activity (Fig. 6C, 7B). Here, the activity of citronellol is congruent with the activity of citral and geraniol and hence we assume its specific low representation in the drone EAG to be indeed due to a reduced number of sensitive ORNs or sensilla.

Furthermore, the odor- and sex-specific activity we found in the AL may underlie a common concept of a hardwired architecture in the glomerular organization, as reported in honeybees (Joerges et al., 1997; Sachse et al., 1999) and in fruit flies (reviewed in Laissue and Vosshall, 2008). However, this hardwired innervation pattern is also shown to be the subject of plastic, modulatory effects. These effects can thereby originate in both an enhanced sensory exposure (Sachse et al., 2007) or a memory & learning induced plasticity (Hourcade et al., 2009). Additionally, there is evidence in the honeybee, of an AL innervation by feedback neurons streaming downwards from the MB (Kirschner et al., 2006). Thus, a comparative study of the AL processing in naïve and experienced animals could shed more light into learning and memory induced modulation of the bumblebee AL network.

Taken together, our results suggest that differences in the peripheral reception of behaviorally relevant olfactory stimuli are not sufficient enough to evaluate the ecological or sex-specific impact of an odorant. Despite a distinct, stimulus-specific EAG activity (Fig. 5A, Fig. 7A), the olfactory processing in the AL seems to re-assess the neural representation of an odorant. Here, an excellent example for our assumption is farnesol, exhibiting an outstanding activity neither in the receptive (Fig. 5A) nor in the learning approaches (Fig. 3A), but a distinct neural representation during olfactory processing in the worker AL (Fig. 6D, bottom panel, Fig. 7, right panels).

keeping and maintenance, Anica Maier and Fabian Rüdenauer for assistance with the PER experiments.

Author contributions:

F.S., and M.S.-B. designed the electrophysiological experiments. J.S and. M.S.-B. designed the behavioral experiments. F.S. and M.S.-B conducted the experiments. F.S., and M.S-B. analyzed the electrophysiological data. F.S., J.S. and M.S-B analyzed the behavioral data. F.S. drafted the manuscript. M.S.-B. and W.R revised the manuscript. T.E., T.S. and J.S. contributed conceptual input and chemical guidance.

References

Abel, R., Rybak, J., and Menzel, R. (2001). Structure and response patterns of olfactory interneurons in the honeybee,Apis mellifera. *J. Comp. Neurol.* 437, 363–383. doi:10.1002/cne.1289.

Ågren, L., and Hallberg, E. (1996). Flagellar sensilla of bumble bee males (Hymenopera, Apidae, Bombus). *Apidologie* 25, 433–444. doi:10.1051/apido:19960601.

Arnold, G., Masson, C., and Budharugsa, S. (1985). Comparative study of the antennal lobes and their afferent pathway in the worker bee and the drone (Apis mellifera). *Cell Tissue Res.* 242, 593–605. doi:10.1007/BF00225425.

Avarguès-Weber, A., Deisig, N., and Giurfa, M. (2011). Visual Cognition in Social Insects. *Annu. Rev. Entomol.* 56, 423–443. doi:10.1146/annurev-ento-120709-144855.

Avarguès-Weber, A., and Mota, T. (2016). Advances and limitations of visual conditioning protocols in harnessed bees. *J. Physiol. Paris* 110, 107–118. doi:10.1016/j.jphysparis.2016.12.006.

Bergman, P., and Bergström, G. (1997). Scent marking, scent origin, and species specificity in male premating behavior of two Scandinavian bumblebees. *Can. Field-Naturalist* 111, 1235–1251. doi:0098 0331/97/0500 I235$12.50/0.

Bergström, G., Kullenberg, B., Ställberg-Stenhagen, S., and Stenhagen, E. (1968). "Studies on natural odoriferous compounds. II. Identification of a 2,3–dihydrofarnesol as the main component of the marking perfume of male bumble bees of the species Bombus terrestris," in *L. Ark. Kemi 28*, 453–469.

Bitterman, M. E., Menzel, R., Fietz, A., and Schäfer, S. (1983). Classical conditioning of proboscis

extension in honeybees (Apis mellifera). *J. Comp. Psychol.* 97, 107–119. doi:10.1037/0735-7036.97.2.107.

Brill, M. F., Reuter, M., Rössler, W., and Strube-Bloss, M. F. (2014). Simultaneous long-term recordings at two neuronal processing stages in behaving honeybees. *J. Vis. Exp.*, 2014. doi:10.3791/51750.

Brill, M. F., Rosenbaum, T., Reus, I., Kleineidam, C. J., Nawrot, M. P., and Rössler, W. (2013). Parallel processing via a dual olfactory pathway in the honeybee. *J. Neurosci.* 33, 2443–56. doi:10.1523/JNEUROSCI.4268-12.2013.

Brockmann, A., Brückner, D., and Crewe, R. M. (1998). The EAG Response Spectra of Workers and Drones to Queen Honeybee Mandibular Gland Components: The Evolution of a Social Signal. *Naturwissenschaften* 85, 283–285. doi:10.1007/s001140050500.

Connolly, J. D. J., and Hill, R. A. (1991). *Dictionary of Terpenoids*. 1st ed. London: CRC Press Available at: http://doi.wiley.com/10.1002/ffj.2730070418.

Dahanukar, A., Hallem, E. A., and Carlson, J. R. (2005). Insect chemoreception. *Curr. Opin. Neurobiol.* 15, 423–430. doi:10.1016/j.conb.2005.06.001.

Daly, K. C., Chandra, S., Durtschi, M. L., and Smith, B. H. (2001). The generalization of an olfactory-based conditioned response reveals unique but overlapping odour representations in the moth Manduca sexta. *J. Exp. Biol.* 204, 3085–3095. doi:10.1242/jeb.204.17.3085.

de Belle, J., and Heisenberg, M. (1994). Associative odor learning in Drosophila abolished by chemical ablation of mushroom bodies. *Science (80-.).* 263, 692–695. doi:10.1126/science.8303280.

Esslen, J., and Kaissling, K. E. (1976). Zahl und Verteilung antennaler Sensillen bei der Honigbiene (Apis mellifera L.). *Zoomorphologie* 83, 227–251. doi:10.1007/BF00993511.

Fachada, N., and C. Rosa, A. (2018). micompm: A MATLAB/Octave toolbox for multivariate independent comparison of observations. *J. Open Source Softw.* 3, 430. doi:10.21105/joss.00430.

Fahrbach, S. E. (2006). Structure of the Mushroom Bodies of the Insect Brain. *Annu. Rev. Entomol.* 51, 209–232. doi:10.1146/annurev.ento.51.110104.150954.

Finke, V., Baracchi, D., Giurfa, M., Scheiner, R., and Avarguès-Weber, A. (2021). Evidence of cognitive specialization in an insect: proficiency is maintained across elemental and higher-order visual learning but not between sensory modalities in honey bees. *J. Exp. Biol.* 224. doi:10.1242/jeb.242470.

Fonta, C., and Masson, C. (1984). Comparative study by electrophysiology of olfactory responses in bumblebees (Bombus hypnorum andBombus terrestris). *J. Chem. Ecol.* 10, 1157–1168. doi:10.1007/BF00988546.

Fonta, C., and Masson, C. (1987). Structural and functional studies of the peripheral olfactory nervous system of male and female bumble-bees (Bombus hypnorum and Bombus terrestris). *Chem. Senses* 12, 53–69. doi:10.1093/chemse/12.1.53.

Fonta, C., and Masson, C. (1982). Analyse De l'Équipement Sensoriel Antennaire Du Bourdon Bombus Hypnorum L. *Apidologie* 13, 247–263. doi:10.1051/apido:19820305.

Free, J. B. (1987). *Pheromones of Social Bees*. 1st ed. Dordrecht: Springer Netherlands.

Galizia, G. C., Joerges, J., Küttner, A., Faber, T., and Menzel, R. (1997). A semi-in-vivo preparation for optical recording of the insect brain. *J. Neurosci. Methods* 76, 61–69. doi:10.1016/S0165-0270(97)00080-0.

Getz, W. M., and Akers, R. P. (1993). Olfactory response characteristics and tuning structure of placodes in the honey bee Apis mellifera L. *Apidologie* 24, 195–217. doi:10.1051/apido:19930303.

Giurfa, M. (2007). Behavioral and neural analysis of associative learning in the honeybee: a taste from the magic well. *J. Comp. Physiol. A* 193, 801–824. doi:10.1007/s00359-007-0235-9.

Giurfa, M., and Sandoz, J.-C. (2012). Invertebrate learning and memory: Fifty years of olfactory conditioning of the proboscis extension response in honeybees. *Learn. Mem.* 19, 54–66. doi:10.1101/lm.024711.111.

Granero, A. M., Guerra Sanz, J. M., Egea Gonzalez, F. J., Martinez Vidal, J. L., Dornhaus, A., Ghani, J., et al. (2005). Chemical compounds of the foraging recruitment pheromone in bumblebees. *Naturwissenschaften* 92, 371–374. doi:10.1007/s00114-005-0002-0.

Groh, C., Lu, Z., Meinertzhagen, I. A., and Rössler, W. (2012). Age-related plasticity in the synaptic ultrastructure of neurons in the mushroom body calyx of the adult honeybee Apis mellifera. *J. Comp. Neurol.* 520, 3509–3527. doi:10.1002/cne.23102.

Groh, C., and Rössler, W. (2008). Caste-specific postembryonic development of primary and secondary olfactory centers in the female honeybee brain. *Arthropod Struct. Dev.* 37, 459–468. doi:10.1016/j.asd.2008.04.001.

Groh, C., and Rössler, W. (2020). Analysis of Synaptic Microcircuits in the Mushroom Bodies of the Honeybee. *Insects* 11, 43. doi:10.3390/insects11010043.

Gronenberg, W. (1987). Anatomical and physiological properties of feedback neurons of the mushroom bodies in the bee brain. *Exp. Biol.* 46, 115–25. Available at: http://www.ncbi.nlm.nih.gov/pubmed/3582581.

Grünewald, B. (1999). Morphology of feedback neurons in the mushroom body of the honeybee, Apis mellifera. *J. Comp. Neurol.* 404, 114. doi:10.1002/(SICI)1096-9861(19990201)404:1<114::AID-CNE9>3.3.CO;2-R.

Guerrieri, F., Schubert, M., Sandoz, J.-C., and Giurfa, M. (2005). Perceptual and Neural Olfactory Similarity in Honeybees. *PLoS Biol.* 3, e60. doi:10.1371/journal.pbio.0030060.

Haehnel, M., and Menzel, R. (2010). Sensory Representation and Learning-Related Plasticity in Mushroom Body Extrinsic Feedback Neurons of the Protocerebral Tract. *Front. Syst. Neurosci.* 4, 1–13. doi:10.3389/fnsys.2010.00161.

Hammer, M. (1993). An identified neuron mediates the unconditioned stimulus in associative olfactory learning in honeybees. *Nature* 366, 59–63. doi:10.1038/366059a0.

Hefetz, A., Batra, S. W. T., and Blum, M. S. (1979). Linalool, neral and geranial in the mandibular glands of Colletes bees — an aggregation pheromone. *Experientia* 35, 319–320. doi:10.1007/BF01964324.

Homberg, U. (1984). Processing of antennal information in extrinsic mushroom body neurons of the bee brain. *J. Comp. Physiol. A* 154, 825–836. doi:10.1007/BF00610683.

Hourcade, B., Perisse, E., Devaud, J.-M., and Sandoz, J.-C. (2009). Long-term memory shapes the primary olfactory center of an insect brain. *Learn. Mem.* 16, 607–615. doi:10.1101/lm.1445609.

Howard, S. R., Avarguès-Weber, A., Garcia, J. E., Greentree, A. D., and Dyer, A. G. (2018). Numerical ordering of zero in honey bees. *Science (80-.).* 360, 1124–1126. doi:10.1126/science.aar4975.

Imamura, K., Mataga, N., and Mori, K. (1992). Coding of odor molecules by mitral/tufted cells in rabbit

olfactory bulb. I. Aliphatic compounds. *J. Neurophysiol.* 68, 1986–2002. doi:10.1152/jn.1992.68.6.1986.

Joerges, J., Küttner, A., Galizia, C. G., and Menzel, R. (1997). Representations of odours and odour mixtures visualized in the honeybee brain. *Nature* 387, 285–288. doi:10.1038/387285a0.

Katoh, K., Koshimoto, H., Tani, A., and Mori, K. (1993). Coding of odor molecules by mitral/tufted cells in rabbit olfactory bulb. II. Aromatic compounds. *J. Neurophysiol.* 70, 2161–2175. doi:10.1152/jn.1993.70.5.2161.

Kirschner, S., Kleineidam, C. J., Zube, C., Rybak, J., Grünewald, B., and Rössler, W. (2006). Dual olfactory pathway in the honeybee, Apis mellifera. *J. Comp. Neurol.* 499, 933–952. doi:10.1002/cne.21158.

Kropf, J., Kelber, C., Bieringer, K., and Rössler, W. (2014). Olfactory subsystems in the honeybee: sensory supply and sex specificity. *Cell Tissue Res.*, 583–595. doi:10.1007/s00441-014-1892-y.

Kropf, J., and Rössler, W. (2018). In-situ recording of ionic currents in projection neurons and Kenyon cells in the olfactory pathway of the honeybee. *PLoS One* 13, e0191425. doi:10.1371/journal.pone.0191425.

Kullenberg, B., Bergstrom, G., Ställberg-Stenhagen, S., Liaaen-Jensen, S., Lamvik, A., Sunde, E., et al. (1970). Volatile Components of the Cephalic Marking Secretion of Male Bumble Bees. *Acta Chem. Scand.* 24, 1481–1483. doi:10.3891/acta.chem.scand.24-1481.

Lacher, V. (1964). Elektrophysiologische Untersuchungen an einzelnen Rezeptoren für Geruch, Kohlendioxyd, Luftfeuchtigkeit und Tempratur auf den Antennen der Arbeitsbiene und der Drohne (Apis mellifica L.). *Z. Vgl. Physiol.* 48, 587–623. doi:10.1007/BF00333743.

Laissue, P. P., and Vosshall, L. B. (2008). "The Olfactory Sensory Map in Drosophila," in *Brain Development in Drosophila melanogaster* (New York, NY: Springer New York), 102–114. doi:10.1007/978-0-387-78261-4_7.

Laloi, D., Sandoz, J. C., Picard-Nizou, A. L., Marchesi, A., Pouvreau, A., Taséi, J. N., et al. (1999). Olfactory conditioning of the proboscis extension in bumble bees. *Entomol. Exp. Appl.* 90, 123–129. doi:10.1023/A:1003598301272.

Laska, M., Galizia, G. C., Giurfa, M., and Menzel, R. (1999). Olfactory discrimination ability and odor structure-activity relationships in honeybees. *Chem. Senses* 24, 429–438. doi:10.1093/chemse/24.4.429.

Laska, M., and Hübener, F. (2001). Olfactory discrimination ability for homologous series of aliphatic ketones and acetic esters. *Behav. Brain Res.* 119, 193–201. doi:10.1016/S0166-4328(00)00348-X.

Lichtenstein, L., Lichtenstein, M., and Spaethe, J. (2018). Length of stimulus presentation and visual angle are critical for efficient visual PER conditioning in the restrained honey bee, Apis mellifera . *J. Exp. Biol.* 221, jeb179622. doi:10.1242/jeb.179622.

Lichtenstein, L., Sommerlandt, F. M. J., and Spaethe, J. (2015). Dumb and lazy? A comparison of color learning and memory retrieval in drones and workers of the buff-tailed bumblebee, bombus terrestris, by means of per conditioning. *PLoS One* 10, 1–18. doi:10.1371/journal.pone.0134248.

Linster, C., and Hasselmo, M. (1999). Behavioral Responses to Aliphatic Aldehydes Can Be Predicted From Known Electrophysiological Responses of Mitral Cells in the Olfactory Bulb. *Physiol. Behav.* 66, 497–502. doi:10.1016/S0031-9384(98)00324-2.

Loukola, O. J., Solvi, C., Coscos, L., and Chittka, L. (2017). Bumblebees show cognitive flexibility by improving on an observed complex behavior. *Science (80-.).* 355, 833–836.

doi:10.1126/science.aag2360.

Luxová, A., Urbanová, K., Valterová, I., Terzo, M., and Borg-Karlson, A.-K. (2004). Absolute configuration of chiral terpenes in marking pheromones of bumblebees and cuckoo bumblebees. *Chirality* 16, 228–233. doi:10.1002/chir.20017.

Matsumoto, Y., Menzel, R., Sandoz, J.-C., and Giurfa, M. (2012). Revisiting olfactory classical conditioning of the proboscis extension response in honey bees: A step toward standardized procedures. *J. Neurosci. Methods* 211, 159–167. doi:10.1016/j.jneumeth.2012.08.018.

Mauelshagen, J. (1993). Neural correlates of olfactory learning paradigms in an identified neuron in the honeybee brain. *J. Neurophysiol.* 69, 609–625. doi:10.1152/jn.1993.69.2.609.

Menzel, R. (2012). The honeybee as a model for understanding the basis of cognition. *Nat. Rev. Neurosci.* 13, 758–768. doi:10.1038/nrn3357.

Menzel, R. (2014). The insect mushroom body, an experience-dependent recoding device. *J. Physiol.* 108, 84–95. doi:10.1016/j.jphysparis.2014.07.004.

Mertes, M., Carcaud, J., and Sandoz, J.-C. (2021). Olfactory coding in the antennal lobe of the bumble bee Bombus terrestris. *Sci. Rep.* 11, 10947. doi:10.1038/s41598-021-90400-6.

Müller, D., Abel, R., Brandt, R., Zöckler, M., and Menzel, R. (2002). Differential parallel processing of olfactory information in the honeybee, Apis mellifera L. *J. Comp. Physiol. A Neuroethol. Sensory, Neural, Behav. Physiol.* 188, 359–370. doi:10.1007/s00359-002-0310-1.

Nagaraja, N., and Bruckner, D. (2013). Olfactory learning and memory recall in drones of hive honeybee species. *J. Entomol. Res.* 37, 29–32.

Nishino, H., Nishikawa, M., Mizunami, M., and Yokohari, F. (2009). Functional and topographic segregation of glomeruli revealed by local staining of antennal sensory neurons in the honeybee Apis mellifera. *J. Comp. Neurol.* 515, 161–180. doi:10.1002/cne.22064.

Nouvian, M., Reinhard, J., and Giurfa, M. (2016). The defensive response of the honeybee Apis mellifera. *J. Exp. Biol.* 219, 3505–3517. doi:10.1242/jeb.143016.

Nunes, T. M., Nascimento, F. S., Turatti, I. C., Lopes, N. P., and Zucchi, R. (2008). Nestmate recognition in a stingless bee: does the similarity of chemical cues determine guard acceptance? *Anim. Behav.* 75, 1165–1171. doi:10.1016/j.anbehav.2007.08.028.

Parrey, A. H., Raina, R. H., Saddam, B., Pathak, P., Kumar, S., Uniyal, V. P., et al. (2021). Role of Bumblebees (Hymenoptera: Apidae) in Pollination of High Land Ecosystems: A Review. *Agric. Rev.* I, 1–6. doi:10.18805/ag.R-2159.

Riveros, A. J., and Gronenberg, W. (2009). Olfactory learning and memory in the bumblebee Bombus occidentalis. *Naturwissenschaften* 96, 851–856. doi:10.1007/s00114-009-0532-y.

Robacker, D. C., and Hendry, L. B. (1977). Neral and geranial: Components of the sex pheromone of the parasitic wasp, Itoplectis conquisitor. *J. Chem. Ecol.* 3, 563–577. doi:10.1007/BF00989077.

Robertson, H. M., and Wanner, K. W. (2006). The chemoreceptor superfamily in the honey bee, Apis mellifera: Expansion of the odorant, but not gustatory, receptor family. *Genome Res.* 16, 1395–1403. doi:10.1101/gr.5057506.

Rother, L., Kraft, N., Smith, D. B., el Jundi, B., Gill, R. J., and Pfeiffer, K. (2021). A micro-CT-based standard brain atlas of the bumblebee. *Cell Tissue Res.* 386, 29–45. doi:10.1007/s00441-021-03482-z.

Rybak, J., Kuß, A., Lamecker, H., Zachow, S., Hege, H.-C., Lienhard, M., et al. (2010). The Digital Bee Brain: Integrating and Managing Neurons in a Common 3D Reference System. *Front. Syst. Neurosci.* 4, 15. doi:10.3389/fnsys.2010.00030.

Rybak, J., and Menzel, R. (1993). Anatomy of the mushroom bodies in the honey bee brain: the neuronal connections of the alpha-lobe. *J. Comp. Neurol.* 334, 444–65. doi:10.1002/cne.903340309.

Sachse, S., Rappert, A., and Galizia, C. G. (1999). The spatial representation of chemical structures in the antennal lobe of honeybees: steps towards the olfactory code. *Eur. J. Neurosci.* 11, 3970–3982. doi:10.1046/j.1460-9568.1999.00826.x.

Sachse, S., Rueckert, E., Keller, A., Okada, R., Tanaka, N. K., Ito, K., et al. (2007). Activity-Dependent Plasticity in an Olfactory Circuit. *Neuron* 56, 838–850. doi:10.1016/j.neuron.2007.10.035.

Sadd, B. M., Barribeau, S. M., Bloch, G., de Graaf, D. C., Dearden, P., Elsik, C. G., et al. (2015). The genomes of two key bumblebee species with primitive eusocial organization. *Genome Biol.* 16, 76. doi:10.1186/s13059-015-0623-3.

Sandoz, J.-C. (2006). Odour-evoked responses to queen pheromone components and to plant odours using optical imaging in the antennal lobe of the honey bee drone Apis mellifera L. *J. Exp. Biol.* 209, 3587–3598. doi:10.1242/jeb.02423.

Schmalz, F., Jundi, B., Rössler, W., and Strube-bloss, M. (2022). Categorizing Visual Information in Subpopulations of Honeybee Mushroom Body Output Neurons. *Front. Physiol.* 13, 1–11. doi:10.3389/fphys.2022.866807.

Shang, L., Wang, Y., Wang, P., Wang, S., and Ren, B. (2010). Application of Rough Set Analysis in Species and Caste Discrimination of Bumblebees (Hymenoptera: Apidae: Bombus) Based on Antennal Sensilla. *Ann. Entomol. Soc. Am.* 103, 654–660. doi:10.1603/AN10017.

Smith, B. H., and Menzel, R. (1989). The use of electromyogram recordings to quantify odourant discrimination in the honey bee, Apis mellifera. *J. Insect Physiol.* 35, 369–375. doi:10.1016/0022-1910(89)90110-8.

Sommerlandt, F. M. J., Rössler, W., and Spaethe, J. (2014). Elemental and non-elemental olfactory learning using PER conditioning in the bumblebee, Bombus terrestris. *Apidologie* 45, 106–115. doi:10.1007/s13592-013-0227-4.

Spaethe, J., Brockmann, A., Halbig, C., and Tautz, J. (2007). Size determines antennal sensitivity and behavioral threshold to odors in bumblebee workers. *Naturwissenschaften* 94, 733–739. doi:10.1007/s00114-007-0251-1.

Srinivasan, M. V. (2010). Honey Bees as a Model for Vision, Perception, and Cognition. *Annu. Rev. Entomol.* 55, 267–284. doi:10.1146/annurev.ento.010908.164537.

Strausfeld, N. J. (2002). Organization of the honey bee mushroom body: Representation of the calyx within the vertical and gamma lobes. *J. Comp. Neurol.* 450, 4–33. doi:10.1002/cne.10285.

Strube-Bloss, M. F., Brown, A., Spaethe, J., Schmitt, T., and Rössler, W. (2015). Extracting the behaviorally relevant stimulus: Unique neural representation of farnesol, a component of the recruitment pheromone of Bombus terrestris. *PLoS One* 10, 1–16. doi:10.1371/journal.pone.0137413.

Strube-Bloss, M. F., Herrera-Valdez, M. A., and Smith, B. H. (2012). Ensemble Response in Mushroom Body Output Neurons of the Honey Bee Outpaces Spatiotemporal Odor Processing Two Synapses Earlier in the Antennal Lobe. *PLoS One* 7, e50322. doi:10.1371/journal.pone.0050322.

Strube-Bloss, M. F., Nawrot, M. P., and Menzel, R. (2011). Mushroom Body Output Neurons Encode Odor-Reward Associations. *J. Neurosci.* 31, 3129–3140. doi:10.1523/jneurosci.2583-10.2011.

Strube-Bloss, M. F., Nawrot, M. P., and Menzel, R. (2016). Neural correlates of side-specific odour memory in mushroom body output neurons. *Proc. R. Soc. B Biol. Sci.* 283, 20161270. doi:10.1098/rspb.2016.1270.

Szyszka, P. (2008). Associative and non-associative plasticity in Kenyon cells of the honeybee mushroom body. *Front. Syst. Neurosci.* 2, 1–10. doi:10.3389/neuro.06.003.2008.

Trhlin, M., and Rajchard, J. (2011). &nbsp;Chemical communication in the honeybee (Apis mellifera L.): a review. *Vet. Med. (Praha).* 56, 265–273. doi:10.17221/1543-vetmed.

Vareschi, E. (1971). Duftunterscheidung bei der Honigbiene -- und Verhahensreaktionen. *Z. Vgl. Physiol.* 75, 143–173. doi:143. doi:10.1007/BF00335260.

von Frisch, K. (1914). *Der farbensinn und Formensinn der Biene.* Jena,: Fischer doi:10.5962/bhl.title.11736.

Wanner, K. W., Nichols, A. S., Walden, K. K. O., Brockmann, A., Luetje, C. W., and Robertson, H. M. (2007). A honey bee odorant receptor for the queen substance 9-oxo-2-decenoic acid. *Proc. Natl. Acad. Sci.* 104, 14383–14388. doi:10.1073/pnas.0705459104.

Yamagata, N., Schmuker, M., Szyszka, P., Mizunami, M., and Menzel, R. (2009). Differential odor processing in two olfactory pathways in the honeybee. *Front. Syst. Neurosci.* 3, 16. doi:10.3389/neuro.06.016.2009.

Zwaka, H., Bartels, R., Grünewald, B., and Menzel, R. (2018). Neural Organization of A3 Mushroom Body Extrinsic Neurons in the Honeybee Brain. *Front. Neuroanat.* 12, 1–11. doi:10.3389/fnana.2018.00057.

Supplemental Data
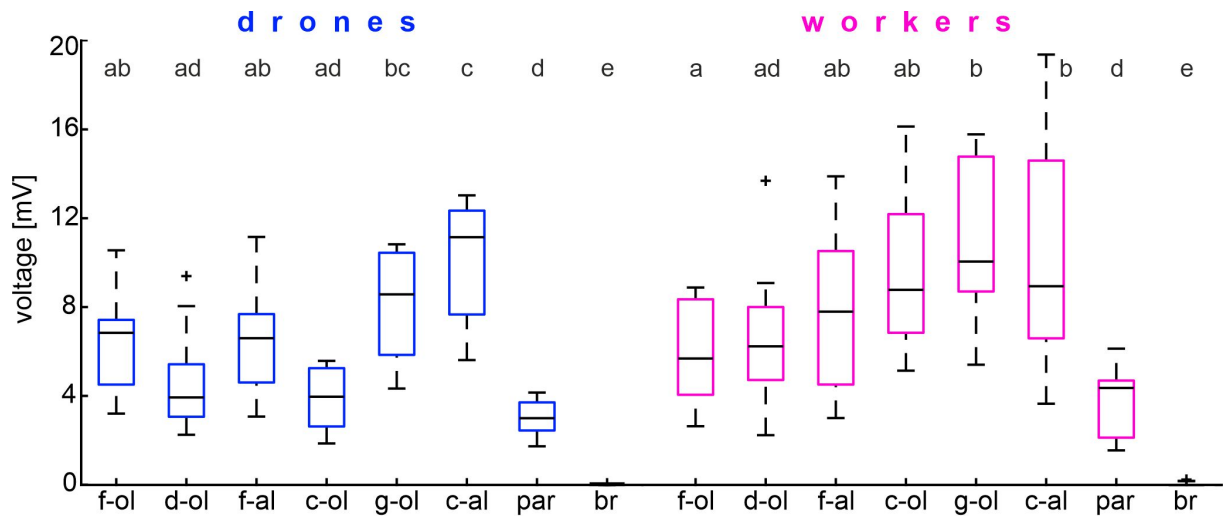
S1. Maximum EAG amplitudes of bumblebee drones and workers. Maximum EAG values of 11 drones (left panel, blue) and 13 workers (right panel, magenta) during 500 ms after stimulus on-set. Same letters indicate shared significance levels (repeated measurements ANOVA, post-hoc test: Tukey-Kramer, $p < 0.05$). Abbreviations: f-ol: farnesol, d-ol: 2,3-dihydrofarnesol, f-al: farnesal, c-ol: citronellol, g-ol: geraniol, c-al: citral, par: paraffin, br: base rate, n.s.: not significant. repeated measurements ANOVA : Drones: rmANOVA, $F_{(0,7)}=76.1$, $p = 1.46e-13$, Workers: rmANOVA, $F_{(0,7)}=44.9$, $p = 3.11e-13$.
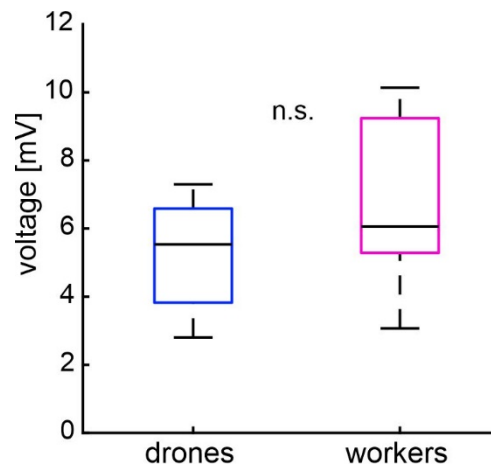
S2. Comparison of mean EAG activity of drones and workers. Drones (blue) and workers (magenta) show no overall difference in the mean EAG activity. Wilcoxon rank sum test: $p > 0.05$. n.s.: not significant.
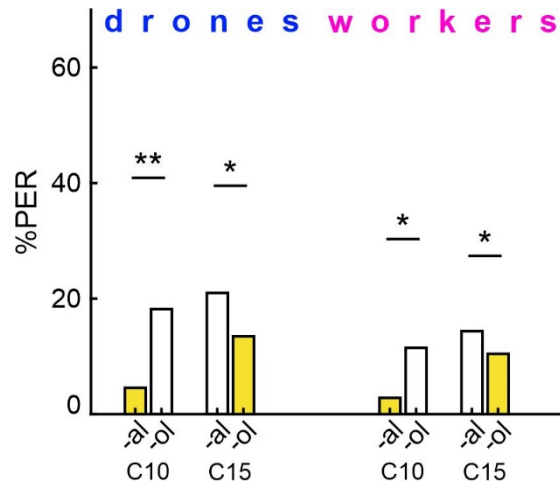
Figure S3. Averaged PER rate during retention test in dependency of odor moiety. Both drones and workers show no generalization of the PER towards novel odor molecules sharing the same functional group as the CS. On the contrary, PER rate in both sexes is dominated by a generalization to the carbon chain length for both presented terpene classes (C10, C15). Bars show averaged PER to all presented novel stimuli, grouped in aldehydes (-al) and alcohols (-ol). Yellow filled bars indicate functional group of the CS. Odor classification: Aldehydes: Citral (C10), farnesal (C15); Alcohols: Citronellol (C10), geraniol (C10), farnesol (C15), 2,3-dihydrofarnesol (C15). Chi² test: *p < 0.05, **p < 0.01. For detailed statistics see table S7 & S8.
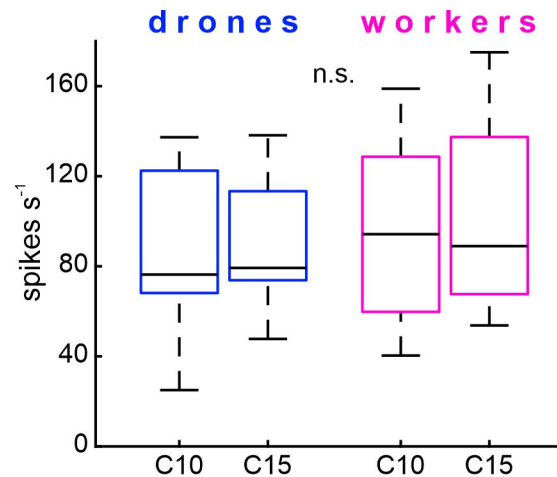
S4. Representation of molecule size at the AL output. Mean spike rate of AL neurons. Data shows pooled monoterpene and sesquiterpenes evoked activity for drones (blue) and workers (magenta). Wilcoxon rank sum test: p > 0.05. n.s.: not significant.

Table S1. Chi² test for 10th acquisition trial paired vs. unpaired in drones.

Drones (n-count: paired/unpaired)	Chi2stat	p
Geraniol (51/27)	27.41	1.65e-07
Citral (40/25)	23.03	1.60e-06
Citronellol (51/28)	30.24	3.81e-08
Farnesol (42/26)	28.04	1.20e-07
Farnesal (54/33)	30.60	3.20e-08
2,3-Dihydrofarnesol (46/26)	30.80	2.90e-08

Table S2. Chi² test for 10th acquisition trial paired vs. unpaired in workers.

Workers (n-count: paired/unpaired)	Chi2stat	p
Geraniol (49/25)	39.73	2.92e-10
Citral (43/25)	21.61	3.34e-06
Citronellol (43/25)	27.57	1.52e-07
Farnesol (58/25)	28.78	8.12e-08
Farnesal (65/25)	26.59	2.52e-07
2,3-Dihydrofarnesol (45/25)	22.46	2.14e-06

Table S3. Cross-matrix of workers retention tests.

CS+	test stimulus					
	g-ol	c-al	c-ol	f-ol	f-al	d-ol
Geraniol						
n-count (pos./neg. responses)	(38/11)	(10/23)	(7/25)	(2/30)	(1/24)	(1/24)
Chi2stat		18.13	24.30	39.37	34.86	34.86
p		2.05e-05	1.03e-06	1.75e-09	5.88e-09	5.88e-09
Citral						
n-count	(9/16)	(27/16)	(5/20)	(0/27)	(1/24)	(0/27)
Chi2stat	4.55		11.61	27.59	22.55	27.59
p	0.0328		8.15e-04	3.73e-07	3.38e-06	3.73e-07
Citronellol						
n-count	(5/21)	(7/19)	(29/14)	(1/24)	(1/25)	(1/25)
Chi2stat	15.06	10.66		25.80	26.66	26.66
p	1.29e-04	0.001		6.28e-07	6.03e-07	6.03e-07
Farnesol						
n-count	(2/41)	(0/29)	(3/35)	(31/27)	(7/31)	(7/19)
Chi2stat	26.72	24.08	20.82		11.77	5.09
p	1.17e-06	2.31e-06	8.37e-06		7.49e-04	0.0239
Farnesal						
n-count	(0/34)	(1/45)	(0/39)	(8/40)	(41/24)	(7/21)
Chi2stat	36.60	42.47	40.60	24.21		11.36
p	2.40e-09	3.57e-10	4.63e-10	1.08e-06		7.49e-04
2,3-Dihydrofarnesol						
n-count	(1/28)	(0/27)	(0/28)	(7/18)	(7/19)	(30/15)
Chi2stat	28.95	30.85	31.68	9.64	10.43	
p	1.24e-07	6.92e-08	6.92e-08	0.00190	0.0015	

Table S4. Cross-matrix of drones retention tests.

CS+	test stimulus					
	g-ol	c-al	c-ol	f-ol	f-al	d-ol
Geraniol						
n-count (pos./neg. responses)	(33/18)	(14/20)	(9/18)	(2/31)	(5/29)	(1/24)
Chi2stat		4.56	6.99	28.35	20.63	25.00
p		0.0325	0.0102	5.05e-07	9.27e-06	1.43e-06
Citral						
n-count	(12/19)	(28/12)	(12/23)	(0/30)	(2/28)	(3/23)
Chi2stat	6.95		9.56	35.00	28.07	21.62
p	0.00837		0.00248	1.65e-08	2.90e-07	5.53e-06
Citronellol						
n-count	(10/25)	(9/25)	(37/14)	(2/33)	(0/27)	(1/25)
Chi2stat	16.19	17.44		37.40	37.26	32.51
p	5.70e-05	3.68e-05		2.58e-09	2.58e-09	1.97e-08
Farnesol						
n-count	(0/30)	(1/33)	(1/33)	(31/11)	(13/18)	(10/15)
Chi2stat	38.88	38.71	38.71		7.56	7.54
p	8.18e-10	8.18e-10	8.18e-10		0.00602	0.00602
Farnesal						
n-count	(0/35)	(1/35)	(2/32)	(8/21)	(41/13)	(8/20)
Chi2stat	49.27	46.43	40.96	18.23		17.19
p	1.11e-11	2.37e-11	2.57e-10	2.44e-05		3.37e-05
2,3-Dihydrofarnesol						
n-count	(1/27)	(2/27)	(2/23)	(8/18)	(9/21)	(31/15)
Chi2stat	28.88	26.41	22.96	8.97	10.18	
p	3.84e-07	6.88e-07	2.73e-06	0.00273	0.00176	

Table S5. Retention test for pooled C10 and C15 comparison in drones.

CS vs control	Chi2stat	p
C10 vs C15	59.13	1.47e-14
C15 vs C10	74.95	4.82e-18

Table S6. Retention test for pooled C10 and C15 comparison in workers.

CS vs control	Chi2stat	p
C10 vs C15	44.68	2.31e-11
C15 vs C10	74.95	4.82e-18

Table S7. Retention test for pooled aldehydes and alcohols comparison in drones.

CS vs control	Chi2stat	p
aldehydes vs alcohols	7.45	0.0064
alcohols vs aldehydes	5.93	0.0149

Table S8. Retention test for pooled aldehydes and alcohols comparison in workers.

CS vs control	Chi2stat	p
aldehydes vs alcohols	4.79	0.0286
		Yates-correction: 0.049
alcohols vs aldehydes	2.04	0.153

Table S9. Vapor pressures.

Odor	Vapor pressure [mm Hg]
Monoterpenes:	
Geraniol	3.0e-2
Citral I	9.13e-2
Citronellol	2.00e-2
Sesquiterpenes:	
Farnesol	3.94e-5
Farnesal	1.87e-5
2,3-Dihydrofarnesol	6.00e-5

Categorizing visual information in subpopulations of honeybee mushroom body output neurons

Fabian Schmalz[1], Basil el Jundi[1], Wolfgang Rössler[1], Martin Strube-Bloss[2]*

[1] Behavioral Physiology and Sociobiology (Zoology II), Biozentrum, University of Würzburg, Würzburg, Germany

[2] Department of Biological Cybernetics and Theoretical Biology, University of Bielefeld, Bielefeld, Germany

[*] Correspondence:
Martin Strube-Bloss
martin.strube-bloss@uni-bielefeld.de

Keywords: Mushroom Body Output Neurons, Categorization, Multi-Unit Electrophysiology, Vision, Olfaction, Honeybee, Vertical Lobe, Multimodal

The article can be downloaded from:

https://www.frontiersin.org/articles/10.3389/fnbeh.2017.00226/full

Abstract

Multisensory integration plays a central role in perception, as all behaviors usually require the input of different sensory signals. For instance, for a foraging honeybee the association of a food source includes the combination of olfactory and visual cues to be categorized as a flower. Moreover, homing after successful foraging using celestial cues and the panoramic scenery may be dominated by visual cues. Hence, dependent on the context, one modality might be leading and influence the processing of other modalities. To unravel the complex neural mechanisms behind this process we studied honeybee mushroom body output neurons (MBON). MBONs represent the first processing level after olfactory-visual convergence in the honeybee brain. This was physiologically confirmed in our previous study by characterizing a subpopulation of multisensory MBONs. These neurons categorize incoming sensory inputs into olfactory, visual, and olfactory-visual information. However, in addition to multisensory units a prominent population of MBONs was sensitive to visual cues only. Therefore, we asked which visual features might be represented at this high-order integration level. Using extracellular, multi-unit recordings in combination with visual and olfactory stimulation, we separated MBONs with multisensory responses from purely visually driven MBONs. Further analysis revealed, for the first time, that visually driven MBONs of both groups encode detailed aspects within this individual modality, such as light intensity and light identity. Moreover, we show that these features are separated by different MBON subpopulations, for example by extracting information about brightness and wavelength. Most interestingly, the latter MBON population was tuned to separate UV-light from other light stimuli, which were only poorly differentiated from each other. A third MBON subpopulation was neither tuned to brightness nor to wavelength and encoded the general presence of light. Taken together, our results support the view that the mushroom body, a high-order sensory integration, learning and memory center in the insect brain, categorizes sensory information by separating different behaviorally relevant aspects of the multisensory scenery and that these categories are channeled into distinct MBON subpopulations.

1. Introduction

Daily foraging is an essential routine in a honeybee's life and comes with various challenges, like the detection of valuable resources and the subsequent commuting between hive and most profitable resources. Since von Frisch's early research, we know that both processes rely heavily on sophisticated perception of visual information accompanied by memory formation (von Frisch, 1914, 1949; Srinivasan, 2010). On one hand, bees use their trichromatic vision to

scan the environment for color or contrast patterns of exploitable food sources (von Frisch, 1914; Peitsch et al., 1992; Lunau, 1993; Heiling et al., 2003; Srinivasan, 2010). On the other hand, they orient themselves using various visual cues, e.g. landmarks and panoramic cues, the pattern of polarized skylight, or the sun, among others (Srinivasan and Zhang, 2004).

Visual input received by photoreceptors of the compound eye is processed in the lamina, medulla, and lobula complex of the optic lobe before it is sent via visual projection neurons (PN) to the mushroom body (MB), the center for multimodal integration as well as learning and memory formation (Homberg, 1984; de Belle and Heisenberg, 1994; Menzel and Giurfa, 2001; Menzel, 2014). The visual PNs form three distinct tracts, originating in the upper medulla (the anterior superior optic tract, ASOT),the lower medulla (anterior inferior optic tract, AIOT) and in the lobula complex (lobular optic tract, LOT, Ehmer and Gronenberg 2002; Groh and Rössler 2020). All three optic tracts project into two sub compartments of the MB calyx, the collar (CO) and the basal ring (BR) region. In addition, the MB receives sensory input to the calyx region from multiple other modalities, like olfaction or gustation (Menzel and Giurfa, 2001; Schröter and Menzel, 2003; Menzel, 2014). The olfactory input to the MB originates from ~800-900 PNs of the antennal lobe (AL) innervating the MB calyx lip (LI) and BR region via two main tracts, the medial (m-ALT) and the lateral (l-ALT) antennal-lobe tract (Müller et al., 2002; Kirschner et al., 2006; Brill et al., 2013). Both visual and olfactory PNs diverge onto ~184.000 Kenyon Cells (KC), the MB principal neurons (Fahrbach, 2006; Groh and Rössler, 2020). Following this connectivity, a first olfactory-visual convergence exists in the BR. Bundles of KC axo-dendrites extend through in the pedunculus region and project further to the MB output regions, the medial (ML) and vertical lobes (VL). The ML and VL are organized into distinct strata, reflecting the concentric organization of KC dendrites in MB calyces. In the VL, terminals of the CO region form a layer that is between the mid layer of the VL comprising KC terminals of the LI region, and the upper most layer containing KC terminals of the BR region (Ehmer and Gronenberg, 2002; Strausfeld, 2002; Zwaka et al., 2018). However, the ventral layer of the VL, the so-called gamma lobe, is not supplied by KC axons from one specific calyx region, but rather by axons from a specific KC class, class II KCs (clawed). Dendrites of clawed KCs are not restricted to a single compartment of the calyx but are distributed across all three compartments of the calyx, thus receiving input from multiple modalities (Strausfeld, 2002).

Approximately 400 mushroom body output neurons (MBON) innervate virtually all strata of the VL (Gronenberg, 1987; Rybak and Menzel, 1993; Grünewald, 1999; Strausfeld, 2002). MBON somata are organized in seven disctinct clusters distributed in different regions of the

deutocerebrum and protocerebrum (Rybak and Menzel, 1993). These groups of MBONs relay information to different brain regions like the superior, intermediate and lateral protocerebral lobes (honeybee: Mauelshagen 1993; Homberg 1984; cockroach: Li and Strausfeld 1997), the contralateral brain hemisphere (Rybak and Menzel, 1993; Strausfeld, 2002), and the central complex (Hulse et al., 2021). Some MBONs (A3/PCT cluster) are GABA-ergic and feed back to the MB calyx input region (Gronenberg, 1987; Li and Strausfeld, 1997; Grünewald, 1999; Strausfeld, 2002; Zwaka et al., 2018). Furthermore, individual MBONs, like the antennal lobe feedback neuron (ALF-1) connect layers in the VL with large areas within the AL (Kirschner et al., 2006). Physiological studies found MBONs responding to stimuli of single or multiple modalities, reflecting the multimodal information processed by presynaptic KCs (Gronenberg, 1987; Strube-Bloss and Rössler, 2018).

So far, detailed information on the representation of stimulus specificity or sensitivity at the MBON level is sparse, as most studies focused on learning-related plasticity in MBONs (Menzel and Manz, 2005; Okada et al., 2007; Strube-Bloss et al., 2011; Filla and Menzel, 2015). Most interestingly, initially insensitive MBONs can be recruited to encode the odor reward association (Strube-Bloss et al., 2011) which can include complex stimulus features like odor identity and stimulation side (Strube-Bloss et al., 2016). However, also in naïve honeybees multimodal MBONs combine olfactory-visual stimulus features to categorize olfactory, visual and olfactory-visual compound stimuli (Strube-Bloss and Rössler, 2018). The latter study showed that a substantial proportion of recorded MBONs (~ 42%) were sensitive to visual cues only. Together with 32% of MBONs responding to both (visual and olfactory) modalities, light sensitive MBONs comprise up to ~74% of the MBON population at this processing level. Here we asked which visual features are represented at this high-order integration level by presenting visual stimuli varying in wavelength (identity) and brightness (intensity) to honeybees while performing multichannel extracellular recordings from the input region of the MBONs. Furthermore, we included an odor stimulus to identify the proportion of multimodal MBONs involved in visual processing to be in turn able, to concentrate analysis specifically to the population of unimodal, visual sensitive MBONs.
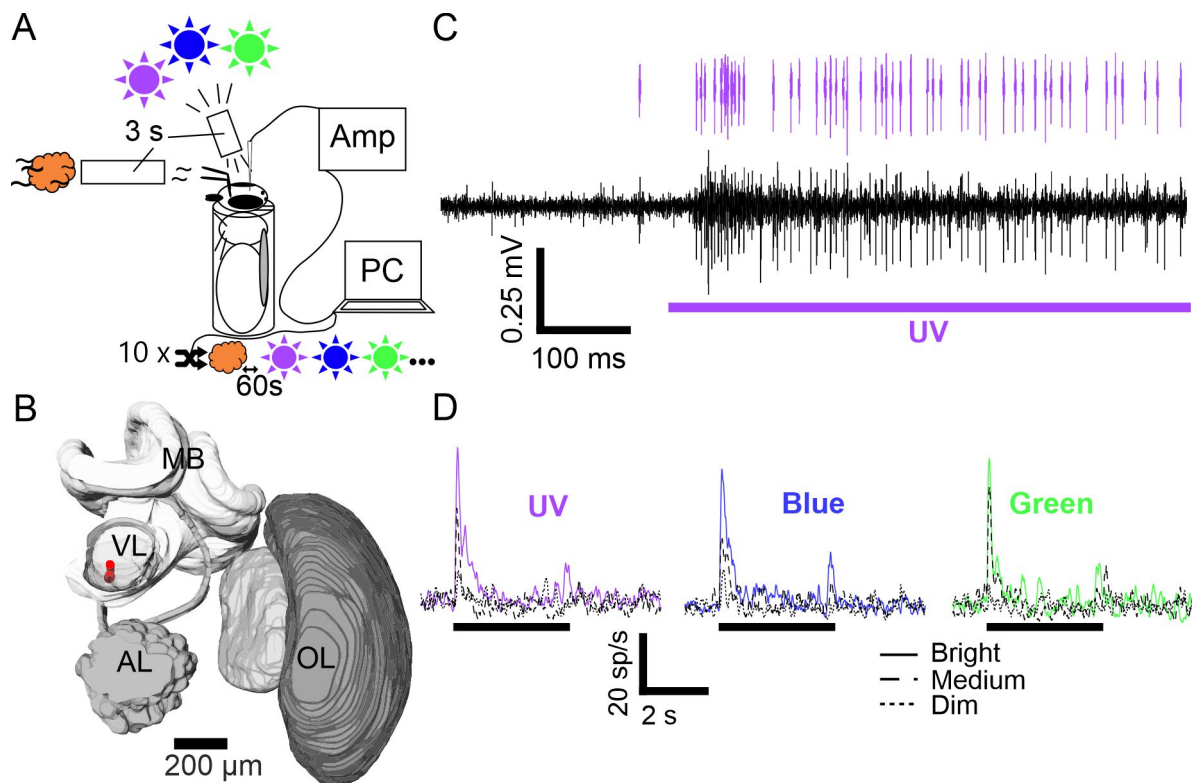
Figure 1. Stimulus setup, electrode position and mushroom body output neuron (MBON) activity. (A) Animals were harnessed in metal tubes and stimulated with UV, blue and green light (purple, blue and green sun) and one olfactory (orange cloud) cue. Each stimulus was presented ten times for three seconds. Stimulus order was pseudorandomized with an inter-stimulus interval of 60 s and controlled via PC. Signals were pre-amplified (AMP) and subsequently digitized. **(B)** 3D brain reconstruction of one examined animal. Electrode position is shown in red. Abbreviations: MB: Mushroom body, VL: Vertical lobe, AL: Antennal lobe, OL: Optic lobe. **(C)** Raw data trace showing 250 ms baseline activity before stimulus on-set (UV bright, magenta bar), followed by distinct spike activity after stimulus on-set. Magenta bars aligned on top of recording indicate spikes of one exemplary Unit, assigned to the respective timings. **(D)** Averaged spike rate of one exemplary neuron is shown for stimulation with UV, blue, and green at three intensities (cp. figure inset). Black bar indicates stimulation.

2. Material & Methods:

2.1 Animals:

Honeybee foragers *(Apis mellifera carnica)* were collected at our local bee station and kept in an incubator (35°C, 50-65% relative humidity, maximum storage time 48h). The bees had access to 50% sucrose diluted in water *ad libitum*. Prior to the experiment, bees were chilled on ice and harnessed in metal tubes where their head capsules were fixed by strong dental wax (Deiberit 502, SILADENT Dr. Böhme & Schöps GmbH, Goslar, Germany) and their antennae immobilized by low melting point paraffin wax (eicosane, Sigma-Aldrich, Taufkirchen,

Germany). Antennae were fixed at the scapus, according to their pupal position, close to the compound eyes but without any coverage of nearby ommatidia. The flagellum stays hereby loose and can freely move. The head capsule was opened and all glands, trachea and the neural sheath above the MBs were carefully removed to gain full access to the vertical lobes (VL). In total, we tested 55 honeybees.

2.2 Stimulation:

Visual Stimulation:

Three monochromatic LEDs emitting UV (360-400nm, TRU Components, Conrad, Hirschhaid, Germany), blue (450-490nm, Avago Technologies, Broadcom Inc., San José, CA, USA) and green (510-550nm, Avago Technologies, Broadcom Inc., San José, CA, USA) light respectively were used. The light was guided through two acrylic glass rods (Plexiglas®, diameter: 10mm, length: 100mm), each illuminating one compound eye of the test animals. The scattering characteristics of the acrylic glass rods thereby generated a homogenous, diffused light beam. Each wavelength was presented at three intensity levels (bright, medium and dim, table 1). The photon count of each stimulus was measured at the position of the bee's compound eye using a spectrometer (Maya2000 Pro, Ocean Insight, Orlando, FL, USA).

Table 1: Light intensity of the used visual stimuli [photons/cm²/s]

	Bright	Medium	Dim
UV	$1.14*10^{14}$	$3.30*10^{13}$	$4.63*10^{12}$
Blue	$1.57*10^{14}$	$2.00*10^{13}$	$2.35*10^{12}$
Green	$4.20*10^{14}$	$2.20*10^{13}$	$1.72*10^{12}$
Control flashlight (white light: 410-770 nm)	$4.56*10^{14}$		

Olfactory Stimulation:

We used a custom-made olfactometer (adapted from Galizia et al., 1997; Strube-Bloss et al., 2011) in the following way. A charcoal washed air stream (25 ml/s) was split and guided through both a Teflon tube (diameter 10 mm, constant air stream) and a solenoid valve (LEE HDI 3 Port, LEE Hydraulische Miniaturkomponenten GmbH, Sulzbach, Germany). In the off-position, the valve gated the airstream constantly through a 5 ml syringe, loaded with an empty filter paper (1 cm²). During odor stimulation, the solenoid valve switched on and directed the

air stream for three seconds through a second 5ml syringe, containing filter paper soaked with 10 µl odor solution. Both syringe needles (19G Neoject, DISPOMED GmbH & Co. KG, Gelnhausen, Germany) injected into the constant airstream that was orientated towards the antennae. The odor solution consisted of a 50/50 mixture of geraniol (W250716, Sigma-Aldrich Chemie GmbH, Taufkirchen, Germany) and citronellol (W230901, Sigma-Aldrich Chemie GmbH, Taufkirchen, Germany), diluted 1:100 in paraffin oil (76235, Sigma-Aldrich Chemie GmbH, Taufkirchen, Germany). Odors were chosen due to their natural occurrence in the scent of flowers and bee pheromones (Luxová et al., 2004; Chen and Viljoen, 2010; Trhlin and Rajchard, 2011).

Stimulation protocol and automated application:

Since we aimed to characterize visually driven MBONs, we started the experimental protocol only after the confirmation of neural activity caused by stimulation with white light (flashlight). Both, olfactory as well as visual stimulation was applied using the Trial Control software (Neuralynx Inc., Bozeman, MT, USA). Customized scripts enabled a fully automated stimulation via TTL-pulses, generated by a Neuralynx acquisition system unit (DL 4SX 16ch System, Neuralynx Inc., Bozeman, MT, USA). Each stimulus lasted three seconds and all stimuli were presented ten times in a pseudo-randomized order (random, but not more than two presentations of the same stimulus in a row) at an inter-stimulus interval of one minute (Fig. 1 A/D).

2.3 Electrophysiology:

Triode building and subsequent implantation follows the detailed description of our earlier publications (Strube-Bloss et al., 2011; Brill et al., 2014; Strube-Bloss and Rössler, 2018). In short, three polyurethane insulated copper wires (P155, Elektrisola, Reichshof-Eckenhagen, Germany) were glued together using dental wax (64103015S1 Pinnacle, DeguDent GmbH, Hanau, Germany). The single wires were connected to an electrode interface board (EIB-18; Neuralynx Inc., Bozeman, MT, USA), mounted to a customized electrode holder. The impedance of each electrode channel was controlled for a value between 1.5-2.5 MΩ, using a nanoZ kit (Multi Channel Systems MCS GmbH, Reutlingen, Germany). After pre-amplification by a head stage (HS-16, Neuralynx Inc., Bozeman, MT, USA) signals of the three single wires were digitalized and pair-wise subtracted online to exclude global noise, using the Cheetah acquisition software (Cheetah 6.4, Neuralynx Inc., Bozeman, MT, USA). We applied a high-pass filter (above 300-400 Hz) and recorded at a sampling rate of 30 kHz. A silver wire (AG-

8T, Science-Products, Hofheim, Germany) served as reference electrode and was inserted posteriorly in the hemolymph of the head capsule. The triode was positioned at the ventral side of the VL at a depth between 10-300 µm (Fig. 1B, also see supplementary material in Strube-Bloss and Rössler, 2018). To prevent electrode drift and desiccation of the brain tissue, we sealed the brain surface with two component, surgical silicon (KWIK-SIL Sarasota, FL, USA).

2.4 Visualization of electrode position:

Before recording, the triode was immersed in ALEXA 647 Hydrazide (A20502, Thermo Fisher Scientific GmbH, Dreieich, Germany) or in a 50/50 mixture of Micro-Ruby (D7162, Thermo Fisher Scientific GmbH, Dreieich, Germany) and ALEXA 647 Hydrazide diluted in 0.5 M KCl. After the experiment, the triode was removed and the brain was dissected out of the head capsule and fixated overnight in a 4% formaldehyde/phosphate-buffered saline (PBS), under dark conditions at 4°C. On the next day, the brain was washed 3 x 10 min in PBS and dehydrated in an increasing ethanol series (30%, 50%, 70%, 90%, 95%, 2x100%; 10 min each) and subsequently cleared and mounted in methyl salicylate. We used a SP2 confocal microscope (Leica, Wetzlar, Germany) with a 10x water immersion objective to scan the brain samples and reconstruct the triode position in three-dimensions using the software Amira (Thermo Fisher Scientific GmbH, Dreieich, Germany).

2.5 Spike sorting

We applied a semi-automatic spike sorting technique using Spike2 (Cambridge Electronic Design, Cambridge, UK) on single channels (monotrode sorting) or on double channels (stereotrode sorting). Spike templates were generated based on waveform and threshold (± 3 x standard deviation above baseline) and all matching events grouped. We used the implemented principal component analysis (PCA) to analyze matching events for a clear separation throughout the recorded spike train and monitored the inter spike interval times (ISI), to exclude groups containing intervals below 1 ms. The spikes fitting into the final templates were assigned to individual units (Fig. 1C) and corresponding timestamps exported to MATLAB (MathWorks, Natick, MA, USA).
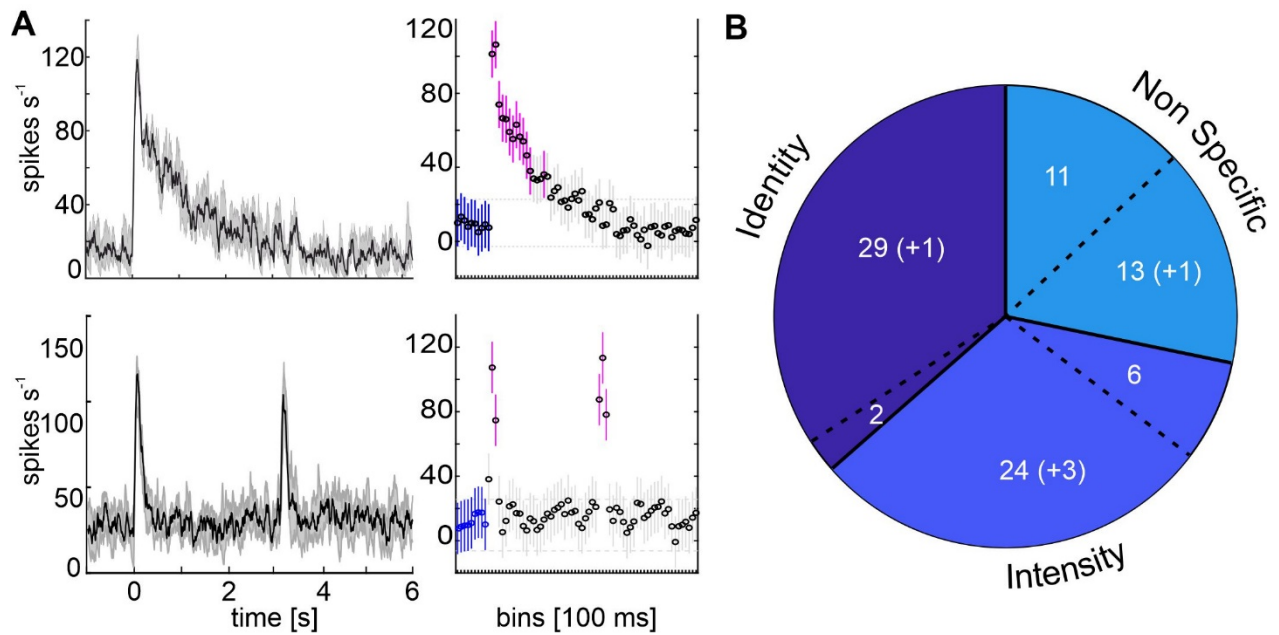
Figure 2. Response detection and proportion of MBON subpopulations. (A) Left charts show the mean spike activity of one phasic-tonically (top) and one phasically (bottom) responding representative example unit. Stimulation starts at time zero. Mean (solid black line) and standard deviation (shaded grey area) are indicated for 10 trials. Right charts show the activity in 100ms bins for the baseline activity before stimulus on-set (blue) and bins with significant variances (magenta; rmANOVA, post-hoc test: Tukey-Kramer, $p < 0.05$). Stimulation starts at 0 s and lasts 3 s. **(B)** Classification by neural coding behavior. 31 units differentiated between wavelengths (Identity), two of them were multimodal responding to odor stimulation as well (separated by a dashed line). 30 units did not discriminate between wavelengths within the same intensity level, but differentiated between brightness within each color (Intensity), six of them were multimodal. A third group neither differentiated between wavelengths or brightness but showed significant responses (Non Specific), eleven of them responded multimodally. Numbers in parentheses indicate units who exhibit their short term activity after visual stimulation (Fig.4).

2.6 Analysis

Analysis and statistics were performed in MATLAB, using the 'Statistics and Machine Learning' and the FIND toolboxes (Meier et al., 2008). To evaluate the response detection, spike rate, principal component analysis (PCA) and Euclidean distances, we used baseline corrected data. Baseline correction was calculated by subtracting the mean activity of each trial's first 500 ms (3-2.5 seconds before stimulus onset) from the full recording. Unit activity during stimulation was rated as a response when at least one bin (100 ms) showed a significant variance to the pre-stimulus bins (Fig. 2A, repeated measurements ANOVA, followed by a multiple comparison Tukey-Kramer correction, $p < 0.05$). Only units responding to presented stimuli were taken into the analysis. Neuron classification was based on the distribution of the maximum responses rates during 500 ms after stimulus onset across all ten trials (Fig. 3A-C,

left panels). Analysis of subgroup response consistency used the maximum spike rate for each stimulus during stimulation onset, normalized to the maximum spike rate of all stimuli (Fig. 3A-C, right panels). Furthermore, we organized the data in stimulus-dependent population vectors using averaged response rates and performed a principal component analysis (PCA; Supplementary Figure S3). Factor loadings of the PCA data were additionally used to organize single units according to the contributed variance values (Fig. 5A). Euclidean distances (L²-Norm) were calculated using a pairwise subtraction of a population vector couple $(v^a - v^b)$ as $d(t) = (\sum (v_i^a(t) - v_i^b(t))^2)^{1/2}$.

3. Results:

3.1 Visual and olfactory-visual driven MBONs

Our goal was to further characterize the visual representation after olfactory-visual convergence at a high-order integration center, the honeybee's mushroom body. Due to the focus of our recordings to units that only fulfilled the visual biased pre-control, we could already exclude purely olfactory driven MBONs and narrow the examined population down to visual and olfactory-visual MBONs. Subsequent spike sorting and response detection analyses confirmed the intended absence of olfactory, non-visual sensitive MBONs. To differentiate between purely visually driven and multimodal MBONs, we included an odor mixture into our stimulation protocol. Since MBONs generalize between different odors (Strube-Bloss et al., 2011) and respond reliably to each unimodal element of a presented compound (Strube-Bloss and Rössler, 2018), one olfactory stimulus seems to be sufficient to control for multimodal activity. Following our criteria, we selected 71 unimodal, purely visually driven units and 19 multimodal units out of 55 bees, resembling 79% and 21 % of the examined MBON population.

### 3.2 Color identity and intensity coding in MBON subpopulations

Analyzing the coding properties of visually driven MBONs revealed three populations of MBONs. The largest group (34%) comprised 31 units that exhibited wavelength specific responses, including two neurons showing multimodal activity (Identity, Fig. 2B). These units showed specific activity to a certain wavelength, especially to UV light. Thereby 14 units showed a strong tuning towards UV light, but did not differentiate between blue or green light (e.g. see exemplary identity-coding unit, Fig. 3B, left panel). Another 6 units significantly distinguished between UV and green light, but did not separate UV and blue or blue and green. Furthermore, 2 units separated UV and blue light, but in turn did not distinguish between UV

and green or blue and green. In addition, 3 units exhibited specific activity towards green light, but did not differ between UV or blue. Remaining 4 units distinguished only between blue and green light and exhibited no significant differences between both colors and UV. Finally, we did not find any unit that was specifically tuned towards blue light, thus not distinguishing between UV and green light. Although, some units encoded brightness effects, this activity was often restricted to a specific wavelength (see Fig. 3B, left panel: Exemplary unit encodes stimulus intensity limited to the UV-spectrum). The second group consists of 30 units (33%) that showed specific activity towards stimulus intensity, regardless of wavelength variances (Intensity, Fig. 2B, 3A). Six neurons in this group responded to both presented modalities. A third group of 24 (27%) visually driven units showed significant responses independent of light identity or intensity. These units are classified as non-specific coding (NonS) and comprise 13 unimodal and 11 multimodal units. A detailed overview of the population response activity of intensity and non-specific coding units is shown in the Supplementary Figure S2, for activity of unimodal, identity coding neurons see paragraph 3.4 and Fig. 5.

3.3 Short term activity increases after visual stimulation

Comparing the baseline activity and different phases after stimulus offset, we separated five units from the previous analyses. These purely visually driven units exhibit a significantly increased spontaneous activity after stimulus offset (Fig. 4A) and therefore are referred to as V_{post} units. This elevated post-stimulus activity lasted for a few seconds after stimulus offset but always returned to baseline level after 60 seconds, before the onset of the following stimulation trial. No multimodal unit was found to exhibit such a characteristic post stimulus activity. This activity was independent of previous stimulus' wavelength or intensity (Fig. 4B) and was expressed by neurons of all three classified subgroups. One unit was classified as identity coding unit, three units were categorized as intensity coding units, and one unit as non-specifically coding unit. In addition, we found that the V_{post} neurons exhibited the shortest inter spike intervals (ISI) and, thus, the highest neural activity rate of all characterized uni- and multimodal MBON subgroups (Supplementary Figure S1).
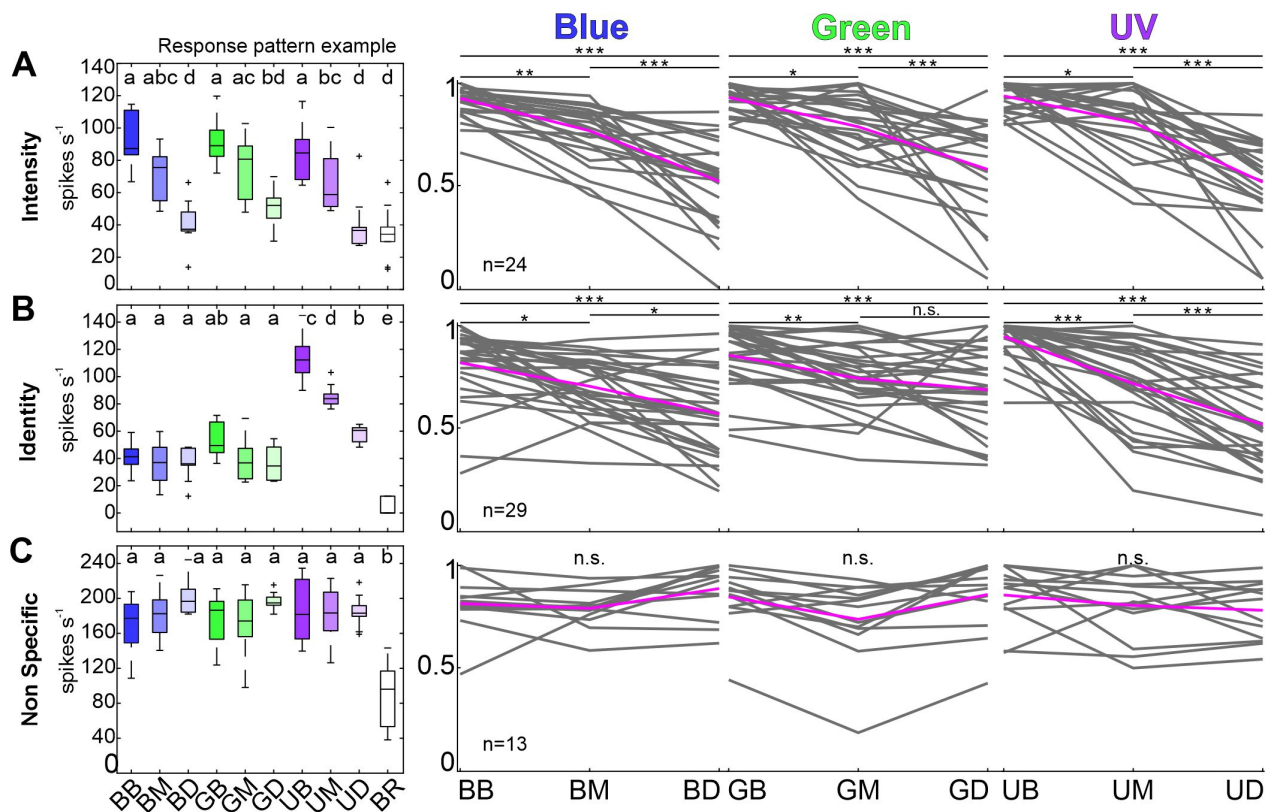
Figure 3. Individual response pattern of unimodal, visually sensitive MBON subpopulations. (A) Example of **one** intensity coding MBON (left most). Boxplots are colored in shades of the respective wavelength (cp. headings on the right), white box corresponds to baseline activity. Same letters indicate shared variance levels (rmANOVA, post-hoc test: Tukey-Kramer, $p < 0.05$). Right panels depict individual response maxima of all neurons in the respective group during 500 ms after stimulus on-set. Depicted maxima are normalized to the maximum light response for each single unit. Single unit activity is shown in grey, mean activity across all units in magenta. Neural activity of the Identity coding subpopulation **(B)** and the Non Specific group **(C)** is presented as described in (A). Activity of multimodal units is not shown. Asterisks mark variances between intensity levels (rmANOVA, post-hoc test: Tukey-Kramer, $p < 0.05$). Abbreviations: BB: Blue Bright, BM: Blue Medium, BD: Blue Dim, GB: Green Bright, GM: Green Medium, GD: Green Dim, UB: UV Bright, UM: UV Medium, UD: UV Dim, BR: Baseline activity.

3.4 Identity coding MBONs separate UV light information

Analysis of individual identity-coding MBONs revealed a high number of neurons encoding stimulus intensity exclusively for UV-light (Fig. 3B). To analyze how the different wavelengths might be specifically encoded by the subpopulation of unimodal, identity coding MBONs, we calculated pairwise Euclidian distances (ED) between population vectors (Fig. 5) and performed a principal component analysis (PCA, Supplementary Figure S3). At the highest intensity, the ED between population response to UV and green or UV and blue light was very prominent and outlasted the stimulus presentation. The same phenomenon occurred in the PCA, in which the trajectory of UV shows a distinct separation from blue and green (Supplementary

Figure S3). In contrast, the discrimination between blue and green light induced activity was rather low (Fig. 5B, Supplementary Figure S3). The same was true for medium and dim light conditions (Fig. 5C). We therefore conclude that it is indeed the UV-light stimulus that is categorized by the unimodal identity-coding MBON subpopulation.
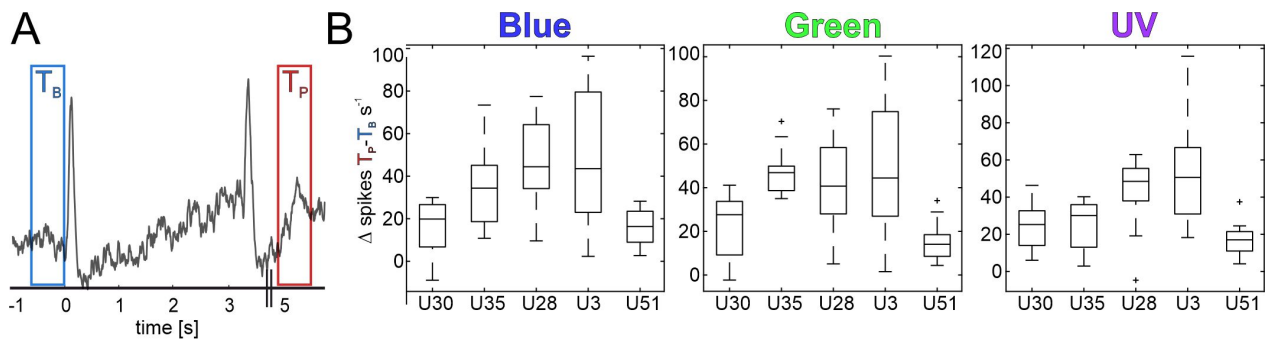
Figure 4. Five MBONs show significant activity after visual stimulation (V_{post}). (A) Mean activity of an exemplary unit, increasing its activity after stimulus off set. Two 500 ms time windows mark time T_B, 500 ms before stimulus on-set (blue) and time T_P, 2 s after stimulus off-set (red). Stimulus starts at time 0 s and lasts 3 s. **(B)** Difference of maximum spike rate between T_P and T_B for all post-stimulus active neurons during bright stimulation. All shown values exhibit significant differences (Wilcoxon signed rank tests, $p < 0.05$).

3.5 MBON response dynamics are not reflected in subgroup classification

Analyses of the MBON response patterns revealed differences in the burst duration after stimulus onset; units either showed a phasic response to the stimulus onset or exhibited a phasic-tonic response, which sometimes lasted throughout the entire stimulus duration (Fig. 2A). Units were rated as *phasic* units when a fast, sharp burst of APs occurred after stimulus onset and lasted for a few hundred milliseconds, before the spike rate dropped back to baseline level. *Phasic-tonic* units also showed an initial phasic onset burst but maintained a significantly increased AP frequency for at least 500 ms. Phasic and phasic-tonic responses were relatively equally distributed across all subgroups and stimulations. Overall, 58% of the recorded units responded in a phasic manner and 42% in a phasic-tonic manner. Only two subgroups showed an individual, slightly above average proportion of phasic-tonically responding units, the identity- and the multimodal intensity-group. Regarding the maximum spike rate, no significant differences between phasic and phasic-tonic units were found (data not shown).
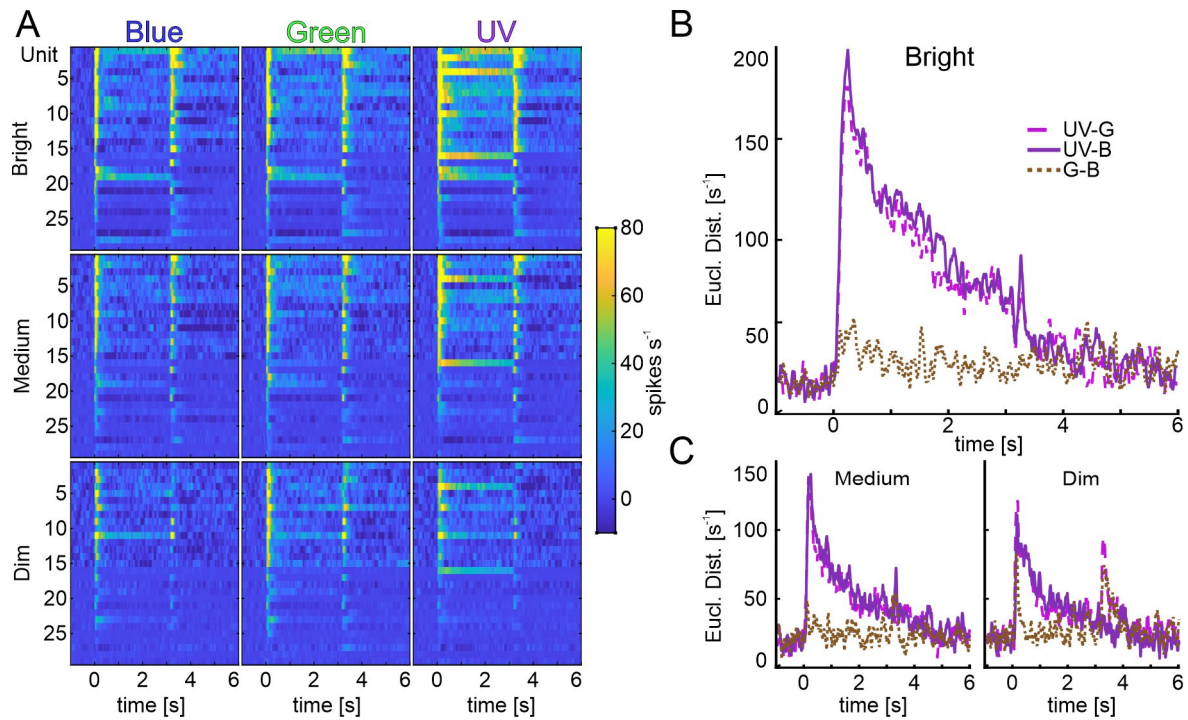
Figure 5. Identity coding MBONs categorize UV-light information. (A) Population vectors of light induced activity of unimodal identity coding MBONs (rows: Brightness; columns: Wavelengths). We performed a principal component analysis to arrange units from top to down, according to their factor loadings of principal component 1 (explaining for 42 % of variance data) **(B)** Pair wise Euclidean distances (ED) between the bright-stimulated population vectors (first column in A; UV-Green: pink, dash-dotted line, UV-Blue: purple, solid line, Green-Blue: brown, dotted line). Note, pairs including UV light induce the highest ED, whereas blue and green pairings exhibit low discrimination rates. **(C)** Data for medium (left panel) and dim (right panel) intensity as described in (B).

4. Discussion

4.1 Extracellular recordings of MBON activity

Performing electrophysiological recordings in a densely packed neuropil is always coupled with the necessity to restrict the recordings or the analysis to the target neuron population, especially while approaching individual neurons extracellularly. As we aimed to gather data from MBONs, we had the choice between the two major output regions of the MBs, the VL and the medial lobe (ML). Since the ML is relatively hard to access due to its deep and dorsally orientated location, even partially covered by the VL, we decided to record from the VL. The position of the VL is thereby close to the brain surface and allows an unobstructed and plain access. With our recordings located in the ventral aspect of the VL, it is hence important to narrow the extraction of neural activity down to the activity of MBONs (axon diameter up to 15 µm, Strube-Bloss et al., 2011). We therefore have to exclude not only activity by Kenyon cell axons (diameter < 0,5 µm, see supplemental data in Strube-Bloss et al. 2011), but also

activity by thin afferent neurons in the protocerebrum (Strausfeld et al., 2000; Strausfeld, 2002) and by passing MB input tracts, namely the anterior superior optic tract (ASOT, diameter ~1,2 µm, Gronenberg 2001), or the medio-lateral antennal lobe tract (ml-ALT). Our triode's design, a very thin bundle of three wires and waiving of gold plating (causing high impedances of ~2 MΩ, whereas gold plated electrodes show impedances below 500 kΩ, Ferguson et al., 2009), guarantees a local and electrical restriction, that both limits the detection of neural signals to the immediate proximity around the electrode's tip and excludes weaker signals due to its high impedance. In addition, the differential recording from all pairwise channel combinations to excludes signals that are not in close vicinity of the electrode tip. Thus, activity of fine KC axons or ASOT neurons is either lost in the background noise level or does not pass the signal threshold in the subsequent spike sorting. Spontaneous neural activity from bypassing axons of the olfactory ml-ALT is sorted out due to its insensitivity to visual stimulations.

4.2 MBONs carry stimulus intensity and identity information

Since the MBs are centers of learning and memory formation most studies of MBONs were focused on olfactory learning and memory induced plasticity (de Belle and Heisenberg, 1994; Menzel and Giurfa, 2001; Menzel, 2014). Although MBs play a key role in multimodal integration and some studies reported visually induced MBON activity (Gronenberg, 1987; Mauelshagen, 1993; Rybak and Menzel, 1998), a systematic study on visual processing of MBONs was yet missing. However, in a recent study, we could show that MBONs mainly categorize olfactory, visual and olfactory-visual information, while distinct information about stimulus quality or quantity within a modality was generalized (Strube-Bloss and Rössler, 2018). Although the non-specific coding subgroup confirms this concept of a broad categorization of visual information, our data additionally shows encoding of stimulus intensity and identity in distinct MBON subpopulations. Until now, information on the representation of stimulus identity or intensity at the level of the MB output is sparse. Studies that actually raised this subject examined the activity of exclusively olfactory MBONs (Strube-Bloss et al., 2011). In other studies, MBONs of the protocerebral-calycal-tract (PCT) cluster, also referred to as A3 neurons were the only identified MBONs, shown to respond multimodally and stimulus-intensity dependent (Haehnel and Menzel, 2010). In contrast to PCT neurons and other multimodal MBONs that arborize in the VL either within a specific layer or across multiple strata (Strausfeld, 2002; Okada et al., 2007; Zwaka et al., 2018), we expect the purely visually driven intensity and identity coding MBONs to restrict their arborizations exclusively to the collar-specific stratum of the VL or to the gamma lobe. The CO stratum and the gamma lobe

are the only strata that can receive purely visual input by either class I KCs from the calyx collar region or by a subset of exclusively visual sensitive class II KCs located in the CO or BR region (Strausfeld, 2002). We assume, that the reported concept of a distinct sparse coding of KCs during olfactory stimulation (Perez-Orive et al., 2002; Szyszka et al., 2005) holds also true for visual stimulation. MBONs responding to this generic coding exhibit a distinct on- and offset activity that is shown for the majority of neurons in this study (Fig. 5A), as well as in MBON populations of the fruit fly (Vrontou et al., 2021).

4.3 Specific categorization of UV light in the vertical lobe

The subpopulation of identity coding MBONs separates UV light from the other presented wavelengths, consistently for all presented intensity levels (Fig. 5B, C). Since we see a robust brightness coding of intensity coding MBONs across all wavelengths (Fig. 3A) and only presented visual stimuli within the same log unit (Tab. 1), we can exclude that this effect is based on stimulation artifacts or experimental settings. Furthermore, we can disregard possible sensitization effects already present at the peripheral level as electroretinographic recordings revealed equal discrimination of visual stimuli of the same wavelength and intensity at the photoreceptor level (*supplements* in Becker et al., 2019). Interestingly, although the EDs between blue and green were small, the distances might increase due to classical conditioning, which had been reported to induce a recruitment of initially insensitive MBONs to encode a reward associated stimulus (Strube-Bloss et al., 2011, 2016). Hence, classical conditioning experiments, in which bees learned to discriminate the very same blue and green light stimuli (Becker et al., 2019) might recruit MBONs to encode the reward associated light, which would result in an increased ED between both wavelengths.

Moreover, we assume that the specific UV activity reflects unique processing and perception of UV light. This hypothesis is supported by behavioral experiments that reported elevated sensitivities of honeybees for UV light (von Helversen, 1972; Labhart, 1974) as well as a prominent modulation of UV perception during cross modal conditioning experiments (Becker et al., 2019). Moreover, the specific perception of UV light reflects its crucial role during daily foraging routines. UV light is not only an essential component during orientation via celestial cues, particularly polarized UV light (von Frisch, 1949; Brines and Gould, 1982; Wehner, 1989), it is also known to play an important role in the processing of flower patterns (von Frisch, 1965; Heiling et al., 2003; Papiorek et al., 2016). Such a distinct representation of UV light in a subpopulation of MBONs will probably channel the UV information further into various

regions, like the protocerebral lobe, including the lateral horn, and potentially modulate decision-making and motor output.

4.4 UV Categorization in the VL: Hardwired or plastic?

MBON activity recorded at the VL has been shown to depend not only on long-term input like learning and recruitment processes (Haehnel and Menzel, 2010, 2012; Strube-Bloss et al., 2011, 2016), it is also known for cockroaches and crickets (Schildberger, 1981; Li and Strausfeld, 1999) that specific combinations of preceding multimodal cues influence MBON activity. Since most of the studies, including our own, used experienced honeybee foragers (von Helversen, 1972; Becker et al., 2019), it is possible that the unique perception of UV is not hardwired but rather the result of learning and experience induced plasticity. Honeybees and other hymenopterans are known to perform learning flights or walks after leaving the hive or nest for the first time (Lindauer, 1952; von Frisch, 1965; Fleischmann et al., 2016; Collett and Zeil, 2018). This behavior enables the insects to perceive sun light for the first time and calibrate their navigational systems to reliably navigate back to the nest (Grob et al., 2019). The change of sensory input is subsequently coupled with a change of tasks that causes a reorganization of calycal structures (reviewed by Groh and Rössler 2020) and thereby possibly affect the VL activity as well. To reliably control for such a long-term or short-term experience dependent plasticity in the perception of UV light, one has to examine MBON activity recorded from the VL of naïve, unexperienced bees and also control for short-term plasticity caused by multimodal stimulation. The second concept could be a labeled line, meaning that the observed prominent representation is a hardwired prerequisite for using UV light during navigation and orientation tasks. Although the central complex has been shown to be an important neuropil in the insect brain for orientation and navigation (Pfeiffer and Homberg, 2014; Hensgen et al., 2021), there is little information of a direct connection of the central complex and the MBs in honeybees that could explain such a unique categorization of UV light. Furthermore, it is not clear yet how much UV- information, or even polarization information, is relayed to the MBs. Nevertheless, we expect distinct connections of the MBs and the central complex in the honeybee, since this pathway may be conserved in neopteran insects and such connections have been reported in the monarch butterfly (TU-neuron, Heinze et al., 2013) and the fruit fly (multiple MBONs, Hulse et al., 2021; ppl1 neurons, Krashes et al., 2009 and Liu et al., 2012).

4.5 Short-term memory after stimulus offset

Olfactory and visual learning in the honeybee have been described extensively in conditioning studies over the last decades (Bitterman et al., 1983; Avarguès-Weber et al., 2011; Dobrin and Fahrbach, 2012; Giurfa and Sandoz, 2012; Lichtenstein et al., 2018). Visual conditioning heavily relies on the temporal relationship between reward associated stimulus and reward. It is most effective when both stimuli are presented with an overlap of three seconds at the end of the visual stimulus (reviewed in Avarguès-Weber and Mota 2016). Since details of the underlying neuronal and molecular processes necessary for associative learning are still unclear, we can only speculate and formulate models (Smith et al., 2008). So far, research mainly covered age and experience influences on structural plasticity of microglomerular circuits in the MB calyx (Groh and Rössler, 2020), the essential role of neuromodulators in the network (Hammer and Menzel, 1995, 1998; Schwaerzel et al., 2003), and, additionally, modulatory input to the MB calycal region by GABAergic feedback MBONs (Gronenberg, 1987; Grünewald, 1999; Ganeshina and Menzel, 2001; Haehnel and Menzel, 2010; Zwaka et al., 2018), and other (octopaminergic) extrinsic neurons (Hammer, 1993; Mauelshagen, 1993; Blenau et al., 1999; Okada et al., 2007). Furthermore, a distinct increase or decrease of neural activity following a stimulus reward association has been described for olfactory MBONs and the multimodal PE1 neuron (Okada et al. 2007; Strube-Bloss et al., 2011; 2016). The unique activity increase of the V_{post} group (Fig. 4) could thereby be part of such experience-related modulations that have been already reported for similar concepts in studies in mouse models (Han et al., 2008; Yu et al., 2021). The increased network activity can act as a prerequisite to integrate other simultaneously occurring modalities, like a reward representation, similar to the concept of coincidence detection at the KC level (Perez-Orive et al., 2002). The momentary increased activity of the V_{post} neurons may act as a short-term (trace) memory and either enable the successful association of paired stimuli or, conversely, prohibit a robust connection to the reward if the interval between reward and stimulus becomes too long resulting in an unsuccessful (un-paired) association (Giurfa, 2007).

Conflict of Interest:

Author contributions:

Funding:

References

Avarguès-Weber, A., Deisig, N., and Giurfa, M. (2011). Visual Cognition in Social Insects. *Annu. Rev. Entomol.* 56, 423–443. doi:10.1146/annurev-ento-120709-144855.

Avarguès-Weber, A., and Mota, T. (2016). Advances and limitations of visual conditioning protocols in harnessed bees. *J. Physiol. Paris* 110, 107–118. doi:10.1016/j.jphysparis.2016.12.006.

Becker, M. C., Rössler, W., and Strube-Bloss, M. F. (2019). UV-light perception is modulated by the odour element of an olfactory-visual compound in restrained honeybees. *J. Exp. Biol.* 222, jeb.201483. doi:10.1242/jeb.201483.

Bitterman, M. E., Menzel, R., Fietz, A., and Schäfer, S. (1983). Classical conditioning of proboscis extension in honeybees (Apis mellifera). *J. Comp. Psychol.* 97, 107–119. doi:10.1037/0735-7036.97.2.107.

Blenau, W., Schmidt, M., Faensen, D., and Schürmann, F.-W. (1999). Neurons with dopamine-like immunoreactivity target mushroom body Kenyon cell somata in the brain of some hymenopteran insects. *Int. J. Insect Morphol. Embryol.* 28, 203–210. doi:10.1016/S0020-7322(99)00025-2.

Brill, M. F., Reuter, M., Rössler, W., and Strube-Bloss, M. F. (2014). Simultaneous long-term recordings at two neuronal processing stages in behaving honeybees. *J. Vis. Exp.*, 2014. doi:10.3791/51750.

Brill, M. F., Rosenbaum, T., Reus, I., Kleineidam, C. J., Nawrot, M. P., and Rössler, W. (2013). Parallel processing via a dual olfactory pathway in the honeybee. *J. Neurosci.* 33, 2443–56. doi:10.1523/JNEUROSCI.4268-12.2013.

Brines, M. L., and Gould, J. L. (1982). Skylight Polarization patterns and Animal Orientation. *J. Exp. Biol.* 96, 69–91. doi:10.1242/jeb.96.1.69.

Chen, W., and Viljoen, A. M. (2010). Geraniol — A review of a commercially important fragrance material. *South African J. Bot.* 76, 643–651. doi:10.1016/j.sajb.2010.05.008.

Collett, T. S., and Zeil, J. (2018). Insect learning flights and walks. *Curr. Biol.* 28, R984–R988. doi:10.1016/j.cub.2018.04.050.

de Belle, J., and Heisenberg, M. (1994). Associative odor learning in Drosophila abolished by chemical ablation of mushroom bodies. *Science (80-.).* 263, 692–695. doi:10.1126/science.8303280.

Dobrin, S. E., and Fahrbach, S. E. (2012). Visual Associative Learning in Restrained Honey Bees with Intact Antennae. *PLoS One* 7, e37666. doi:10.1371/journal.pone.0037666.

Ehmer, B., and Gronenberg, W. (2002). Segregation of visual input to the mushroom bodies in the honeybee (Apis mellifera). *J. Comp. Neurol.* 451, 362–373. doi:10.1002/cne.10355.

Fahrbach, S. E. (2006). Structure Of The Mushroom Bodies Of The Insect Brain. *Annu. Rev. Entomol.* 51, 209–232. doi:10.1146/annurev.ento.51.110104.150954.

Ferguson, J. E., Boldt, C., and Redish, A. D. (2009). Creating low-impedance tetrodes by electroplating with additives. *Sens. Actuators. A. Phys.* 156, 388–393. doi:10.1016/j.sna.2009.10.001.

Filla, I., and Menzel, R. (2015). Mushroom body extrinsic neurons in the honeybee (Apis mellifera) brain integrate context and cue values upon attentional stimulus selection. *J. Neurophysiol.* 114, 2005–2014. doi:10.1152/jn.00776.2014.

Fleischmann, P. N., Christian, M., Müller, V. L., Rössler, W., and Wehner, R. (2016). Ontogeny of learning walks and the acquisition of landmark information in desert ants, Cataglyphis fortis. *J. Exp. Biol.* 219, 3137–3145. doi:10.1242/jeb.140459.

Galizia, G. C., Joerges, J., Küttner, A., Faber, T., and Menzel, R. (1997). A semi-in-vivo preparation for optical recording of the insect brain. *J. Neurosci. Methods* 76, 61–69. doi:10.1016/S0165-0270(97)00080-0.

Ganeshina, O., and Menzel, R. (2001). GABA-immunoreactive neurons in the mushroom bodies of the honeybee: An electron microscopic study. *J. Comp. Neurol.* 437, 335–349. doi:10.1002/cne.1287.

Giurfa, M. (2007). Behavioral and neural analysis of associative learning in the honeybee: a taste from the magic well. *J. Comp. Physiol. A* 193, 801–824. doi:10.1007/s00359-007-0235-9.

Giurfa, M., and Sandoz, J.-C. (2012). Invertebrate learning and memory: Fifty years of olfactory conditioning of the proboscis extension response in honeybees. *Learn. Mem.* 19, 54–66. doi:10.1101/lm.024711.111.

Grob, R., Fleischmann, P. N., and Rössler, W. (2019). Learning to navigate – how desert ants calibrate their compass systems. *Neuroforum* 25, 109–120. doi:10.1515/nf-2018-0011.

Groh, C., and Rössler, W. (2020). Analysis of Synaptic Microcircuits in the Mushroom Bodies of the Honeybee. *Insects* 11, 43. doi:10.3390/insects11010043.

Gronenberg, W. (1987). Anatomical and physiological properties of feedback neurons of the mushroom bodies in the bee brain. *Exp. Biol.* 46, 115–25.
Available at: http://www.ncbi.nlm.nih.gov/pubmed/3582581.

Gronenberg, W. (2001). Subdivisions of hymenopteran mushroom body calyces by their afferent supply. *J. Comp. Neurol.* 435, 474–489. doi:10.1002/cne.1045.

Grünewald, B. (1999). Morphology of feedback neurons in the mushroom body of the honeybee, Apis mellifera. *J. Comp. Neurol.* 404, 114. doi:10.1002/(SICI)1096-9861(19990201)404:1<114::AID-CNE9>3.3.CO;2-R.

Haehnel, M., and Menzel, R. (2010). Sensory Representation and Learning-Related Plasticity in Mushroom Body Extrinsic Feedback Neurons of the Protocerebral Tract. *Front. Syst. Neurosci.* 4, 1–13. doi:10.3389/fnsys.2010.00161.

Haehnel, M., and Menzel, R. (2012). Long-term memory and response generalization in mushroom body extrinsic neurons in the honeybee Apis mellifera. *J. Exp. Biol.* 215, 559–565. doi:10.1242/jeb.059626.

Hammer, M. (1993). An identified neuron mediates the unconditioned stimulus in associative olfactory learning in honeybees. *Nature* 366, 59–63. doi:10.1038/366059a0.

Hammer, M., and Menzel, R. (1995). Learning and memory in the honeybee. *J. Neurosci.* 15, 1617–30.
Available at: http://linkinghub.elsevier.com/retrieve/pii/S0960982205010419.

Hammer, M., and Menzel, R. (1998). Multiple sites of associative odor learning as revealed by local brain microinjections of octopamine in honeybees. *Learn. Mem.* 5, 146–56. Available at: https://www.ncbi.nlm.nih.gov/pmc/articles/PMC311245/pdf/x2.pdf.

Han, F., Caporale, N., and Dan, Y. (2008). Reverberation of Recent Visual Experience in Spontaneous Cortical Waves. *Neuron* 60, 321–327. doi:10.1016/j.neuron.2008.08.026.

Heiling, A. M., Herberstein, M. E., and Chittka, L. (2003). Crab-spiders manipulate flower signals. *Nature* 421, 334–334. doi:10.1038/421334a.

Heinze, S., Florman, J., Asokaraj, S., el Jundi, B., and Reppert, S. M. (2013). Anatomical basis of sun compass navigation II: The neuronal composition of the central complex of the monarch butterfly. *J. Comp. Neurol.* 521, 267–298. doi:10.1002/cne.23214.

Hensgen, R., England, L., Homberg, U., and Pfeiffer, K. (2021). Neuroarchitecture of the central complex in the brain of the honeybee: Neuronal cell types. *J. Comp. Neurol.* 529, 159–186. doi:10.1002/cne.24941.

Homberg, U. (1984). Processing of antennal information in extrinsic mushroom body neurons of the bee brain. *J. Comp. Physiol. A* 154, 825–836. doi:10.1007/BF00610683.

Hulse, B. K., Haberkern, H., Franconville, R., Turner-Evans, D. B., Takemura, S., Wolff, T., et al. (2021). A connectome of the Drosophila central complex reveals network motifs suitable for flexible navigation and context-dependent action selection. *Elife* 10. doi:10.7554/eLife.66039.

Kirschner, S., Kleineidam, C. J., Zube, C., Rybak, J., Grünewald, B., and Rössler, W. (2006). Dual olfactory pathway in the honeybee, Apis mellifera. *J. Comp. Neurol.* 499, 933–952. doi:10.1002/cne.21158.

Krashes, M. J., DasGupta, S., Vreede, A., White, B., Armstrong, J. D., and Waddell, S. (2009). A Neural Circuit Mechanism Integrating Motivational State with Memory Expression in Drosophila. *Cell* 139, 416–427. doi:10.1016/j.cell.2009.08.035.

Labhart, T. (1974). Behavioral analysis of light intensity discrimination and spectral sensitivity in the honey bee,Apis mellifera. *J. Comp. Physiol. ? A* 95, 203–216. doi:10.1007/BF00625444.

Li, Y., and Strausfeld, N. J. (1997). Morphology and sensory modality of mushroom body extrinsic neurons in the brain of the cockroach, Periplaneta americana. *J. Comp. Neurol.* 387, 631–50. doi:10.1002/(SICI)1096-9861(19971103)387:4<631::AID-CNE9>3.0.CO;2-3.

Li, Y., and Strausfeld, N. J. (1999). Multimodal efferent and recurrent neurons in the medial lobes of cockroach mushroom bodies. *J. Comp. Neurol.* 409, 647–663. doi:10.1002/(SICI)1096-9861(19990712)409:4<647::AID-CNE9>3.0.CO;2-3.

Lichtenstein, L., Lichtenstein, M., and Spaethe, J. (2018). Length of stimulus presentation and visual angle are critical for efficient visual PER conditioning in the restrained honey bee, Apis mellifera . *J. Exp. Biol.* 221, jeb179622. doi:10.1242/jeb.179622.

Lindauer, M. (1952). Ein Beitrag zur Frage der Arbeitsteilung im Bienenstaat. *Z. Vgl. Physiol.* 34, 299–345. doi:10.1007/BF00298048.

Liu, Q., Liu, S., Kodama, L., Driscoll, M. R., and Wu, M. N. (2012). Two dopaminergic neurons signal to the dorsal fan-shaped body to promote wakefulness in Drosophila. *Curr. Biol.* 22, 2114–2123. doi:10.1016/j.cub.2012.09.008.

Lunau, K. (1993). Interspecific diversity and uniformity of flower colour patterns as cues for learned discrimination and innate detection of flowers. *Experientia* 49, 1002–1010. doi:10.1007/BF02125649.

Luxová, A., Urbanová, K., Valterová, I., Terzo, M., and Borg-Karlson, A.-K. (2004). Absolute

configuration of chiral terpenes in marking pheromones of bumblebees and cuckoo bumblebees. *Chirality* 16, 228–233. doi:10.1002/chir.20017.

Mauelshagen, J. (1993). Neural correlates of olfactory learning paradigms in an identified neuron in the honeybee brain. *J. Neurophysiol.* 69, 609–625. doi:10.1152/jn.1993.69.2.609.

Meier, R., Egert, U., Aertsen, A., and Nawrot, M. P. (2008). FIND — A unified framework for neural data analysis. *Neural Networks* 21, 1085–1093. doi:10.1016/j.neunet.2008.06.019.

Menzel, R. (2014). The insect mushroom body, an experience-dependent recoding device. *J. Physiol.* 108, 84–95. doi:10.1016/j.jphysparis.2014.07.004.

Menzel, R., and Giurfa, M. (2001). Cognitive architecture of a mini-brain: the honeybee. *Trends Cogn. Sci.* 5, 62–71. doi:10.1016/S1364-6613(00)01601-6.

Menzel, R., and Manz, G. (2005). Neural plasticity of mushroom body-extrinsic neurons in the honeybee brain. *J. Exp. Biol.* 208, 4317–4332. doi:10.1242/jeb.01908.

Müller, D., Abel, R., Brandt, R., Zöckler, M., and Menzel, R. (2002). Differential parallel processing of olfactory information in the honeybee, Apis mellifera L. *J. Comp. Physiol. A Neuroethol. Sensory, Neural, Behav. Physiol.* 188, 359–370. doi:10.1007/s00359-002-0310-1.

Okada, R., Rybak, J., Manz, G., and Menzel, R. (2007). Learning-Related Plasticity in PE1 and Other Mushroom Body-Extrinsic Neurons in the Honeybee Brain. *J. Neurosci.* 27, 11736–11747. doi:10.1523/JNEUROSCI.2216-07.2007.

Papiorek, S., Junker, R. R., Alves-dos-Santos, I., Melo, G. A. R., Amaral-Neto, L. P., Sazima, M., et al. (2016). Bees, birds and yellow flowers: pollinator-dependent convergent evolution of UV patterns. *Plant Biol.* 18, 46–55. doi:10.1111/plb.12322.

Peitsch, D., Fietz, A., Hertel, H., Souza, J., Ventura, D., and Menzel, R. (1992). The spectral input systems of hymenopteran insects and their receptor-based colour vision. *J. Comp. Physiol. A* 170, 23–40. doi:10.1007/BF00190398.

Perez-Orive, J., Mazor, O., Turner, G. C., Cassenaer, S., Wilson, R. I., and Laurent, G. (2002). Oscillations and Sparsening of Odor Representations in the Mushroom Body. *Science (80-.).* 297, 359–365. doi:10.1126/science.1070502.

Pfeiffer, K., and Homberg, U. (2014). Organization and functional roles of the central complex in the insect brain. *Annu. Rev. Entomol.* 59, 165–184. doi:10.1146/annurev-ento-011613-162031.

Rybak, J., and Menzel, R. (1993). Anatomy of the mushroom bodies in the honey bee brain: the neuronal connections of the alpha-lobe. *J. Comp. Neurol.* 334, 444–65. doi:10.1002/cne.903340309.

Rybak, J., and Menzel, R. (1998). Integrative properties of the Pe1 neuron, a unique mushroom body output neuron. *Learn. Mem.* 5, 133–145. doi:10.1101/lm.5.1.133.

Schildberger, K. (1981). Some physiological features of mushroom-body linked fibers in the house cricket brain. *Naturwissenschaften* 68, 623–624. doi:10.1007/BF00398621.

Schröter, U., and Menzel, R. (2003). A new ascending sensory tract to the calyces of the honeybee mushroom body, the subesophageal-calycal tract. *J. Comp. Neurol.* 465, 168–178. doi:10.1002/cne.10843.

Schwaerzel, M., Monastirioti, M., Scholz, H., Friggi-Grelin, F., Birman, S., and Heisenberg, M. (2003). Dopamine and Octopamine Differentiate between Aversive and Appetitive Olfactory Memories in Drosophila. *J. Neurosci.* 23, 10495–10502. doi:10.1523/JNEUROSCI.23-33-10495.2003.

Smith, D., Wessnitzer, J., and Webb, B. (2008). A model of associative learning in the mushroom body. *Biol. Cybern.* 99, 89–103. doi:10.1007/s00422-008-0241-1.

Srinivasan, M. V. (2010). Honey Bees as a Model for Vision, Perception, and Cognition. *Annu. Rev. Entomol.* 55, 267–284. doi:10.1146/annurev.ento.010908.164537.

Srinivasan, M. V., and Zhang, S. (2004). Visual motor computations in insects. *Annu. Rev. Neurosci.* 27, 679–96. doi:10.1146/annurev.neuro.27.070203.144343.

Strausfeld, N. J. (2002). Organization of the honey bee mushroom body: Representation of the calyx within the vertical and gamma lobes. *J. Comp. Neurol.* 450, 4–33. doi:10.1002/cne.10285.

Strausfeld, N. J., Homberg, U., Kloppenburg, P., and Kloppenberg, P. (2000). Parallel organization in honey bee mushroom bodies by peptidergic Kenyon cells. *J. Comp. Neurol.* 424, 179–95. doi:10.1002/1096-9861(20000814)424:1<179::AID-CNE13>3.0.CO;2-K.

Strube-Bloss, M. F., Nawrot, M. P., and Menzel, R. (2011). Mushroom Body Output Neurons Encode Odor-Reward Associations. *J. Neurosci.* 31, 3129–3140. doi:10.1523/JNEUROSCI.2583-10.2011.

Strube-Bloss, M. F., Nawrot, M. P., and Menzel, R. (2016). Neural correlates of side-specific odour memory in mushroom body output neurons. *Proc. R. Soc. B Biol. Sci.* 283, 20161270. doi:10.1098/rspb.2016.1270.

Strube-Bloss, M. F., and Rössler, W. (2018). Multimodal integration and stimulus categorization in putative mushroom body output neurons of the honeybee. *R. Soc. Open Sci.* 5, 171785. doi:10.1098/rsos.171785.

Szyszka, P., Ditzen, M., Galkin, A., Galizia, G. C., and Menzel, R. (2005). Sparsening and Temporal Sharpening of Olfactory Representations in the Honeybee Mushroom Bodies. *J. Neurophysiol.* 94, 3303–3313. doi:10.1152/jn.00397.2005.

Trhlin, M., and Rajchard, J. (2011). &nbsp;Chemical communication in the honeybee (Apis mellifera L.): a review. *Vet. Med. (Praha).* 56, 265–273. doi:10.17221/1543-VETMED.

von Frisch, K. (1914). *Der farbensinn und Formensinn der Biene.* Jena,: Fischer, doi:10.5962/bhl.title.11736.

von Frisch, K. (1949). The Polarization of the Sky Light as a Factor in the Bees' Dances. *Experientia* 5, 142–8. doi:10.1007/BF02174424.

von Frisch, K. (1965). *Tanzsprache und Orientierung der Bienen.* Berlin, Heidelberg: Springer Berlin Heidelberg doi:10.1007/978-3-642-94916-6.

von Helversen, O. (1972). Zur spektralen Unterschiedsempfindlichkeit der Honigbiene. *J. Comp. Physiol.* 80, 439–472. doi:10.1007/BF00696438.

Vrontou, E., Groschner, L. N., Szydlowski, S., Brain, R., Krebbers, A., and Miesenböck, G. (2021). Response competition between neurons and antineurons in the mushroom body. *Curr. Biol.* 31, 4911-4922.e4. doi:10.1016/j.cub.2021.09.008.

Wehner, R. (1989). The Hymenopteran Skylight Compass: Matched Filtering and Parallel Coding. *J. Exp. Biol.* 146, 63–85. doi:10.1242/jeb.146.1.63.

Yu, Q., Fu, H., Wang, G., Zhang, J., and Yan, B. (2021). Short-Term Visual Experience Leads to Potentiation of Spontaneous Activity in Mouse Superior Colliculus. *Neurosci. Bull.* 37, 353–368. doi:10.1007/s12264-020-00622-3.

Zwaka, H., Bartels, R., Grünewald, B., and Menzel, R. (2018). Neural Organization of A3 Mushroom Body Extrinsic Neurons in the Honeybee Brain. *Front. Neuroanat.* 12, 1–11. doi:10.3389/fnana.2018.00057.
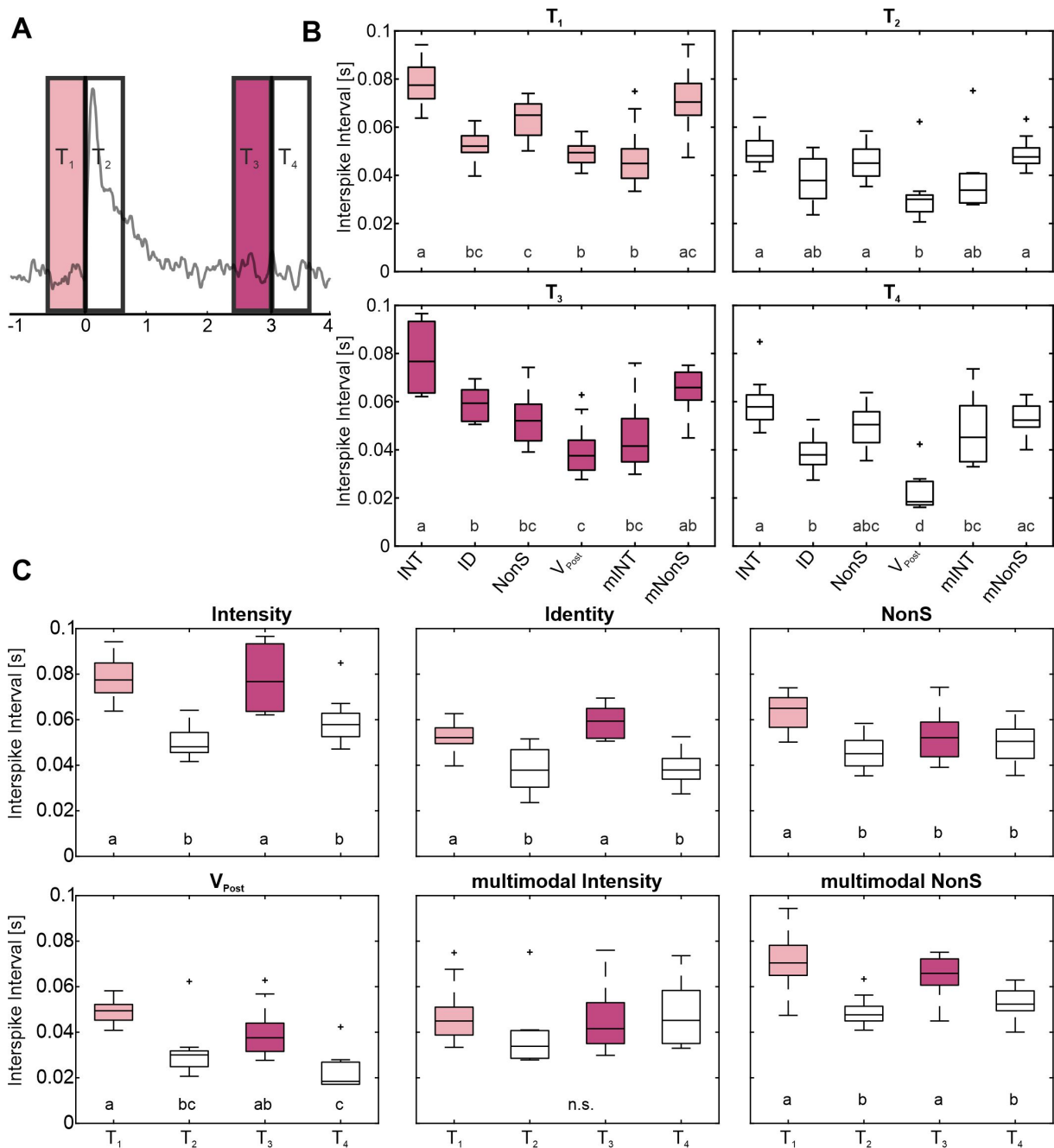
Figure S1. Interspike intervals of MBON subgroups. (A) Exemplary activity of one MBON. Boxes show four 500 ms time windows during which mean interspike intervals (ISI) are calculated: T_1: 500 ms before stimulus on-set, T_2: stimulus on-set, T_3: 500 ms before stimulus off-set, T_4: 500 ms after stimulus off-set. Stimulus starts at 0 s and lasts 3 s. (B) ISI are shown for all examined MBON subgroups at T_{1-4} (except multimodal Identity neurons, due to their little n-size). Same letters indicate shared variance levels groups (one-way ANOVA, post-hoc test: Tukey-Kramer, $p < 0.05$). (C) Group specific comparison of ISI at T_{1-4} (one-way ANOVA, post-hoc test: Tukey-Kramer, $p < 0.05$). Abbreviations: INT: Intensity, ID: Identity, NonS: Non-specific, V_{Post}: Visual post-stimulus active, mINT: Multimodal Intensity, mNonS: Multimodal NonS.
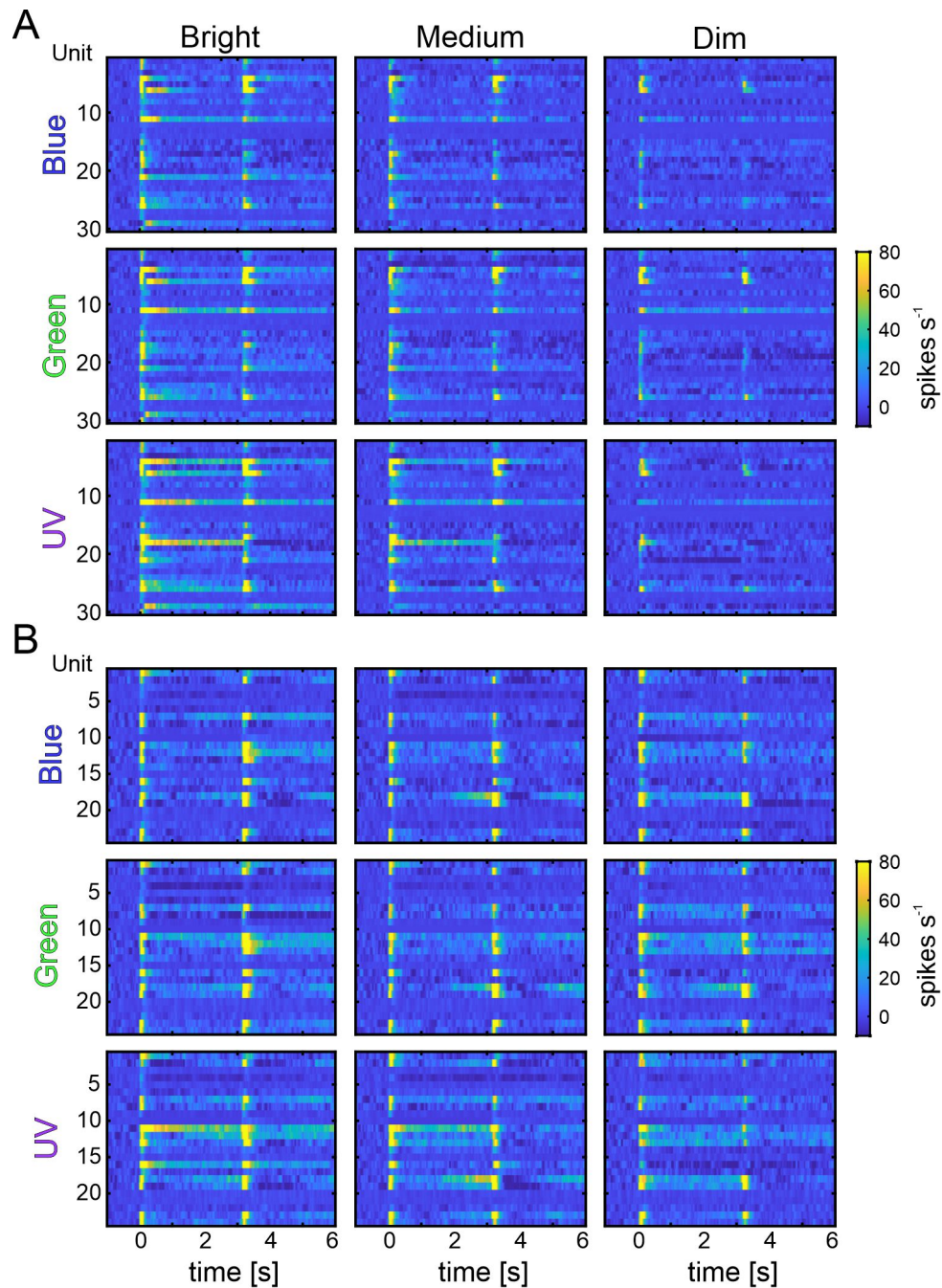
Figure S2. Neural activity of Intensity and Non-specific coding neurons (A) Population vectors of light induced activity of intensity coding MBONs (Rows: Wavelengths; Columns: Brightness). Each heat map shows activity of unimodal (first 24 units) and multimodal (units 22-30) intensity coding neurons. **(B)** Population vectors of light induced activity of non-specific coding MBONs, as explained in A. Each heat map shows activity of unimodal (first 13 units) and multimodal (units 14-24) non-specific coding neurons. Color bar indicates spike activity.
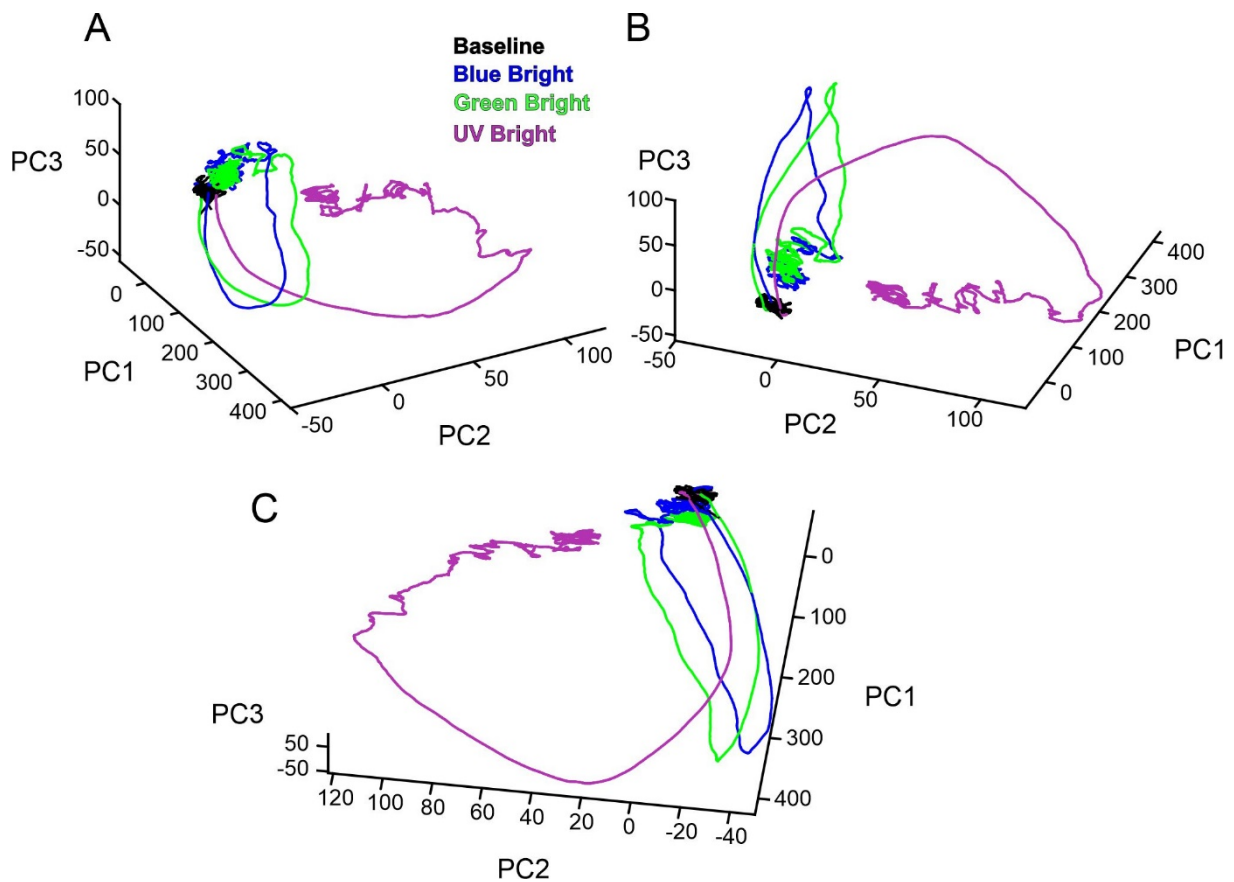
Figure S3. Principal component analyses of unimodal, identity coding MBONs
(A) Trajectories of first three principal components show a clear separation of populational activity. 100 ms of baseline are displayed in black, followed by three seconds stimulation with blue bright (blue), green bright (green) and UV bright (magenta). PC1, PC2 and PC3 explain for 42 %, 17% and 9% of variance data, respectively. Interestingly, in contrast blue and green light, UV light seems to elicit distinct tonic activity. Azimuth: 64, Elongation: 47(B) and (C). Data as explained in A. Azimuth: 69 and -98 Elongation: -53 and -83.

4. General discussion

To this day, the understanding of the distinct processing of behaviorally relevant stimuli by the sensory system of bumblebees and honeybees is still incomplete. In the course of this thesis, I was able to gain more insight on this subject by combining behavioral and electrophysiological approaches at different levels along the olfactory and visual sensory pathways.

In chapter 2, I examined sex-specific differences in the olfactory processing of bumblebee workers and drones. Analyses of their behavior revealed a strong generalization towards the odorant molecule size during conditioning and memory experiments in both sexes. Experiments along the olfactory pathway found receptive activity at the antennae level to be stimulus- and sex-specific. Interestingly, in both sexes, distinct stimulus representation found at the antennae was not reflected in the antennal lobe activity. On the contrary, stimuli with a rather low peripheral profile, stood out in the antennal lobe activity, e.g. 2,3-dihydrofarnesol and farnesol, both components of sex-specific pheromones. This effect was especially pronounced in the female antennal lobe activity, corroborating recent findings of a unique farnesol representation.

In chapter 3, I broadened our understanding of modality representation in the honeybee vertical lobe and showed for the first time an encoding of intensity and identity of visual stimuli, resulting in a new classification of visual MBONs. Additionally, I found a unique processing of UV light specifically linked to a just defined stimulus-identity coding group. In the following, I will discuss features of the processing of behaviorally relevant stimuli including the findings in chapters 2 and 3 in both bumblebees & honeybees and give insights on subsequent approaches based on the elaborated results. Finally, I will conclude with my personal remarks on this research topic.

4. 1 Peripheral stimulus representation as insufficient indication of behavioral impact

We see certain stimuli in chapter 2 (e.g. citronellol, farnesol) to evoke distinctly different neural activity at the EAG level and in the AL. I assume this transition of the neural representation from the receptor level to the AL is connected to the ecological role of the respective odor, e.g. farnesol as a major component of the bumblebee recruitment pheromone. Studies in honeybees and ants found, that the glomerular organization in the female AL is distinctly different from the male AL (Nishino et al., 2009; Kelber et al., 2010;

Nishikawa et al., 2012). In particular, ORNs from the worker-specific *Sensilla basiconica* are prevalently innervating the glomerular T3 cluster in honeybees and the T6 cluster in *Atta vollenweiderei* (Kelber et al., 2010; Kropf et al., 2014). Moreover, the T3 cluster in honeybees is shown to be distinctly reduced in males (Nishino et al., 2009), a likely consequence of the missing ORN input from *S. basiconica* (Kropf et al., 2014). This innervation by *S. basiconica* has been theorized to act as input of a specific sensory pathway for social tasks in *Camponotus japonicus* (Nishikawa et al., 2012). Due to striking similarities in bumblebees and honeybees, regarding the sensory input (honeybee: e.g. Lacher, 1964; Esslen and Kaissling, 1976; Getz and Akers, 1993; bumblebee: e.g. Fonta and Masson, 1987; Ågren and Hallberg, 1996) and neural architecture (honeybee: e.g. Arnold et al., 1985; Rybak et al., 2010; bumbleebee: e.g. Mertes et al., 2021; Rother et al., 2021), such a conserved, worker-specific layout of the glomerular innervation pattern can be the neural substrate in the female AL for the distinct representation of key odorants like farnesol. Thus, subsequent research on this topic should consider selective stainings of olfactory sensilla, especially of *S. basiconica*, to gain more insights on a possible, sex-specific, neural prerequisite in the female AL of *B. terrestris*.

We also find striking differences between sensory representations and central brain representations of visual stimuli. The processing of visual information in the MBON population of the honeybee VL was found to be specifically tuned towards stimulation with UV-light (chapter 3, Fig. 5 B,C), whereas electroretinographic (ERG) examinations in a previous study showed no distinct differences of the discrimination between the same visual stimuli (supplementary material in Becker et al., 2019). A specific processing of UV has also been reported in behavioral approaches that found not only an elevated sensitivity towards UV light (von Helversen, 1972; Labhart, 1974), but also a modulated role of UV-perception during cross-modal conditioning experiments (Becker et al., 2019). In general, the perception of UV light has been found to play an important role in the honeybee ecology, not only for the detection of flower patterns (von Frisch, 1965; Thompson et al., 1972; Heiling et al., 2003; Papiorek et al., 2016), but also as key component during navigation and orientation by celestial cues, like polarized light (von Frisch, 1949; Brines and Gould, 1982; Wehner, 1989). Interestingly, polarized skylight is thereby received through a distinct area in the retina of several insect species, the dorsal rim area (DRA, Labhart and Meyer, 1999). In honeybees, the reception of polarized light is mediated via UV-sensitive retinulacells in ommatidia of the DRA,

expressing non-twisted rhabdomeres, orthogonally aligned to each other and thus being able to absorb UV light of certain oscillation planes (Schinz, 1975; Labhart and Meyer, 1999). Since several studies showed connections of the insect MB and the central complex (e.g. Liu et al., 2012; Heinze et al., 2013; Hulse et al., 2021), the designated neuropil for orientation and navigation (Pfeiffer and Homberg, 2014; Hensgen et al., 2021), further experiments should investigate a possible impact of polarized light on the activity of the identity-coding MBONs. An expansion of the stimulation set-up to include polarized light would in turn require a reassessment of the representation of specifically polarized UV light in the periphery and the VL.

In general, our results support the view, that a rather low neural activity in the periphery allows hardly a comprehensive assumption about the neural or behavioral relevance of a stimulus, since impactful modulation may initially occur after a first stage of processing, e.g. in the AL or the OL. Despite the fact, that little is known about the specific neural circuits underlying the processing of key stimuli in honeybees or bumblebees, research of courtship behavior in fruit flies shows, that behaviorally relevant processes are affecting the neural circuits after a first processing of both, olfactory and visual cues. During the stimulation with sex pheromones, a specific behaviorally relevant circuit receives its crucial input from olfactory PNs, subsequent to a first processing in the AL (Ruta et al., 2010). Moreover, a modulation of another behaviorally relevant circuitry has been reported in the visual pathway. Here, the gain of visual PNs originating in the fly lobula is modulated by sexual arousal and thus influencing the subsequent visual pathway and courtship behavior (Hindmarsh Sten et al., 2021).

4.2. Plasticity induced modulation of sensory processing

Plasticity in insects is occurring in multiple levels along the olfactory pathway, e.g. at the antennal level, in the AL or in the MB (reviewed in Anton and Rössler, 2021) and has been well researched in various species, e.g. in honeybees (e.g. Groh et al., 2006; Jernigan et al., 2020), moths (e.g. Greiner et al., 2002; Guerrieri et al., 2012), and blood-feeding bugs (e.g. Bodin et al., 2009; Reisenman, 2014). The intensity and on-set of plasticity depends on various biotic and abiotic factors, including state-dependency, age-related effects, environmental aspects or learning & memory processes (reviewed in Anton and Rössler, 2021). At the antennal level, plasticity is reported to be induced by memory effects, like olfactory learning (Claudianos et

al., 2014), by state dependent factors, like circadian rhythms (reviewed in Gadenne et al., 2016), by nutritional effects, e.g. in fruit flies (Jung et al., 2018), or by mating status, e.g. in moths and hymenopterans (moths: e.g. Martel et al., 2009; Saveer et al., 2012; hymenopterans: Ghaninia et al., 2017; Lenschow et al., 2018). Until this day, the occurrence of plasticity in bumblebee antennae has not been specifically examined. Since our EAG experiments were performed only during the activity period of the animals (~10 am-4 pm), comprised non-reproductive workers & unmated drones, and guaranteed an ad-libitum access to sucrose solution, we assume antennal plasticity induced by state dependent factors to be unlikely. Nevertheless, future experiments should control for plastic effects at the antennal level in regard of learning and memory dependent changes in OR expression, as shown in honeybees (Claudianos et al., 2014).

In the AL, studies in honeybees found a distinct plasticity linked to maturation and polyethism (Winnington et al., 1996; Wang et al., 2005; Jernigan et al., 2020). Due to the fact that bumblebee workers do not exhibit polyethism but alloethism, advanced insights to an alloethism-induced plasticity in the AL would require a specific separation of task- and age-related test groups. So far, AL volume in bumblebees was shown to exhibit plastic changes only in correlation with age but not with sensory exposure (Jones et al., 2013). However, specific glomeruli in the fruit fly have been shown to exhibit plastic volume changes and interneuron activity due to sensory exposure to CO_2 (Sachse et al., 2007). A volume change in a single glomerulus is very distinct in the well-mapped fly AL (52 glomeruli, Vosshall et al., 2000), but would probably be lost in the volume of the averaged bumblebee AL (~158 glomeruli, Mertes et al., 2021). In addition, crucial varying factors of the stimulus (e.g. the usage of a potential noxious stimuli vs harmless plant odors, different exposure protocols, or neglect of reversibility effects in bumblebees), need to be taken into account when investigating bumblebee AL plasticity. AL activity in the honeybee was shown to be modulated by olfactory learning and memory induced plasticity (Rath et al., 2011) leading to increased glomerular activity towards the rewarded CS stimulus. Similar to honeybees, ALs of bumblebees show activity patterns reflecting the chemical structure of the olfactory stimulus (Mertes et al., 2021). Thus, subsequent experiments, long-term monitoring the glomerular activity during conditioning experiments, would not only allow gaining insights in learning & memory related plasticity in the AL, but also add more information to the generalization

effects we found in our PER approaches (chapter 2, Fig 3, right panels).

The specific categorization of UV light found in the honeybee MBONs (chapter 3, par. 3.4) can be either base on a hardwired concept with innate UV tuning or be induced by plasticity effects. To examine such effects of sensory exposure & experience related plasticity in the MB circuits, honeybees and ants have established as valuable models over the last decades (e.g. Hourcade et al., 2010; Stieb et al., 2010; Groh et al., 2012; Muenz et al., 2015; Scholl et al., 2015). In short, a polyethism induced transition from indoor duties to outdoor tasks has been shown to evoke plasticity in the MB lip and collar of honeybees and desert ants, resulting in a decrease of the synaptic boutons and an increase of volume (Stieb et al., 2010; Muenz et al., 2015). During this specific transition, honeybees and ants display signature learning flights or walks to calibrate their navigational system (e.g. Lindauer, 1952; von Frisch, 1965; Fleischmann et al., 2016; Collett and Zeil, 2018). Neuroanatomical approaches in *Cataglyphis noda* showed, that the exposure to the natural polarization pattern is crucial for the mentioned plasticity in the collar region (Grob et al., 2017). In addition, early sensory (visual) exposure has been shown to induce similar effects in both the honeybee (Scholl et al., 2014) and the desert ant (Stieb et al., 2010). Moreover, plastic changes in the MB are thereby not only restricted to the calycal input, but are also occurring in extrinsic MBONs, innervating the ML and VL (reviewed in Groh and Rössler, 2020). Until today, research investigating plastic effects in the MB output mostly neglected visual effects and focused on olfactory learning induced aspects (e.g. Menzel and Giurfa, 2001; Haehnel and Menzel, 2010; Strube-Bloss et al., 2011). While studies about visual processing in MBONs are already sparse (see chapter 3, par. 4.2), information about visual learning induced plasticity in the MBs is even more elusive. Neuroanatomical examinations in carpenter ants found color-learning to induce plasticity most notably along the visual pathway, i.e. in the OL, the anterior optic tubercle and the central complex, but not condensed in the MB (Yilmaz et al., 2019). The OL as a potential area for visual-learning induced plasticity is also assumed by molecular approaches that showed increased expression of learning-related genetic markers in both the MB and the OL after visual conditioning (Avalos et al., 2021). Wherever precisely located, the influence of visual-learning plasticity needs to be appreciated during examinations of the MB and its output regions. An inclusion of data from naïve honeybees could thus control for effects of visual-learning or sensory-exposure induced plasticity on the specific MBON tuning in the VL (chapter

3, par. 3.4) and give more insights to the question of a plastic or hardwired UV-categorization in visual MBONs (chapter 3, par. 4.4).

4.3 Categorization of sensory input in the mushroom body output of the honeybee

Although research in the honeybee MB output lobes in the last decades mainly investigated olfactory processing and plasticity induced effects (e.g. Haehnel and Menzel, 2010; Strube-Bloss et al., 2011, 2016; Menzel, 2014), several studies found processing of additional modalities, mostly vision (e.g. Gronenberg, 1987; Mauelshagen, 1993; Rybak and Menzel, 1998). Recently, extracellular approaches in the VL showed MBONs to categorize modality-specific for olfactory, visual and olfactory-visual information (Strube-Bloss and Rössler, 2018), thus reflecting the layer-specific architecture of the calycal MB input (lip: olfactory input, collar: visual input, basal ring: olfactory and visual input). Moreover, around 20 % of the recorded MBONs showed no responses to any of the presented stimuli and were assumed to be silent, with the capability for a plastic recruitment, or tuned to different modalities (e.g. gustation). However, information about the representation of stimulus identity or intensity is sparse. Until this day, only olfactory processing MBONs have been found to encode information about stimulus intensity (Haehnel and Menzel, 2010; Strube-Bloss et al., 2011). Our findings in chapter 3 (Fig. 2B, 3, left panels) show for the first time the representation of visual intensity and identity at the MB output. We were able to classify unimodal (purely visually driven) and multimodal (olfactory-visually driven) MBONs according to their neural activity in three distinct groups: Identity-, intensity- and non-specific coding MBONs (Fig. 1).
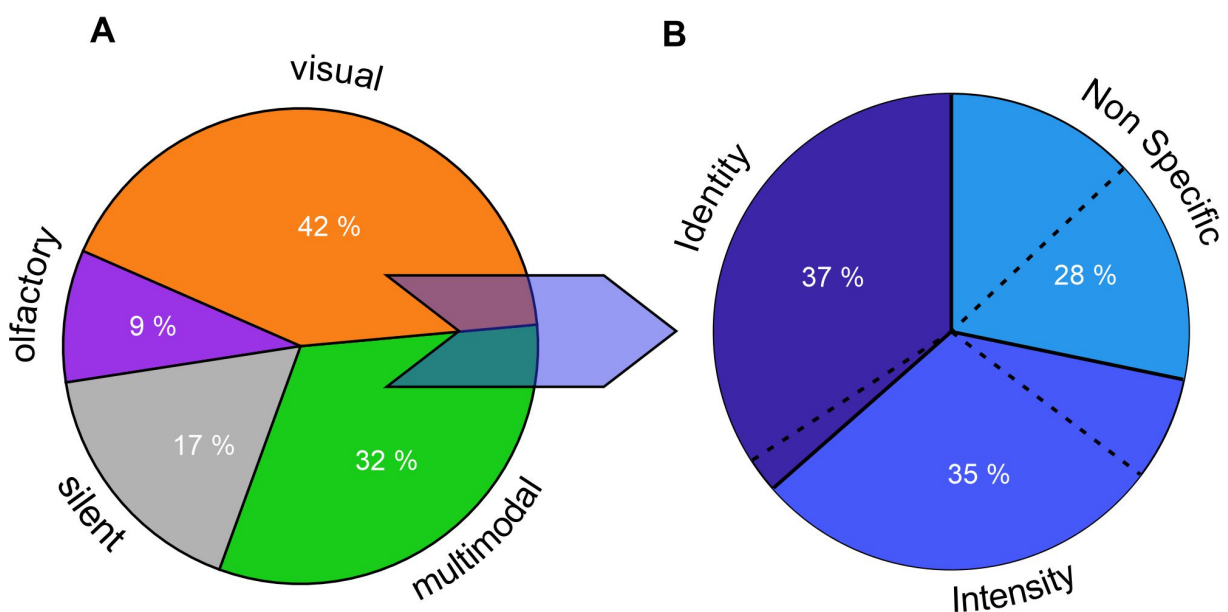
Figure 1: Response tuning of MBONs. (A) Proportion of MBON tuning, adapted from Strube-Bloss and Rössler (2018). 32 % of recorded MBONs encode olfactory and visual information and are labeled as multimodal (green). 51 % of examined units responded only to one modality, 42 % visual (orange) and 9 % olfactory stimuli (purple). 17 % of recorded neurons did not respond to olfactory or visual stimulation (silent, grey). **(B)** Classification of visual sensitive MBONs described in chapter 2 (Fig. 2) comprising uni- and multimodal visual sensitive units (indicated by blue arrow). Chart shows MBONs, grouped according to their response activity. Neurons coding for stimulus identity (37 %, Identity, dark blue), stimulus intensity (35 %, Intensity, medium blue) and simply for stimulus on-set, without any intensity or identity coding aspects (28 %, Non Specific, light blue). Dashed lines indicate proportion of multimodal units, consistently occurring in smaller portions in all groups. For details see chapter 2 (Par. 3.2).

Interestingly, the subclass of unimodal identity coding MBONs exhibits a specific tuning towards stimulation with UV light. As discussed in the previous paragraph, we can only speculate about a possible hardwiring or experience-related plasticity causing this specific categorization towards UV (chapter 3, par. 4.4) and its attribution to foraging or navigational processes. In the honeybee, little is known about a connection of MBONs and the central complex, linking this specific UV representation with navigation or orientation processes. Interestingly, research in the fruit fly gained more insight to this barely comprehended connection and found direct and indirect input from MBONs to the central complex and vice versa (Li et al., 2020; Hulse et al., 2021). To increase our understanding of visual processing in the honeybee VL, future research is thus required to not only control for experience-related effects but also include intracellular and neuroanatomical approaches to enable an identification of MBONs on a cellular level. A subsequent analysis of the innervation pattern of identified MBONs will not only allow an association of electrophysiological classification (chapter 3, Fig. 2, Strube-Bloss and Rössler, 2018) and neuroanatomical mapping (Rybak and Menzel, 1993; Strausfeld, 2002) but also provide more information about the calycal input of the MBONs. So far, we can only draw conclusions about the calycal input of the examined MBONs from their modality tuning and the respective layer-architecture of the VL (Strausfeld, 2002). Doing so, we assume e.g. purely visually-driven MBONs to receive their calycal input either by class I KCs located in the collar region or by exclusively visual sensitive class II KCs of the CO or BR region. Interestingly, the calyx collar and basal ring have been reported to additionally receive gustatory input via the subesophageal-calycal tract (Schröter and Menzel, 2003), a sensory modality that has barely received any examination in the VL so far. Whereas neuroanatomical approaches in the fruit fly showed specific MBONs to convey not only

gustatory information but also thermo- and hygrosensory input (Li et al., 2020), studies in honeybee MBONs lack corresponding information so far. A well suited candidate to close this gap of knowledge in the honeybee are MBONs of the A3 or protocerebral-calycal-tract (PCT) cluster, the only identified MBONs to encode information about gustatory (Gronenberg, 1987; Haehnel and Menzel, 2010) and mechanosensory input (Gronenberg, 1987).

4.4 Closing remarks

In the course of this thesis, I was able to gain a profound knowledge of the processing of behaviorally relevant stimuli in both the buff-tailed bumblebee and the honeybee. Both species have a remarkable physiology and behavior that suits them for future research about sex-specific processing of olfactory cues or the integration of visual stimuli. Throughout this dissertation, it became evident that it is not sufficient to reduce a stimulus-induced effect to its sole neural activity, but also consider the ensemble of intrinsic and extrinsic effects on the neural circuitry. For example, a further investigation of the MBON population or AL activity should therefore not only rely on additional stimulus modalities (e.g. mechanical, gustatory stimuli) and techniques (e.g. intracellular recordings, calcium imaging), but also implement context dependent aspects, e.g. tethered recordings in a virtual arena during walking or even flying state. With plenty of these proposed approaches already established in the honeybee and bumblebee, these species represent highly attractive models for the current and future research in the field of neuroethology.

"…if you feel the heat around the corner."

Neil McCauley

Bibliography

Abdullah, N., Hamzah, A., Ramli, J., Mardan, M., and Mardani, M. (1990). Identification of Nasonov Pheromones and the Effects of Synthetic Pheromones on the Clustering Activity of the Asiatic Honeybee (APis Cerana). *Pertanika* 13, 189–194.
 Available at: https://core.ac.uk/download/pdf/12222141.pdf.

Ache, B. W., and Young, J. M. (2005). Olfaction: Diverse species, conserved principles. *Neuron* 48, 417–430. doi:10.1016/j.neuron.2005.10.022.

Agi, E., Langen, M., Altschuler, S. J., Wu, L. F., Zimmermann, T., and Hiesinger, P. R. (2014). The Evolution and Development of Neural Superposition. *J. Neurogenet.* 28, 216–232. doi:10.3109/01677063.2014.922557.

Ågren, L., and Hallberg, E. (1996). Flagellar sensilla of bumble bee males (Hymenopera, Apidae, Bombus). *Apidologie* 25, 433–444. doi:10.1051/apido:19960601.

Anton, S., and Homberg, U. (1999). "Antennal Lobe Structure," in *Insect Olfaction* (Berlin, Heidelberg: Springer Berlin Heidelberg), 97–124. doi:10.1007/978-3-662-07911-9_5.

Anton, S., and Rössler, W. (2021). Plasticity and modulation of olfactory circuits in insects. *Cell Tissue Res.* 383, 149–164. doi:10.1007/s00441-020-03329-z.

Arnold, G., Masson, C., and Budharugsa, S. (1985). Comparative study of the antennal lobes and their afferent pathway in the worker bee and the drone (Apis mellifera). *Cell Tissue Res.* 242, 593–605. doi:10.1007/BF00225425.

Aso, Y., Hattori, D., Yu, Y., Johnston, R. M., Iyer, N. A., Ngo, T. T. B., et al. (2014). The neuronal architecture of the mushroom body provides a logic for associative learning. *Elife* 3, e04577. doi:10.7554/eLife.04577.

Avalos, A., Traniello, I. M., Claudio, E. P., and Giray, T. (2021). Parallel mechanisms of visual memory formation across distinct regions of the honey bee brain. *J. Exp. Biol.* 224. doi:10.1242/jeb.242292.

Avarguès-Weber, A., and Mota, T. (2016). Advances and limitations of visual conditioning protocols in harnessed bees. *J. Physiol. Paris* 110, 107–118. doi:10.1016/j.jphysparis.2016.12.006.

Becker, M. C., Rössler, W., and Strube-Bloss, M. F. (2019). UV-light perception is modulated by the odour element of an olfactory-visual compound in restrained honeybees. *J. Exp. Biol.* 222, jeb.201483. doi:10.1242/jeb.201483.

Bergman, P., and Bergström, G. (1997). Scent marking, scent origin, and species specificity in male premating behavior of two Scandinavian bumblebees. *Can. Field-Naturalist* 111, 1235–1251. doi:0098 0331/97/0500 I235$12.50/0.

Bergström, G., Kullenberg, B., Ställberg-Stenhagen, S., and Stenhagen, E. (1968). "Studies on natural odoriferous compounds. II. Identification of a 2,3–dihydrofarnesol as the main component of the marking perfume of male bumble bees of the species Bombus terrestris," in *L. Ark. Kemi 28*, 453–469.

Bhatnagar, K. P., and Meisami, E. (1998). Vomeronasal organ in bats and primates: Extremes of structural variability and its phylogenetic implications. *Microsc. Res. Tech.* 43, 465–475. doi:10.1002/(SICI)1097-0029(19981215)43:6<465::AID-JEMT1>3.0.CO;2-1.

Bitterman, M. E., Menzel, R., Fietz, A., and Schäfer, S. (1983). Classical conditioning of proboscis extension in honeybees (Apis mellifera). *J. Comp. Psychol.* 97, 107–119. doi:10.1037/0735-

7036.97.2.107.

Bodin, A., Vinauger, C., and Lazzari, C. R. (2009). Behavioural and physiological state dependency of host seeking in the bloodsucking insect Rhodnius prolixus. *J. Exp. Biol.* 212, 2386–2393. doi:10.1242/jeb.030668.

Briand, L., Eloit, C., Nespoulous, C., Bézirard, V., Huet, J.-C., Henry, C., et al. (2002). Evidence of an Odorant-Binding Protein in the Human Olfactory Mucus: Location, Structural Characterization, and Odorant-Binding Properties. *Biochemistry* 41, 7241–7252. doi:10.1021/bi015916c.

Brill, M. F., Rosenbaum, T., Reus, I., Kleineidam, C. J., Nawrot, M. P., and Rössler, W. (2013). Parallel processing via a dual olfactory pathway in the honeybee. *J. Neurosci.* 33, 2443–56. doi:10.1523/JNEUROSCI.4268-12.2013.

Brines, M. L., and Gould, J. L. (1982). Skylight Polarization patterns and Animal Orientation. *J. Exp. Biol.* 96, 69–91. doi:10.1242/jeb.96.1.69.

Brockmann, A., and Brückner, D. (2001). Structural differences in the drone olfactory system of two phylogenetically distant Apis species, A. florea and A. mellifera. *Naturwissenschaften* 88, 78–81. doi:10.1007/s001140000199.

Buck, L., and Axel, R. (1991). A novel multigene family may encode odorant receptors: A molecular basis for odor recognition. *Cell* 65, 175–187. doi:10.1016/0092-8674(91)90418-X.

Bushdid, C., Magnasco, M. O., Vosshall, L. B., and Keller, A. (2014). Humans Can Discriminate More than 1 Trillion Olfactory Stimuli. *Science (80-.).* 343, 1370–1372. doi:10.1126/science.1249168.

Claudianos, C., Lim, J., Young, M., Yan, S., Cristino, A. S., Newcomb, R. D., et al. (2014). Odor memories regulate olfactory receptor expression in the sensory periphery. *Eur. J. Neurosci.* 39, 1642–1654. doi:10.1111/ejn.12539.

Collett, T. S., and Zeil, J. (2018). Insect learning flights and walks. *Curr. Biol.* 28, R984–R988. doi:10.1016/j.cub.2018.04.050.

Couto, A., Alenius, M., and Dickson, B. J. (2005). Molecular, Anatomical, and Functional Organization of the Drosophila Olfactory System. *Curr. Biol.* 15, 1535–1547. doi:10.1016/j.cub.2005.07.034.

de Belle, J., and Heisenberg, M. (1994). Associative odor learning in Drosophila abolished by chemical ablation of mushroom bodies. *Science (80-.).* 263, 692–695. doi:10.1126/science.8303280.

Do, M. T. H., and Yau, K.-W. (2010). Intrinsically Photosensitive Retinal Ganglion Cells. *Physiol. Rev.* 90, 1547–1581. doi:10.1152/physrev.00013.2010.

Dornhaus, A., and Chittka, L. (2001). Food alert in bumblebees (Bombus terrestris): possible mechanisms and evolutionary implications. *Behav. Ecol. Sociobiol.* 50, 570–576. doi:10.1007/s002650100395.

Dyer, A. G., Paulk, A. C., and Reser, D. H. (2011). Colour processing in complex environments: insights from the visual system of bees. *Proc Biol Sci* 278, 952–959. doi:10.1098/rspb.2010.2412.

Elofsson, R. (1970). Brain and Eyes of Zygentoma (Thysanura). *Insect Syst. Evol.* 1, 1–20. doi:10.1163/187631270X00294.

Esslen, J., and Kaissling, K. E. (1976). Zahl und Verteilung antennaler Sensillen bei der Honigbiene (Apis mellifera L.). *Zoomorphologie* 83, 227–251. doi:10.1007/BF00993511.

Fan, J., Francis, F., Liu, Y., Chen, J. L., and Cheng, D. F. (2011). Review An overview of odorant-binding protein functions in insect peripheral olfactory reception. *Genet. Mol. Res.* 10, 3056–3069.

doi:10.4238/2011.December.8.2.

Fleischmann, P. N., Christian, M., Müller, V. L., Rössler, W., and Wehner, R. (2016). Ontogeny of learning walks and the acquisition of landmark information in desert ants, Cataglyphis fortis. *J. Exp. Biol.* 219, 3137–3145. doi:10.1242/jeb.140459.

Fleischmann, P. N., Grob, R., Müller, V. L., Wehner, R., and Rössler, W. (2018). The Geomagnetic Field Is a Compass Cue in Cataglyphis Ant Navigation. *Curr. Biol.* 28, 1440-1444.e2. doi:10.1016/j.cub.2018.03.043.

Fonta, C., and Masson, C. (1987). Structural and functional studies of the peripheral olfactory nervous system of male and female bumble-bees (Bombus hypnorum and Bombus terrestris). *Chem. Senses* 12, 53–69. doi:10.1093/chemse/12.1.53.

Foret, S., and Maleszka, R. (2006). Function and evolution of a gene family encoding odorant binding-like proteins in a social insect, the honey bee (Apis mellifera). *Genome Res.* 16, 1404–1413. doi:10.1101/gr.5075706.

Free, J. B. (1987). *Pheromones of Social Bees*. 1st ed. Dordrecht: Springer Netherlands.

Gadenne, C., Barrozo, R. B., and Anton, S. (2016). Plasticity in Insect Olfaction: To Smell or Not to Smell? *Annu. Rev. Entomol.* 61, 317–333. doi:10.1146/annurev-ento-010715-023523.

Getz, W. M., and Akers, R. P. (1993). Olfactory response characteristics and tuning structure of placodes in the honey bee Apis mellifera L. *Apidologie* 24, 195–217. doi:10.1051/apido:19930303.

Ghaninia, M., Haight, K., Berger, S. L., Reinberg, D., Zwiebel, L. J., Ray, A., et al. (2017). Chemosensory sensitivity reflects reproductive status in the ant Harpegnathos saltator. *Sci. Rep.* 7, 3732. doi:10.1038/s41598-017-03964-7.

Gibbs, R. A., Metzker, M. L., Muzny, D. M., Sodergren, E. J., Scherer, S., Scott, G., et al. (2004). Genome sequence of the Brown Norway rat yields insights into mammalian evolution. *Nature* 428, 493–521. doi:10.1038/nature02426.

Gilad, Y., Wiebe, V., Przeworski, M., Lancet, D., and Pääbo, S. (2004). Loss of Olfactory Receptor Genes Coincides with the Acquisition of Full Trichromatic Vision in Primates. *PLoS Biol.* 2, e5. doi:10.1371/journal.pbio.0020005.

Gilad, Y., Wiebe, V., Przeworski, M., Lancet, D., and Pääbo, S. (2007). Correction: Loss of Olfactory Receptor Genes Coincides with the Acquisition of Full Trichromatic Vision in Primates. *PLoS Biol.* 5, e148. doi:10.1371/journal.pbio.0050148.

Giurfa, M., and Sandoz, J.-C. (2012). Invertebrate learning and memory: Fifty years of olfactory conditioning of the proboscis extension response in honeybees. *Learn. Mem.* 19, 54–66. doi:10.1101/lm.024711.111.

Goulson, D. (2010). *Bumblebees: Behaviour, Ecology, and Conservation*. 2nd ed. New York, NY: Oxford University Press.

Grammer, K., Fink, B., and Neave, N. (2005). Human pheromones and sexual attraction. *Eur. J. Obstet. Gynecol. Reprod. Biol.* 118, 135–142. doi:10.1016/j.ejogrb.2004.08.010.

Granero, A. M., Guerra Sanz, J. M., Egea Gonzalez, F. J., Martinez Vidal, J. L., Dornhaus, A., Ghani, J., et al. (2005). Chemical compounds of the foraging recruitment pheromone in bumblebees. *Naturwissenschaften* 92, 371–374. doi:10.1007/s00114-005-0002-0.

Greiner, B., Gadenne, C., and Anton, S. (2002). Central processing of plant volatiles in Agrotis ipsilon

males is age-independent in contrast to sex pheromone processing. *Chem. Senses* 27, 45–48. doi:10.1093/chemse/27.1.45.

Grill-Spector, K., and Malach, R. (2004). The Human Visual Cortex. *Annu. Rev. Neurosci.* 27, 649–677. doi:10.1146/annurev.neuro.27.070203.144220.

Grob, R., Fleischmann, P. N., Grübel, K., Wehner, R., and Rössler, W. (2017). The Role of Celestial Compass Information in Cataglyphis Ants during Learning Walks and for Neuroplasticity in the Central Complex and Mushroom Bodies. *Front. Behav. Neurosci.* 11, 1–14. doi:10.3389/fnbeh.2017.00226.

Groh, C., Ahrens, D., and Rössler, W. (2006). Environment- and Age-Dependent Plasticity of Synaptic Complexes in the Mushroom Bodies of Honeybee Queens. *Brain. Behav. Evol.* 68, 1–14. doi:10.1159/000092309.

Groh, C., Lu, Z., Meinertzhagen, I. A., and Rössler, W. (2012). Age-related plasticity in the synaptic ultrastructure of neurons in the mushroom body calyx of the adult honeybee Apis mellifera. *J. Comp. Neurol.* 520, 3509–3527. doi:10.1002/cne.23102.

Groh, C., and Rössler, W. (2020). Analysis of Synaptic Microcircuits in the Mushroom Bodies of the Honeybee. *Insects* 11, 43. doi:10.3390/insects11010043.

Gronenberg, W. (1987). Anatomical and physiological properties of feedback neurons of the mushroom bodies in the bee brain. *Exp. Biol.* 46, 115–25. Available at: http://www.ncbi.nlm.nih.gov/pubmed/3582581.

Guerrieri, F., Gemeno, C., Monsempes, C., Anton, S., Jacquin-Joly, E., Lucas, P., et al. (2012). Experience-dependent modulation of antennal sensitivity and input to antennal lobes in male moths (Spodoptera littoralis) pre-exposed to sex pheromone. *J. Exp. Biol.* 215, 2334–2341. doi:10.1242/jeb.060988.

Haehnel, M., and Menzel, R. (2010). Sensory Representation and Learning-Related Plasticity in Mushroom Body Extrinsic Feedback Neurons of the Protocerebral Tract. *Front. Syst. Neurosci.* 4, 1–13. doi:10.3389/fnsys.2010.00161.

Hardie, R. C., and Raghu, P. (2001). Visual transduction in Drosophila. *Nature* 413, 186–93. doi:10.1038/35093002.

Heiling, A. M., Herberstein, M. E., and Chittka, L. (2003). Crab-spiders manipulate flower signals. *Nature* 421, 334–334. doi:10.1038/421334a.

Heinze, S., Florman, J., Asokaraj, S., el Jundi, B., and Reppert, S. M. (2013). Anatomical basis of sun compass navigation II: The neuronal composition of the central complex of the monarch butterfly. *J. Comp. Neurol.* 521, 267–298. doi:10.1002/cne.23214.

Hensgen, R., England, L., Homberg, U., and Pfeiffer, K. (2021). Neuroarchitecture of the central complex in the brain of the honeybee: Neuronal cell types. *J. Comp. Neurol.* 529, 159–186. doi:10.1002/cne.24941.

Hildebrand, J. G., and Shepherd, G. M. (1997). Mechanisms of olfactory discrimination: Converging Evidence for Common Principles Across Phyla. *Annu. Rev. Neurosci.* 20, 595–631. doi:10.1146/annurev.neuro.20.1.595.

Hindmarsh Sten, T., Li, R., Otopalik, A., and Ruta, V. (2021). Sexual arousal gates visual processing during Drosophila courtship. *Nature* 595, 549–553. doi:10.1038/s41586-021-03714-w.

Homberg, U. (1984). Processing of antennal information in extrinsic mushroom body neurons of the

bee brain. *J. Comp. Physiol. A* 154, 825–836. doi:10.1007/BF00610683.

Homberg, U., Montague, R. A., and Hildebrand, J. G. (1988). Anatomy of antenno-cerebral pathways in the brain of the sphinx moth Manduca sexta. *Cell Tissue Res.* 254, 255–281. doi:10.1007/BF00225800.

Hourcade, B., Muenz, T. S., Sandoz, J. C., Rossler, W., and Devaud, J. M. (2010). Long-Term Memory Leads to Synaptic Reorganization in the Mushroom Bodies: A Memory Trace in the Insect Brain? *J. Neurosci.* 30, 6461–6465. doi:10.1523/JNEUROSCI.0841-10.2010.

Hulse, B. K., Haberkern, H., Franconville, R., Turner-Evans, D. B., Takemura, S., Wolff, T., et al. (2021). A connectome of the Drosophila central complex reveals network motifs suitable for flexible navigation and context-dependent action selection. *Elife* 10. doi:10.7554/eLife.66039.

Ito, K., Shinomiya, K., Ito, M., Armstrong, J. D., Boyan, G., Hartenstein, V., et al. (2014). A Systematic Nomenclature for the Insect Brain. *Neuron* 81, 755–765. doi:10.1016/j.neuron.2013.12.017.

Jacobs, G. H. (2009). Evolution of colour vision in mammals. *Philos. Trans. R. Soc. B Biol. Sci.* 364, 2957–2967. doi:10.1098/rstb.2009.0039.

Jernigan, C. M., Halby, R., Gerkin, R. C., Sinakevitch, I., Locatelli, F., and Smith, B. H. (2020). Experience-dependent tuning of early olfactory processing in the adult honey bee, Apis mellifera. *J. Exp. Biol.* 223. doi:10.1242/jeb.206748.

Jones, B. M., Leonard, A. S., Papaj, D. R., and Gronenberg, W. (2013). Plasticity of the Worker Bumblebee Brain in Relation to Age and Rearing Environment. *Brain. Behav. Evol.* 82, 250–261. doi:10.1159/000355845.

Jung, J., Kim, D.-I., Han, G.-Y., and Kwon, H. (2018). The Effects of High Fat Diet-Induced Stress on Olfactory Sensitivity, Behaviors, and Transcriptional Profiling in Drosophila melanogaster. *Int. J. Mol. Sci.* 19, 2855. doi:10.3390/ijms19102855.

Keeling, C. I., Plettner, E., and Slessor, K. N. (2004). "Hymenopteran Semiochemicals," in, 133–177. doi:10.1007/b95452.

Kelber, C., Rössler, W., and Kleineidam, C. J. (2010). Phenotypic plasticity in number of glomeruli and sensory innervation of the antennal lobe in leaf-cutting ant workers (A. vollenweideri). *Dev. Neurobiol.* 70, 222–234. doi:10.1002/dneu.20782.

Keverne, E. B. (1999). The Vomeronasal Organ. *Science (80-.).* 286, 716–720. doi:10.1126/science.286.5440.716.

Kinoshita, M., and Homberg, U. (2017). "Insect Brains: Minute Structures Controlling Complex Behaviors," in, 123–151. doi:10.1007/978-4-431-56469-0_6.

Kirschner, S., Kleineidam, C. J., Zube, C., Rybak, J., Grünewald, B., and Rössler, W. (2006). Dual olfactory pathway in the honeybee, Apis mellifera. *J. Comp. Neurol.* 499, 933–952. doi:10.1002/cne.21158.

Krieger, G. M., Duchateau, M.-J., Van Doorn, A., Ibarra, F., Francke, W., and Ayasse, M. (2006). Identification of Queen Sex Pheromone Components of the Bumblebee Bombus terrestris. *J. Chem. Ecol.* 32, 453–471. doi:10.1007/s10886-005-9013-8.

Kropf, J., Kelber, C., Bieringer, K., and Rössler, W. (2014). Olfactory subsystems in the honeybee: sensory supply and sex specificity. *Cell Tissue Res.*, 583–595. doi:10.1007/s00441-014-1892-y.

Kropf, J., and Rössler, W. (2018). In-situ recording of ionic currents in projection neurons and Kenyon cells in the olfactory pathway of the honeybee. *PLoS One* 13, e0191425. doi:10.1371/journal.pone.0191425.

Kullenberg, B., Bergstrom, G., Ställberg-Stenhagen, S., Liaaen-Jensen, S., Lamvik, A., Sunde, E., et al. (1970). Volatile Components of the Cephalic Marking Secretion of Male Bumble Bees. *Acta Chem. Scand.* 24, 1481–1483. doi:10.3891/acta.chem.scand.24-1481.

Labhart, T. (1974). Behavioral analysis of light intensity discrimination and spectral sensitivity in the honey bee,Apis mellifera. *J. Comp. Physiol. ? A* 95, 203–216. doi:10.1007/BF00625444.

Labhart, T., and Meyer, E. P. (1999). Detectors for polarized skylight in insects: a survey of ommatidial specializations in the dorsal rim area of the compound eye. *Microsc. Res. Tech.* 47, 368–379. doi:10.1002/(SICI)1097-0029(19991215)47:6<368::AID-JEMT2>3.0.CO;2-Q.

Lacher, V. (1964). Elektrophysiologische Untersuchungen an einzelnen Rezeptoren für Geruch, Kohlendioxyd, Luftfeuchtigkeit und Tempratur auf den Antennen der Arbeitsbiene und der Drohne (Apis mellifica L.). *Z. Vgl. Physiol.* 48, 587–623. doi:10.1007/BF00333743.

Land, M. F., and Fernald, R. D. (1992). The Evolution of Eyes. *Annu. Rev. Neurosci.* 15, 1–29. doi:10.1146/annurev.ne.15.030192.000245.

Lenschow, M., Cordel, M., Pokorny, T., Mair, M. M., Hofferberth, J., and Ruther, J. (2018). The post-mating switch in the pheromone response of nasonia females is mediated by dopamine and can be reversed by appetitive learning. *Front. Behav. Neurosci.* 12, 1–11. doi:10.3389/fnbeh.2018.00014.

Li, F., Lindsey, J., Marin, E. C., Otto, N., Dreher, M., Dempsey, G., et al. (2020). The connectome of the adult drosophila mushroom body provides insights into function. *Elife* 9, 1–217. doi:10.7554/eLife.62576.

Li, W., and DeVries, S. H. (2006). Bipolar cell pathways for color and luminance vision in a dichromatic mammalian retina. *Nat. Neurosci.* 9, 669–675. doi:10.1038/nn1686.

Li, Y., and Strausfeld, N. J. (1997). Morphology and sensory modality of mushroom body extrinsic neurons in the brain of the cockroach, Periplaneta americana. *J. Comp. Neurol.* 387, 631–50. doi:10.1002/(SICI)1096-9861(19971103)387:4<631::AID-CNE9>3.0.CO;2-3.

Li, Y., and Strausfeld, N. J. (1999). Multimodal efferent and recurrent neurons in the medial lobes of cockroach mushroom bodies. *J. Comp. Neurol.* 409, 647–663. doi:10.1002/(SICI)1096-9861(19990712)409:4<647::AID-CNE9>3.0.CO;2-3.

Lichtenstein, L., Sommerlandt, F. M. J., and Spaethe, J. (2015). Dumb and lazy? A comparison of color learning and memory retrieval in drones and workers of the buff-tailed bumblebee, bombus terrestris, by means of per conditioning. *PLoS One* 10, 1–18. doi:10.1371/journal.pone.0134248.

Lindauer, M. (1952). Ein Beitrag zur Frage der Arbeitsteilung im Bienenstaat. *Z. Vgl. Physiol.* 34, 299–345. doi:10.1007/BF00298048.

Liu, Q., Liu, S., Kodama, L., Driscoll, M. R., and Wu, M. N. (2012). Two dopaminergic neurons signal to the dorsal fan-shaped body to promote wakefulness in Drosophila. *Curr. Biol.* 22, 2114–2123. doi:10.1016/j.cub.2012.09.008.

Lunau, K. (1993). Interspecific diversity and uniformity of flower colour patterns as cues for learned discrimination and innate detection of flowers. *Experientia* 49, 1002–1010. doi:10.1007/BF02125649.

Malnic, B., Hirono, J., Sato, T., and Buck, L. B. (1999). Combinatorial Receptor Codes for Odors. *Cell* 96, 713–723. doi:10.1016/S0092-8674(00)80581-4.

Malun, D., Waldow, U., Kraus, D., and Boeckh, J. (1993). Connections between the deutocerebrum and

the protocerebrum, and neuroanatomy of several classes of deutocerebral projection neurons in the brain of male Periplaneta americana. *J. Comp. Neurol.* 329, 143–162. doi:10.1002/cne.903290202.

Mansur, B. E., Rodrigues, J. R. V., and Mota, T. (2018). Bimodal Patterning Discrimination in Harnessed Honey Bees. *Front. Psychol.* 9, 1–14. doi:10.3389/fpsyg.2018.01529.

Mariette, J., Carcaud, J., and Sandoz, J.-C. (2021). The neuroethology of olfactory sex communication in the honeybee Apis mellifera L. *Cell Tissue Res.* 383, 177–194. doi:10.1007/s00441-020-03401-8.

Martel, V., Anderson, P., Hansson, B. S., and Schlyter, F. (2009). Peripheral modulation of olfaction by physiological state in the Egyptian leaf worm Spodoptera littoralis (Lepidoptera: Noctuidae). *J. Insect Physiol.* 55, 793–797. doi:10.1016/j.jinsphys.2009.04.012.

Matsui, A., Go, Y., and Niimura, Y. (2010). Degeneration of Olfactory Receptor Gene Repertories in Primates: No Direct Link to Full Trichromatic Vision. *Mol. Biol. Evol.* 27, 1192–1200. doi:10.1093/molbev/msq003.

Mauelshagen, J. (1993). Neural correlates of olfactory learning paradigms in an identified neuron in the honeybee brain. *J. Neurophysiol.* 69, 609–625. doi:10.1152/jn.1993.69.2.609.

Menzel, R. (2014). The insect mushroom body, an experience-dependent recoding device. *J. Physiol.* 108, 84–95. doi:10.1016/j.jphysparis.2014.07.004.

Menzel, R., and Giurfa, M. (2001). Cognitive architecture of a mini-brain: the honeybee. *Trends Cogn. Sci.* 5, 62–71. doi:10.1016/S1364-6613(00)01601-6.

Menzel, R., and Greggers, U. (2015). The memory structure of navigation in honeybees. *J. Comp. Physiol. A* 201, 547–561. doi:10.1007/s00359-015-0987-6.

Mertes, M., Carcaud, J., and Sandoz, J.-C. (2021). Olfactory coding in the antennal lobe of the bumble bee Bombus terrestris. *Sci. Rep.* 11, 10947. doi:10.1038/s41598-021-90400-6.

Mobbs, P. G. (1982). The Brain of the Honeybee Apis Mellifera. I. The Connections and Spatial Organization of the Mushroom Bodies. *Philos. Trans. R. Soc. B Biol. Sci.* 298, 309–354. doi:10.1098/rstb.1982.0086.

Modi, M. N., Shuai, Y., and Turner, G. C. (2020). The Drosophila Mushroom Body: From Architecture to Algorithm in a Learning Circuit. *Annu. Rev. Neurosci.* 43, 465–484. doi:10.1146/annurev-neuro-080317-0621333.

Moller, P. (1976). Electric Signals and Schooling Behavior in a Weakly Electric Fish, Marcusenius cyprinoides L. (Mormyriformes). *Science (80-.).* 193, 697–699. doi:10.1126/science.948747.

Mombaerts, P., Wang, F., Dulac, C., Chao, S. K., Nemes, A., Mendelsohn, M., et al. (1996). Visualizing an Olfactory Sensory Map. *Cell* 87, 675–686. doi:10.1016/S0092-8674(00)81387-2.

Mouritsen, H. (2018). Long-distance navigation and magnetoreception in migratory animals. *Nature* 558, 50–59. doi:10.1038/s41586-018-0176-1.

Muenz, T. S., Groh, C., Maisonnasse, A., Le Conte, Y., Plettner, E., and Rössler, W. (2015). Neuronal plasticity in the mushroom body calyx during adult maturation in the honeybee and possible pheromonal influences. *Dev. Neurobiol.* 75, 1368–1384. doi:10.1002/dneu.22290.

Nei, M., Niimura, Y., and Nozawa, M. (2008). The evolution of animal chemosensory receptor gene repertoires: roles of chance and necessity. *Nat. Rev. Genet.* 9, 951–963. doi:10.1038/nrg2480.

Nishikawa, M., Watanabe, H., and Yokohari, F. (2012). Higher brain centers for social tasks in worker ants, Camponotus japonicus. *J. Comp. Neurol.* 520, 1584–1598. doi:10.1002/cne.23001.

Nishino, H., Iwasaki, M., Yasuyama, K., Hongo, H., Watanabe, H., and Mizunami, M. (2012). Visual and olfactory input segregation in the mushroom body calyces in a basal neopteran, the American cockroach. *Arthropod Struct. Dev.* 41, 3–16. doi:10.1016/j.asd.2011.08.005.

Nishino, H., Nishikawa, M., Mizunami, M., and Yokohari, F. (2009). Functional and topographic segregation of glomeruli revealed by local staining of antennal sensory neurons in the honeybee Apis mellifera. *J. Comp. Neurol.* 515, 161–180. doi:10.1002/cne.22064.

O'Donnell, S., Reichardt, M., and Foster, R. (2000). Individual and colony factors in bumble bee division of labor (Bombus bifarius nearcticus Handl; Hymenoptera, Apidae). *Insectes Soc.* 47, 164–170. doi:10.1007/PL00001696.

Paoli, M., and Galizia, G. C. (2021). Olfactory coding in honeybees. *Cell Tissue Res.* 383, 35–58. doi:10.1007/s00441-020-03385-5.

Papiorek, S., Junker, R. R., Alves-dos-Santos, I., Melo, G. A. R., Amaral-Neto, L. P., Sazima, M., et al. (2016). Bees, birds and yellow flowers: pollinator-dependent convergent evolution of UV patterns. *Plant Biol.* 18, 46–55. doi:10.1111/plb.12322.

Peitsch, D., Fietz, A., Hertel, H., Souza, J., Ventura, D., and Menzel, R. (1992). The spectral input systems of hymenopteran insects and their receptor-based colour vision. *J. Comp. Physiol. A* 170, 23–40. doi:10.1007/BF00190398.

Pelosi, P., and Maida, R. (1990). Odorant-binding proteins in vertebrates and insects: similarities and possible common function. *Chem. Senses* 15, 205–215. doi:10.1093/chemse/15.2.205.

Pevsner, J., Reed, R. R., Feinstein, P. G., and Snyder, S. H. (1988). Molecular Cloning of Odorant-Binding Protein: Member of a Ligand Carrier Family. *Science (80-.).* 241, 336–339. doi:10.1126/science.3388043.

Pfeiffer, K., and Homberg, U. (2014). Organization and functional roles of the central complex in the insect brain. *Annu. Rev. Entomol.* 59, 165–184. doi:10.1146/annurev-ento-011613-162031.

Pointer, M. R., and Attridge, G. G. (1998). The number of discernible colours. *Color Res. Appl.* 23, 52–54. doi:10.1002/(SICI)1520-6378(199802)23:1<52::AID-COL8>3.0.CO;2-2.

Quignon, P., Kirkness, E., Cadieu, E., Touleimat, N., Guyon, R., Renier, C., et al. (2003). Comparison of the canine and human olfactory receptor gene repertoires. *Genome Biol.* 4, R80. doi:10.1186/gb-2003-4-12-r80.

Rath, L., Giovanni Galizia, C., and Szyszka, P. (2011). Multiple memory traces after associative learning in the honey bee antennal lobe. *Eur. J. Neurosci.* 34, 352–360. doi:10.1111/j.1460-9568.2011.07753.x.

Reisenman, C. E. (2014). Hunger is the best spice: Effects of starvation in the antennal responses of the blood-sucking bug Rhodnius prolixus. *J. Insect Physiol.* 71, 8–13. doi:10.1016/j.jinsphys.2014.09.009.

Rother, L., Kraft, N., Smith, D. B., el Jundi, B., Gill, R. J., and Pfeiffer, K. (2021). A micro-CT-based standard brain atlas of the bumblebee. *Cell Tissue Res.* 386, 29–45. doi:10.1007/s00441-021-03482-z.

Ruta, V., Datta, S. R., Vasconcelos, M. L., Freeland, J., Looger, L. L., and Axel, R. (2010). A dimorphic pheromone circuit in Drosophila from sensory input to descending output. *Nature* 468, 686–690.

doi:10.1038/nature09554.

Rybak, J., Kuß, A., Lamecker, H., Zachow, S., Hege, H.-C., Lienhard, M., et al. (2010). The Digital Bee Brain: Integrating and Managing Neurons in a Common 3D Reference System. *Front. Syst. Neurosci.* 4, 15. doi:10.3389/fnsys.2010.00030.

Rybak, J., and Menzel, R. (1993). Anatomy of the mushroom bodies in the honey bee brain: the neuronal connections of the alpha-lobe. *J. Comp. Neurol.* 334, 444–65. doi:10.1002/cne.903340309.

Rybak, J., and Menzel, R. (1998). Integrative properties of the Pe1 neuron, a unique mushroom body output neuron. *Learn. Mem.* 5, 133–145. doi:10.1101/lm.5.1.133.

Sachse, S., Rappert, A., and Galizia, C. G. (1999). The spatial representation of chemical structures in the antennal lobe of honeybees: steps towards the olfactory code. *Eur. J. Neurosci.* 11, 3970–3982. doi:10.1046/j.1460-9568.1999.00826.x.

Sachse, S., Rueckert, E., Keller, A., Okada, R., Tanaka, N. K., Ito, K., et al. (2007). Activity-Dependent Plasticity in an Olfactory Circuit. *Neuron* 56, 838–850. doi:10.1016/j.neuron.2007.10.035.

Sandoz, J.-C. (2006). Odour-evoked responses to queen pheromone components and to plant odours using optical imaging in the antennal lobe of the honey bee drone Apis mellifera L. *J. Exp. Biol.* 209, 3587–3598. doi:10.1242/jeb.02423.

Saveer, A. M., Kromann, S. H., Birgersson, G., Bengtsson, M., Lindblom, T., Balkenius, A., et al. (2012). Floral to green: Mating switches moth olfactory coding and preference. *Proc. R. Soc. B Biol. Sci.* 279, 2314–2322. doi:10.1098/rspb.2011.2710.

Schiefner, A., Freier, R., Eichinger, A., and Skerra, A. (2015). Crystal structure of the human odorant binding protein, OBP IIa. *Proteins Struct. Funct. Bioinforma.* 83, 1180–1184. doi:10.1002/prot.24797.

Schinz, R. H. (1975). Structural specialization in the dorsal retina of the bee, Apis mellifera. *Cell Tissue Res.* 162, 23–34. doi:10.1007/BF00223259.

Scholl, C., Kübert, N., Muenz, T. S., and Rössler, W. (2015). CaMKII knockdown affects both early and late phases of olfactory long-term memory in the honeybee. *J. Exp. Biol.* 218, 3788–96. doi:10.1242/jeb.124859.

Scholl, C., Wang, Y., Krischke, M., Mueller, M. J., Amdam, G. V., and Rössler, W. (2014). Light exposure leads to reorganization of microglomeruli in the mushroom bodies and influences juvenile hormone levels in the honeybee. *Dev. Neurobiol.* 74, 1141–1153. doi:10.1002/dneu.22195.

Schröter, U., and Menzel, R. (2003). A new ascending sensory tract to the calyces of the honeybee mushroom body, the subesophageal-calycal tract. *J. Comp. Neurol.* 465, 168–178. doi:10.1002/cne.10843.

Schwarz, S., Narendra, A., and Zeil, J. (2011). The properties of the visual system in the Australian desert ant Melophorus bagoti. *Arthropod Struct. Dev.* 40, 128–34. doi:10.1016/j.asd.2010.10.003.

Seeley, T. D. (1985). *Honeybee Ecology*. Princeton University Press doi:10.1515/9781400857876.

Shepherd, G. M. (1972). Synaptic organization of the mammalian olfactory bulb. *Physiol. Rev.* 52, 864–917. doi:10.1152/physrev.1972.52.4.864.

Sherk, T. E. (1978). Development of the compound eyes of dragonflies (odonata). IV. Development of the adult compound eyes. *J. Exp. Zool.* 203, 183–199. doi:10.1002/jez.1402030202.

Smith, T. D., Garrett, E. C., Bhatnagar, K. P., Bonar, C. J., Bruening, A. E., Dennis, J. C., et al. (2011). The Vomeronasal Organ of New World Monkeys (Platyrrhini). *Anat. Rec. Adv. Integr. Anat. Evol. Biol.* 294, 2158–2178. doi:10.1002/ar.21509.

Soucy, E., Wang, Y., Nirenberg, S., Nathans, J., and Meister, M. (1998). A Novel Signaling Pathway from Rod Photoreceptors to Ganglion Cells in Mammalian Retina. *Neuron* 21, 481–493. doi:10.1016/S0896-6273(00)80560-7.

Srinivasan, M., and Reinhard, J. (2009). "The Role of Scents in Honey Bee Foraging and Recruitment," in, 165–182. doi:10.1201/9781420075618.ch9.

Srinivasan, M. V., and Zhang, S. (2004). Visual motor computations in insects. *Annu. Rev. Neurosci.* 27, 679–96. doi:10.1146/annurev.neuro.27.070203.144343.

Steinbrecht, R. A. (2007). "Structure and Function of Insect Olfactory Sensilla," in *CIBA Foundation Symposia*, 158–183. doi:10.1002/9780470514948.ch13.

Stengl, M., and Funk, N. W. (2013). The role of the coreceptor Orco in insect olfactory transduction. *J. Comp. Physiol. A Neuroethol. Sensory, Neural, Behav. Physiol.* 199, 897–909. doi:10.1007/s00359-013-0837-3.

Sterling, P., and Demb, J. B. (2004). "Retina," in *The Synaptic Organization of the Brain* (Oxford University Press), 217–270. doi:10.1093/acprof:oso/9780195159561.003.0006.

Stieb, S. M., Muenz, T. S., Wehner, R., and Rössler, W. (2010). Visual experience and age affect synaptic organization in the mushroom bodies of the desert ant Cataglyphis fortis. *Dev. Neurobiol.* 70, 408–423. doi:10.1002/dneu.20785.

Stocker, R. F. (2001). Drosophila as a focus in olfactory research: Mapping of olfactory sensilla by fine structure, odor specificity, odorant receptor expression, and central connectivity. *Microsc. Res. Tech.* 55, 284–296. doi:10.1002/jemt.1178.

Stocker, R. F., Lienhard, M. C., Borst, A., and Fischbach, K. F. (1990). Neuronal architecture of the antennal lobe in Drosophila melanogaster. *Cell Tissue Res.* 262, 9–34. doi:10.1007/BF00327741.

Stork, N. E. (2018). How Many Species of Insects and Other Terrestrial Arthropods Are There on Earth? *Annu. Rev. Entomol.* 63, 31–45. doi:10.1146/annurev-ento-020117-043348.

Stout, J. C., and Goulson, D. (2001). The use of conspecific and interspecific scent marks by foraging bumblebees and honeybees. *Anim. Behav.* 62, 183–189. doi:10.1006/anbe.2001.1729.

Strausfeld, N. J. (1976). *Atlas of an Insect Brain*. Berlin, Heidelberg: Springer Berlin Heidelberg doi:10.1007/978-3-642-66179-2.

Strausfeld, N. J. (1989). "Beneath the Compound Eye: Neuroanatomical Analysis and Physiological Correlates in the Study of Insect Vision," in *Facets of Vision* (Berlin, Heidelberg: Springer Berlin Heidelberg), 317–359. doi:10.1007/978-3-642-74082-4_16.

Strausfeld, N. J. (2002). Organization of the honey bee mushroom body: Representation of the calyx within the vertical and gamma lobes. *J. Comp. Neurol.* 450, 4–33. doi:10.1002/cne.10285.

Strausfeld, N. J., and Li, Y. (1999). Organization of olfactory and multimodal afferent neurons supplying the calyx and pedunculus of the cockroach mushroom bodies. *J. Comp. Neurol.* 409, 603–625. doi:10.1002/(SICI)1096-9861(19990712)409:4<603::AID-CNE7>3.0.CO;2-P.

Strausfeld, N. J., Sinakevitch, I., and Vilinsky, I. (2003). The mushroom bodies ofDrosophila melanogaster: An immunocytological and golgi study of Kenyon cell organization in the calyces and lobes. *Microsc. Res. Tech.* 62, 151–169. doi:10.1002/jemt.10368.

Strube-Bloss, M. F., Nawrot, M. P., and Menzel, R. (2011). Mushroom Body Output Neurons Encode Odor-Reward Associations. *J. Neurosci.* 31, 3129–3140. doi:10.1523/JNEUROSCI.2583-10.2011.

Strube-Bloss, M. F., Nawrot, M. P., and Menzel, R. (2016). Neural correlates of side-specific odour memory in mushroom body output neurons. *Proc. R. Soc. B Biol. Sci.* 283, 20161270. doi:10.1098/rspb.2016.1270.

Strube-Bloss, M. F., and Rössler, W. (2018). Multimodal integration and stimulus categorization in putative mushroom body output neurons of the honeybee. *R. Soc. Open Sci.* 5, 171785. doi:10.1098/rsos.171785.

Szyszka, P. (2008). Associative and non-associative plasticity in Kenyon cells of the honeybee mushroom body. *Front. Syst. Neurosci.* 2, 1–10. doi:10.3389/neuro.06.003.2008.

Thompson, W. R., Meinwald, J., Aneshansley, D., and Eisner, T. (1972). Flavonols: Pigments Responsible for Ultraviolet Absorption in Nectar Guide of Flower. *Science (80-.).* 177, 528–530. doi:10.1126/science.177.4048.528.

Trhlin, M., and Rajchard, J. (2011). Chemical communication in the honeybee (Apis mellifera L.): a review. *Vet. Med. (Praha).* 56, 265–273. doi:10.17221/1543-VETMED.

Vogt, K., Aso, Y., Hige, T., Knapek, S., Ichinose, T., Friedrich, A. B., et al. (2016). Direct neural pathways convey distinct visual information to Drosophila mushroom bodies. *Elife* 5, 1–13. doi:10.7554/eLife.14009.

von der Emde, G., Schwarz, S., Gomez, L., Budelli, R., and Grant, K. (1998). Electric fish measure distance in the dark. *Nature* 395, 890–894. doi:10.1038/27655.

von Frisch, K. (1914). *Der farbensinn und Formensinn der Biene.* Jena,: Fischer doi:10.5962/bhl.title.11736.

von Frisch, K. (1949). The Polarization of the Sky Light as a Factor in the Bees' Dances. *Experientia* 5, 142–8. doi:10.1007/BF02174424.

von Frisch, K. (1965). *Tanzsprache und Orientierung der Bienen*. Berlin, Heidelberg: Springer Berlin Heidelberg doi:10.1007/978-3-642-94916-6.

von Helversen, O. (1972). Zur spektralen Unterschiedsempfindlichkeit der Honigbiene. *J. Comp. Physiol.* 80, 439–472. doi:10.1007/BF00696438.

Vosshall, L. B. (2000). Olfaction in Drosophila. *Curr. Opin. Neurobiol.* 10, 498–503. doi:10.1016/S0959-4388(00)00111-2.

Vosshall, L. B., Wong, A. M., and Axel, R. (2000). An Olfactory Sensory Map in the Fly Brain. *Cell* 102, 147–159. doi:10.1016/S0092-8674(00)00021-0.

Wald, G. (1945). Human Vision and the Spectrum. *Science (80-.).* 101, 653–658. doi:10.1126/science.101.2635.653.

Wang, J. W., Wong, A. M., Flores, J., Vosshall, L. B., and Axel, R. (2003). Two-Photon Calcium Imaging Reveals an Odor-Evoked Map of Activity in the Fly Brain. *Cell* 112, 271–282. doi:10.1016/S0092-8674(03)00004-7.

Wang, S., Zhang, S., Sato, K., and Srinivasan, M. V. (2005). Maturation of odor representation in the honeybee antennal lobe. *J. Insect Physiol.* 51, 1244–1254. doi:10.1016/j.jinsphys.2005.07.003.

Wanner, K. W., Nichols, A. S., Walden, K. K. O., Brockmann, A., Luetje, C. W., and Robertson, H. M. (2007). A honey bee odorant receptor for the queen substance 9-oxo-2-decenoic acid. *Proc. Natl.*

Acad. Sci. 104, 14383–14388. doi:10.1073/pnas.0705459104.

Wehner, R. (1989). The Hymenopteran Skylight Compass: Matched Filtering and Parallel Coding. *J. Exp. Biol.* 146, 63–85. doi:10.1242/jeb.146.1.63.

Winnington, A. P., Napper, R. M., and Mercer, A. R. (1996). Structural plasticity of identified glomeruli in the antennal lobes of the adult worker honey bee. *J. Comp. Neurol.* 365, 479–490. doi:10.1002/(SICI)1096-9861(19960212)365:3<479::AID-CNE10>3.0.CO;2-M.

Yilmaz, A., Grübel, K., Spaethe, J., and Rössler, W. (2019). Distributed plasticity in ant visual pathways following colour learning. *Proc. R. Soc. B Biol. Sci.* 286, 20182813. doi:10.1098/rspb.2018.2813.

Young, J. M., Shykind, B. M., Lane, R. P., Tonnes-Priddy, L., Ross, J. A., Walker, M., et al. (2003). Odorant receptor expressed sequence tags demonstrate olfactory expression of over 400 genes, extensive alternate splicing and unequal expression levels. *Genome Biol.* 4, R71. doi:10.1186/gb-2003-4-11-r71.

Zufall, F., and Domingos, A. I. (2018). The structure of Orco and its impact on our understanding of olfaction. *J. Gen. Physiol.* 150, 1602–1605. doi:10.1085/jgp.201812226.

Affidavit

I hereby confirm that my thesis entitled "Processing of behaviorally relevant stimuli at different levels in the bee bra" is the result of my own work. I did not receive any help or support from commercial consultants. All sources and / or materials applied are listed and specified in the thesis.

Furthermore, I confirm that this thesis has not yet been submitted as part of another examination process neither in identical nor in similar form.

Place, Date   Signature

Eidesstattliche Erklärung

Hiermit erkläre ich an Eides statt, die Dissertation „Die Verarbeitung verhaltensrelevanter Stimuli auf unterschiedlichen Ebenen im Bienengehirn" eigenständig, d.h. insbesondere selbständig und ohne Hilfe eines kommerziellen Promotionsberaters, angefertigt und keine anderen als die von mir angegebenen Quellen und Hilfsmittel verwendet zu haben.

Ich erkläre außerdem, dass die Dissertation weder in gleicher noch in ähnlicher Form bereits in einem anderen Prüfungsverfahren vorgelegen hat.

Ort, Datum   Unterschrift

Appendix

Statement of individual author contributions and of legal second publication rights

(If required please use more than one sheet)

Manuscript (Schmalz, F., Eltz, T., Rössler, W., Spaethe, J., Schmitt, T., Strube-Bloss, M. Sex specific processing of olfactory key stimuli in the buff-tailed bumblebee):					
Participated in	**Author Initials,** Responsibility decreasing from left to right				
Study Design	FS	MSB	JS	TE & TS	
Methods Development	FS	MSB	JS		
Data Collection	FS	MSB			
Data Analysis and Interpretation	FS	MSB	JS		
Manuscript Writing					
Writing of Introduction	FS	WR	MSB		
Writing of Materials & Methods	FS	MSB	WR		
Writing of Discussion	FS	MSB	WR		
Writing of First Draft	FS	MSB	WR		
	FS				

Publication (Schmalz, F., Jundi, B., Rössler, W., and Strube-bloss, M. (2022). Categorizing Visual Information in Subpopulations of Honeybee Mushroom Body Output Neurons. *Front. Physiol.* 13, 1–11. doi:10.3389/fphys.2022.866807.):					
Participated in	**Author Initials,** Responsibility decreasing from left to right				
Study Design	FS	MSB			
Methods Development	FS	MSB			
Data Collection	FS				

Data Analysis and Interpretation	FS	BeJ	MSB		
Manuscript Writing					
Writing of Introduction	FS	MSB	WR	BeJ	
Writing of Materials & Methods	FS	MSB	WR	BeJ	
	FS	MSB	WR	BeJ	
Writing of Discussion	FS	MSB	WR	BeJ	
Writing of First Draft	FS				

The doctoral researcher confirms that she/he has obtained permission from both the publishers and the co-authors for legal second publication.

The doctoral researcher and the primary supervisor confirm the correctness of the above mentioned assessment.

Fabian Schmalz

_____

Doctoral Researcher's Name   Date   Place   Signature

_____

Primary Supervisor's Name   Date   Place   Signature

Statement of individual author contributions to figures/tables/chapters included in the manuscripts

(If required please use more than one sheet)

Manuscript (Schmalz, F., Eltz, T., Rössler, W., Spaethe, J., Schmitt, T., Strube-Bloss, M. Sex specific processing of olfactory key stimuli in the buff-tailed bumblebee):

Figure	Author Initials, Responsibility decreasing from left to right				
1	FS				
2	FS				
3	FS*	MSB*			
4	FS				
5	FS				
7	FS				
8	FS				

Explanations (if applicable):

*Equal contributions

Publication (Schmalz, F., el Jundi, B., Rössler, W., and Strube-bloss, M. (2022). Categorizing Visual Information in Subpopulations of Honeybee Mushroom Body Output Neurons. *Front. Physiol.* 13, 1–11. doi:10.3389/fphys.2022.866807.):

Figure	Author Initials, Responsibility decreasing from left to right				
1	FS				
2	FS				
3	FS				
4	FS				
5	FS	MSB			
Table 1	BeJ	FS			

I also confirm my primary supervisor's acceptance.

Fabian Schmalz

_____

Doctoral Researcher's Name   Date   Place   Signature